PSR Report 2474



MAGNETIC SIGNATURES OF SUBMARINES I

Prepared by

P. M. Moser
Pacific-Sierra Research Corporation
Warminster, Pennsylvania 18974

June 1994

Contract N62269-91-C-0533

NAVAL AIR WARFARE CENTER
AIRCRAFT DIVISION WARMINSTER
CODE 5012
WARMINSTER, PENNSYLVANIA 18974

REPORT DOCUMENTATION PAGE

Form Approved
OMB No. 0704-0188

The public reporting burden for this collection of information is estimated to average 1 hour per response, including the time for reviewing instructions, searching existing data sources, gathering and maintaining the data needed, and completing and reviewing the collection of information. Send comments regarding this burden estimate or any other aspect of this collection of information, including suggestions for reducing the burden, to Department of Defense, Washington Headquarters Services, Directorate for Information Operations and Reports (0704-0188), 1215 Jefferson Davis Highway, Suite 1204, Arlington, VA 22202-4302. Respondents should be aware that notwithstanding any other provision of law, no person shall be subject to any penalty for failing to comply with a collection of information if it does not display a currently valid OMB control number.
PLEASE DO NOT RETURN YOUR FORM TO THE ABOVE ADDRESS.

1. REPORT DATE *(DD-MM-YYYY)*	2. REPORT TYPE	3. DATES COVERED *(From - To)*
xx-06-1994	Interim technical	To June 1994

4. TITLE AND SUBTITLE
Magnetic Signatures of Submarines I

5a. CONTRACT NUMBER
N62269-91-C-0533

5b. GRANT NUMBER

5c. PROGRAM ELEMENT NUMBER

6. AUTHOR(S)
Moser, Paul M.

5d. PROJECT NUMBER

5e. TASK NUMBER

5f. WORK UNIT NUMBER

7. PERFORMING ORGANIZATION NAME(S) AND ADDRESS(ES)
Pacific-Sierra Research Corporation
Warminster, PA 18974

8. PERFORMING ORGANIZATION REPORT NUMBER
PSR Report 2474

9. SPONSORING/MONITORING AGENCY NAME(S) AND ADDRESS(ES)
Naval Air Warfare Center Aircraft Division Warminster
Code 5012
Warminster, PA 18974

10. SPONSOR/MONITOR'S ACRONYM(S)
NAWCADWAR

11. SPONSOR/MONITOR'S REPORT NUMBER(S)

12. DISTRIBUTION/AVAILABILITY STATEMENT
Approved for public release, distribution unlimited

13. SUPPLEMENTARY NOTES
See also PSR Report 2629, "Magnetic Signatures of Submarines II" by the same author.

14. ABSTRACT
This report presents a mathematical model of the steady magnetic anomaly produced by a submarine. It consists of several sub-models: the earth's magnetic field as a function of latitude, longitude and date; models for the ferromagnetic moment of the submarine, including induced and permanent components, for both point and extended dipoles; and a model for the magnetic field arising from steady galvanic corrosion currents. The model permits calculation of the magnetic anomaly, as it would be observed by an airborne magnetometer as a function of geographical location, submarine submerged displacement (tonnage), speed, heading and depth, and aircraft altitude, course and speed.

15. SUBJECT TERMS
Submarine, Detection, Magnetic, Signature, Anomaly, Aircraft, Magnetometer, Model, Dipole, Antisubmarine Warfare, Nonacoustic Detection of Submarines

16. SECURITY CLASSIFICATION OF:			17. LIMITATION OF ABSTRACT	18. NUMBER OF PAGES	19a. NAME OF RESPONSIBLE PERSON
a. REPORT	b. ABSTRACT	c. THIS PAGE			19b. TELEPHONE NUMBER *(Include area code)*
unclassified	unclassified	unclassified	unlimited	106	

CONTENTS

FIGURES vi

TABLE 1. Baseline Parameters Assumed for Computations 45

I. INTRODUCTION 1

II. APPROACH 2

III. MAGNETIC FIELD OF THE EARTH 3

IV. MAGNETIC MODEL OF A SUBMARINE 6
- Ferromagnetic Moment 6
- Induced and Equilibrium Moments 6
- Sample Calculation of a Submarine's Induced/Equilibrium Magnetic Moment 8
- Permanent Magnetic Moment 13
- Induced and Permanent Moments in Geographical Coordinates 14
- Vector Loci of Horizontal Moments 16

V. MAGNETIC FIELD AND ANOMALY FROM A FERROMAGNETIC DIPOLE 23
- Point Dipole 23
- Failure of Point Dipole Assumption at Short Range 28

VI. MAGNETIC FIELD AND ANOMALY FROM A STEADY HORIZONTAL ELECTRIC CURRENT ELEMENT 33

VII. DESCRIPTION OF THE MODEL 42

VIII. EXERCISING THE MODEL 45

Example 1. Combined magnetic field of the earth, extended ferromagnetic dipole moment and static electric current moment 46

Example 2. Comparison of ferromagnetic anomalies computed from extended dipole, point dipole, and "$B = M/R^3$" equations 49

CONTENTS (continued)

Example 3. Adjusting an anomaly calculated for a point dipole to approximate one calculated for an extended dipole 51

Example 4. Magnetic anomalies from static horizontal electric current elements 54

Example 5. Combination of magnetic anomalies from ferromagnetic dipole and static electric current element 56

Example 6. Dependence of magnetic anomaly on submarine heading for constant aircraft course direction 58

Example 7. Dependence of separation between extrema of magnetic anomaly on component of dipole moment in direction of sensor aircraft travel 60

Example 8. Dependence of vector components of magnetic induction on submarine heading 62

Example 9. Calculation of magnetic anomalies by exact and approximate methods 64

IX. DISCUSSION 66
Analysis of Magnetic Anomaly Signatures 66
Extended Dipole Model 66
Platform Noise 67
Geological Noise Model 68
Geomagnetic Noise Model 68
Alternating Magnetic Field from Modulation of Corrosion Currents 68

X. CONCLUSIONS / RECOMMENDATIONS 69

XI. REFERENCES 71

APPENDIX A. Symbols, Definitions and Units Used in Appendices 72

APPENDIX B. Reference Framework for Computations 76

CONTENTS (continued)

APPENDIX C. Magnetic Induction from an Infinitesimal ("Point") Ferromagnetic Dipole of Arbitrary Location and Orientation 78

APPENDIX D. Magnetic Induction from an Extended Ferromagnetic Dipole of Arbitrary Length, Location and Orientation 80

APPENDIX E. Magnetic Induction from an Electric Current Element Determined from the Biot-Savart Law 84

APPENDIX F. Magnetic Induction in Air above a Static Horizontal Electric Dipole in Seawater 87

APPENDIX G. Calculation of Earth's Magnetic Field Components in the Vicinity of a Geographical Reference Point 92

APPENDIX H. Computation of Magnetic Anomaly from Components of Magnetic Induction Caused by a Submarine in the Earth's Magnetic Field 95

FIGURES

1. Components and magnitude of the resultant induced/equilibrium magnetic moment of a submarine as a function of heading in submarine-fixed Cartesian coordinates 10

2. Magnitude of the horizontal component of the induced magnetic moment of a submarine as a function of heading in submarine-fixed polar coordinates 10

3. Magnitude of the resultant induced/equilibrium magnetic moment of a submarine as a function of heading in polar coordinates 11

4. Deviation of the induced horizontal moment vector from north as a function of submarine heading 12

5. Elevation angle of induced/equilibrium moment as a function of submarine heading 13

6. Components and resultant of induced and permanent magnetic moment of a 3000-ton submarine in geographical coordinates at 25°N, 58°E as a function of heading 16

7. Plot of the northerly component of the induced magnetic moment as a function of the easterly component 17

8. Inference of submarine heading from the direction of the induced horizontal moment vector 19

9. Loci of magnitude and direction of horizontal component of induced and permanent magnetic moment of a 3000-ton submarine at location 25°N, 58°E as a function of submarine heading for permanent longitudinal moments of 0, $1x10^8$, $3x10^8$, $6x10^8$, $9x10^8$, and $1.5x10^9$ gamma-ft^3 21

10. Maximum deviation of the horizontal moment vector from magnetic north vs. the ratio of permanent to maximum induced longitudinal moment 22

11. Magnetic anomalies calculated for a point dipole for twelve sensor aircraft course directions over the target 26

FIGURES (continued)

12. Comparison of values of magnetic moment obtained with the simple formula $M = B R^3$ to the correct values for a point dipole as a function of sensor course direction 27

13. Separation between extrema of anomaly from a point ferromagnetic dipole as a function of minimum sensor-to-target slant range 28

14. Dependence of calculated magnetic anomaly signature on assumed dipole length for constant magnetic moment 30

15. Linear density of magnetic moment for a prolate spheroidal dipole as a function of position along the dipole axis 31

16. Ratios of magnetic field values referenced to a ferromagnetic source assumed to be a correct representation of a submarine as a function of distance for three types of sources 32

17. Biot-Savart law for the magnetic induction from an infinitesimal electric current element 33

18. Orthogonal components of the magnetic induction from an infinitesimal horizontal electric current element calculated by use of the Biot-Savart Law 34

19. Comparison of magnetic induction from ferromagnetic moments and electric current moments as functions of range perpendicular to the dipole axes 36

20. Equations for the magnetic field above a semi-infinite conducting medium in which a static horizontal electric current dipole is immersed (from Kraichman, 1976) 37

21. Orthogonal components of the magnetic field from a horizontal electric current element calculated by use of Kraichman's equations (3.24), (3.25), and (3.26) 39

22. Magnetic field from a horizontal electric current dipole along a path perpendicular to the dipole axis showing the contributions from the hull current and the seawater return current 40

FIGURES (continued)

23. Magnetic field from a steady electric current dipole in seawater as a function of lateral range and vertical separation between source and sensor 40

24A. Combined magnetic induction of the earth and the extended ferromagnetic and static electric current moments of a submarine 47

24B. Combined magnetic induction of the earth and the extended ferromagnetic and static electric current moments of a submarine 48

25. Comparison of magnetic anomaly signatures calculated by use of point and extended ferromagnetic dipole models 50

26. Comparison of anomalies calculated for extended and point ferromagnetic dipoles for very-low-altitude pass directly over target 51

27. Anomaly from a ferromagnetic dipole modified in magnitude and location to approximate the anomaly from an extended dipole at its extrema 53

28. Comparison of magnetic anomalies calculated for an isolated electric current element and for an electric current element immersed in seawater 55

29. Magnetic anomalies from ferromagnetic dipole, static electric current element, and the combination of the two 57

30. Effect of changes in target submarine heading on calculated magnetic anomaly for constant sensor aircraft heading 59

31. Separation of anomaly extrema calculated from combined extended ferromagnetic dipole and electric current element model for four submarine headings 61

32. Vector components of combined magnetic induction from a ferromagnetic dipole and a static electric current element 63

33. Magnetic anomalies calculated by exact and approximate methods 65

B-1. Coordinate system 76

FIGURES (continued)

D-1. Geometry for extended dipole derivation 80

E-1. Geometry for calculating magnetic induction from an electric current element 84

F-1. Geometry and equations for the magnetic field intensity above a semi-infinite conducting medium in which a static horizontal electric current dipole is immersed (from Kraichman, 1976) 87

G-1. Locations of points at which earth's magnetic field values were determined from IGRF model 92

I. INTRODUCTION

A submarine can cause a local distortion of the earth's naturally occurring magnetic field and thereby produce what is called a "magnetic anomaly." These magnetic effects arise from the "permanent" and induced magnetization of the ferromagnetic material constituting the structure and machinery of the submarine and from galvanic corrosion currents flowing through the submarine and the surrounding water.

Permanent magnetization results from long-term alignment of the submarine with the earth's magnetic field (voyage effect) and is enhanced if the hull is stressed through vibration, mechanical shock or submergence (dive effect) and subsequent relaxation. Over short time periods, the permanent magnetization is independent of the submarine's heading.

Even if a ferromagnetic body is not "permanently" magnetized, it can still produce a local distortion of the fairly uniform magnetic field of the earth. This distortion can be described as if it originates from a temporary, orientation-dependent, induced magnetization of the submarine.

Electric currents produce magnetic fields. Galvanic corrosion currents arise from the difference in electric potential of interconnected dissimilar metals immersed in an electrolytic solution such as a bronze propeller in electrical contact with a steel hull protected against corrosion by attached sacrificial zinc blocks, all immersed in sea water. The potential difference is about 1 volt and the resulting current may range from 1 to 100 amperes. Because of variations in resistance (as a function of propeller shaft angle) between the rotating propeller shaft and its bearings, this current may be modulated at the shaft rate. Thus a submarine may be surrounded by steady and alternating magnetic fields resulting from corrosion currents.

Each of the foregoing contributes to the magnetic signature of a submarine which, at present, represents a potentially rich unexploited source of ASW-relevant information. A study of the magnetic signatures of submarines should establish the basis for optimum processing of signals and yield improved target acquisition range, improved search strategy, target classification, and target heading and depth information.

II. APPROACH

A system model is being developed which yields synthetic magnetic anomaly detector (MAD) signatures corresponding to any realistic combination of target, sensor, environmental, and operational characteristics. The synthetic signatures are then compared to real-world magnetic signatures as a means of validating and amending the model and, ultimately, deducing characteristics of the targets. When completed, the system model will consist of a number of sub-models: a model of the earth's magnetic field, models for the ferromagnetic moment of the submarine, including induced and permanent components, models for the steady magnetic field arising from galvanic corrosion currents, a model for the alternating magnetic field from modulation of corrosion currents, a geomagnetic noise model, a geological noise model, and an integrating model that utilizes all of the above to generate simulated outputs of an airborne sensor such as the AN/ASQ-208 in any realizable encounter geometry.

III. MAGNETIC FIELD OF THE EARTH

The magnetic field of the earth governs the magnetic signature of a submarine in two ways. First, the magnitude and direction of the earth's field, along with the mass, dimensions, and ferromagnetic properties of the submarine and its orientation in the earth's field, determine the induced magnetic moment of the submarine, a measure of its magnetic source strength. Second, a submarine's magnetic field adds vectorially to the earth's field; therefore, a scalar total-field-measuring magnetometer such as the AN/ASQ-208 senses the magnitude of the resultant of the earth's field and the field of the submarine.

To a first approximation, the earth's magnetic field can be considered to originate in any one of several ways: (a) from an earth-sized, uniformly magnetized sphere having a magnetization of 0.08 gauss, (b) from a point dipole of magnetic moment 8.1×10^{25} gauss-cm^3 embedded in the earth near its center, or (c) from an electric current sheet of 1.5×10^9 amperes circulating around the earth and distributed in proportion to the cosine of the latitude.

The magnitude of the equivalent dipole moment of the earth can be expressed alternatively as 2.86×10^{26} gamma-ft^3. The axis of the dipole is tilted 11.5° relative to the geographic axis of the earth and intersects the earth's surface at 78.5°N, 69°W and 78.5°S, 111°E.

The vector field produced by a point magnetic dipole is given by

$$\mathbf{B} = -\mathbf{M}/R^3 + (3\,\mathbf{M}\cdot\mathbf{R})\,\mathbf{R}/R^5 \qquad (1)$$

in which **R** is the radius vector from the dipole to some point P at which the magnetic field is to be calculated, R is the magnitude of **R**, **B** is the magnetic induction vector at P, and **M** is the magnetic moment vector of the dipole. An inspection of equation (1) shows that, at a given distance R, the magnitude B of the magnetic induction is twice as great along the dipole axis (for which $\mathbf{M}\cdot\mathbf{R} = MR$) as along the perpendicular bisector of the dipole (for which $\mathbf{M}\cdot\mathbf{R} = 0$).

If the mean radius of the earth is taken as 6.37×10^8 cm = 2.09×10^7 ft, equation (1) yields a magnitude for the magnetic field at the earth's surface of 0.313 gauss at the magnetic equator and 0.626 gauss at the magnetic poles. Thus, the magnitude of the earth's field varies with distance in the north-south direction at an average rate of about 0.00006 gauss/nmi (6 gamma/nmi). If, in equation (1), one takes the derivative of B with respect to R, one finds that, near the earth's surface, the magnetic field decreases with increasing altitude at the rate of 9 gamma per 1000 ft at the magnetic poles and at half that rate at the equator.

A moderate improvement in calculations of the magnetic field at the earth's surface is obtained by assuming that the dipole is displaced from the earth's center by about 460 km, toward a point in the Pacific Ocean north of New Guinea. The dipole axis has shown no measureable change in direction for nearly 150 years; however, the equivalent dipole is moving (without change in direction) in a north-northwesterly direction.

The magnetic poles of the earth are defined in terms of where the declination (dip angle) is ±90° relative to the earth's surface. In 1975, the north magnetic pole was located at 76.1°N, 100°W. Because the dipole is displaced from the earth's center and because the earth is not a perfect sphere, the point where the dipole axis intersects the earth's surface is about 1160 km (626 nmi) from the north magnetic pole.

Even if the obliquity of the dipole axis and the displacement of the dipole from the center of the earth are taken into account, equation (1) provides only an approximation to the actual surface field and regional deviations of over 0.1 gauss exist. For more accurate calculations, an empirical process of spherical harmonic analysis is used; the main term of the spherical harmonic expression corresponds to the dipole field. (Spherical harmonic analysis is the three-dimensional analog (on a spherical surface) of the Fourier analysis of a complex two-dimensional waveform in terms of a series of harmonically related sine and cosine terms with coefficients that can be adjusted to match any desired waveform. As with Fourier analysis, the accuracy of representation improves with increasing the number of terms.) Magnetic survey data are incorporated into models whose coefficients are updated every five years to accommodate long term (secular) variations. Diurnal and local geological and geomagnetic variations are not addressed.

The National Geophysical Data Center is a national repository for geomagnetic data and models (reference (a)). One model that is available on a floppy disk for use on IBM-compatible personal computers is the International Geomagnetic Reference Field (IGRF) global spherical harmonic model. The IGRF model is of degree n and order m* 10, which requires 120 coefficients (n[n+2]) that are updated every five years; there is an additional set of 120 numbers that define the annual rate of variation of each of the coefficients. The smallest scale size of the field structure that can be represented by such a model (i.e., one "wavelength") equals the circumference of the earth, 21,600 nmi, divided by the degree, which for n = 10 yields 2160 nmi. The CAIN5050 model is of degree and order 50; this yields a "wavelength" of 432 nmi which is sufficient to model the intermediate magnetic anomalies believed to originate in the upper mantle and crust. (The CAIN5050 model presumably requires 2600 coefficients.) To describe small scale geological magnetic anomalies (e.g., a "pixel" size of 250 ft and a "wavelength" of 500 ft) over a 100- by 100-nmi^2 operating area would require 1,481,088 coefficients.

---

* The degree and order are of the associated Legendre polynomial.

In the IGRF model, the earth's magnetism is expressed in terms of its scalar magnetic potential V; to obtain the three orthogonal components of the vector field, partial derivatives of V with respect to each of the three spatial coordinates are taken in accordance with Laplace's equation. The IGRF model permits easy computation of the northward, eastward, and vertically downward components, as well as the total field, horizontal field, declination, and inclination as a function of latitude, longitude, altitude (with respect to the ellipsoid), and calendar date.

IV. MAGNETIC MODEL OF A SUBMARINE

Ferromagnetic Moment

At distances that are large in comparison to the dimensions of a submarine, the ferromagnetic field of a submarine can be considered to originate from a point dipole. In this discussion it is assumed that the submarine hull is constructed of a ferromagnetic material, that its magnetization arises solely from its presence in the earth's magnetic field, and that the submarine can be approximated as a prolate spheroid, whose length is at least eight times greater than its diameter. It is further assumed that the submarine is not using any active signature-modifying equipment. The magnetic dipole moment of a submarine is the vector sum of its induced moment and its permanent moment, each of which may have components in the longitudinal, vertical, and athwartship directions. A submarine is capable of supporting its largest magnetic moments (both induced and permanent) in the longitudinal direction. However, unless the submarine maintains a constant heading for a long period of time (e.g., while on a long voyage), it will have relatively little tendency to acquire a significant permanent horizontal (longitudinal and/or athwartship) magnetization of one particular polarity because its heading will probably vary in a random manner.

If a submarine does acquire a horizontal component of permanent magnetic moment, it is likely to be directed principally along the longitudinal axis and may have either the stern-to-bow or bow-to-stern sense. If the submarine remains for an extended period in, say, the northern hemisphere, where the magnetic field inclination is downward, a downward component of "equilibrium" vertical magnetization will result, independent of the submarine's heading. This component will comprise both permanent and induced magnetization. In addition to the induced and permanent longitudinal dipole moments and the equilibrium vertical dipole moment there are the athwartship components of induced and permanent dipole moment, which, for most orientations, tend to be smaller than the longitudinal moment.

Induced and Equilibrium Moments

In reference (b), Peizer has provided simple formulas for calculating the induced and equilibrium magnetic dipole moments based on the shape and volume enclosed within a steel prolate spheroid approximation of a submarine. These formulas have been generalized somewhat and recast as follows:

$$M_{VE} = V H_V T \quad (2)$$

$$M_{LI} = L H_L T = L H_H T \cos(\beta-\alpha) \quad (3)$$

$$M_{AI} = A H_A T = A H_H T \sin(\beta-\alpha) \quad (4)$$

in which

M_{VE} = equilibrium vertical moment (gamma-ft^3)

M_{LI} = induced longitudinal moment (gamma-ft^3)

M_{AI} = induced athwartship moment (gamma-ft^3)

V = coefficient for vertical component of moment (ft^3/ton)

L = coefficient for longitudinal component of moment (ft^3/ton)

A = coefficient for athwartship component of moment (ft^3/ton)

H_V = vertical component of the earth's field (gamma)

H_L = longitudinal component of the earth's field (gamma)

H_A = athwartship component of the earth's field (gamma)

H_H = horizontal component of the earth's field (gamma)

T = submerged displacement of the submarine (tons)

α = submarine heading (degrees true)

β = local geomagnetic declination (degrees; east, positive).

In equations (2), (3), and (4) the positive directions of M_{VE}, M_{LI}, and M_{HI} are vertically downward, stern-to-bow, and portside-to-starboard, respectively. The positive direction of H_V is, consistent with convention, vertically downward.

Peizer provides values for the coefficients of magnetic moments for six classes of submarines. He gives a single value of V = 5.1 ft^3/ton for all six classes but six values for L

ranging from 10.6 to 16.6 ft^3/ton and a calculated value of L = 11.5 ft^3/ton. He gives three values for A (2.9, 2.9, and 3.6 ft^3/ton) and a suggested value of A = 3.0 ft^3/ton. Peizer's suggested values are in the proportion

$$V : L : A :: 1.70 : 3.83 : 1.00.$$

Schneider (reference (c)) provides a similar approach for estimating magnetic moments and gives "typical values for the axial permeabilities of conventional submarines" in other units. Schneider's values are in the proportion

$$V : L : A :: 1.00 : 4.19 : 1.00.$$

Sample Calculation of a Submarine's Induced/Equilibrium Magnetic Moment

Assume that a KILO class submarine will be operating in the Gulf of Oman on a heading of 030° true at latitude 25°N and longitude 58°E on June 1, 1996. According to *Jane's Fighting Ships* (reference (d)) this vessel displaces 3000 tons of seawater when completely submerged. According to the IGRF model, the earth's magnetic field at that time and place, for zero altitude (relative to the ellipsoid approximating the earth's surface), is given by the following set of values:

Northerly component	34271 nT
Easterly component	662 nT
Downward component	26582 nT
Total field	43377 nT
Horizontal component	34278 nT
Inclination (down)	37.8°
Declination (east)	1.1°.

It should be noted that three properly selected examples of the above seven parameters are sufficient to specify the vector magnetic field.

Therefore, if Peizer's recommended values for V, L, and A are used,

$$M_{VE} = 5.1 \times 26582 \times 3000 = 4.07 \times 10^8 \text{ gamma-ft}^3 \quad (5)$$

$$M_{LI} = 11.5 \times 34278 \times 3000 \times \cos(1.1^\circ - 30^\circ) = 1.035 \times 10^9 \text{ gamma-ft}^3 \quad (6)$$

$$M_{AI} = 3.0 \times 34278 \times 3000 \times \sin(1.1^\circ - 30^\circ) = -1.491 \times 10^8 \text{ gamma-ft}^3. \quad (7)$$

The magnitude M_{HI} of the induced horizontal component is

$$M_{HI} = (M_{LI}^2 + M_{AI}^2)^{1/2} = 1.046 \times 10^9 \text{ gamma-ft}^3. \quad (8)$$

The direction φ_{LI} of the induced horizontal component relative to the longitudinal axis of the submarine is

$$\varphi_{LI} = \arctan(M_{AI}/M_{LI}) = -8.195^\circ. \quad (9)$$

Since the submarine is on an assumed heading of 030° true, the direction of the horizontal component in geographical coordinates is 30° - 8.195° = 21.805° east of true north.

The magnitude M_I of the resultant of the induced and equilibrium moments is

$$M_I = (M_{VE}^2 + M_{LI}^2 + M_{AI}^2)^{1/2} = 1.122 \times 10^9 \text{ gamma-ft}^3. \quad (10)$$

The depression angle θ_I of the resultant vector is

$$\theta_I = \arctan (M_{VE}/M_{HI}) = 21.25^\circ. \quad (11)$$

The magnitudes of the three principal orthogonal components (equilibrium vertical, induced longitudinal, and induced athwartship), the horizontal induced moment, and the resultant magnetic moment as a function of submarine heading are plotted in submarine-fixed Cartesian coordinates in figure 1 for the same 3000-ton submarine located at 25°N, 58°E. In figure 1, the stern-to-bow direction, the portside-to-starboard direction, and the downward direction are considered positive. Thus, the longitudinal (induced) moment takes on positive values when the submarine is on a heading having a northerly component and the athwartship moment is negative for headings with an easterly component. The equilibrium vertical component is independent of heading and, in the northern hemisphere, is directed downward. Figure 2 is a polar plot (in submarine-fixed coordinates) of the magnitude of the horizontal component of induced magnetic moment as a function of submarine heading. Figure 3 is a similar polar plot of the magnitude of the resultant induced/equilibrium magnetic moment vs. heading. Figure 3 shows a smoother curve than figure 2 because of the vector addition of the equilibrium vertical moment, which is independent of heading.

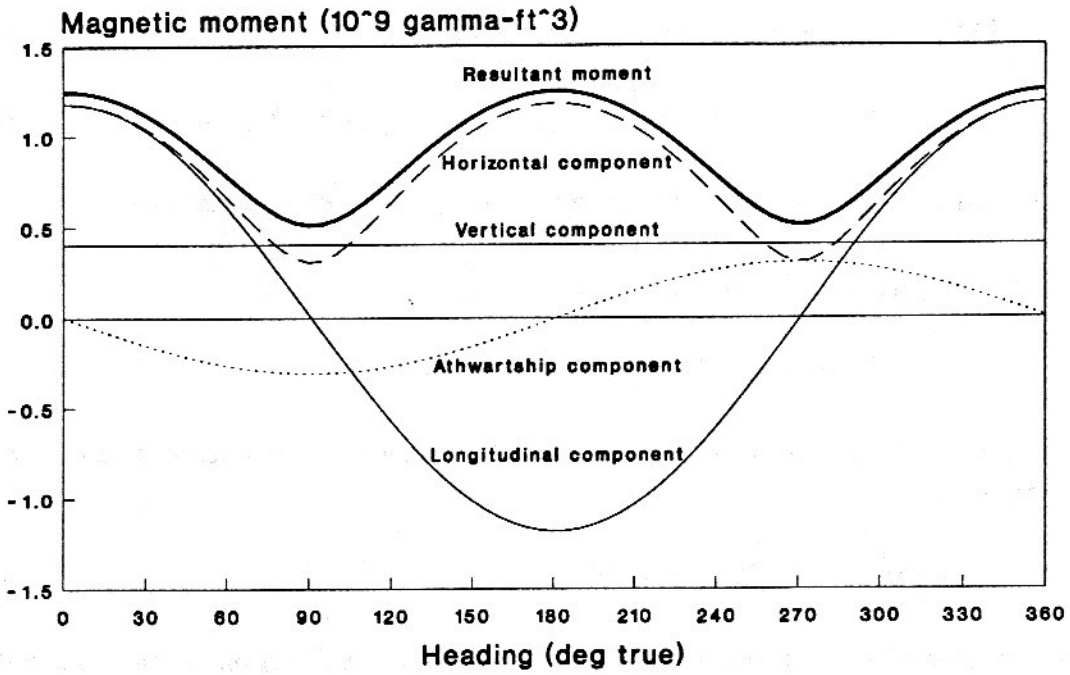


Figure 1. Components and magnitude of the resultant induced/equilibrium magnetic moment of a submarine as a function of heading in submarine-fixed Cartesian coordinates.

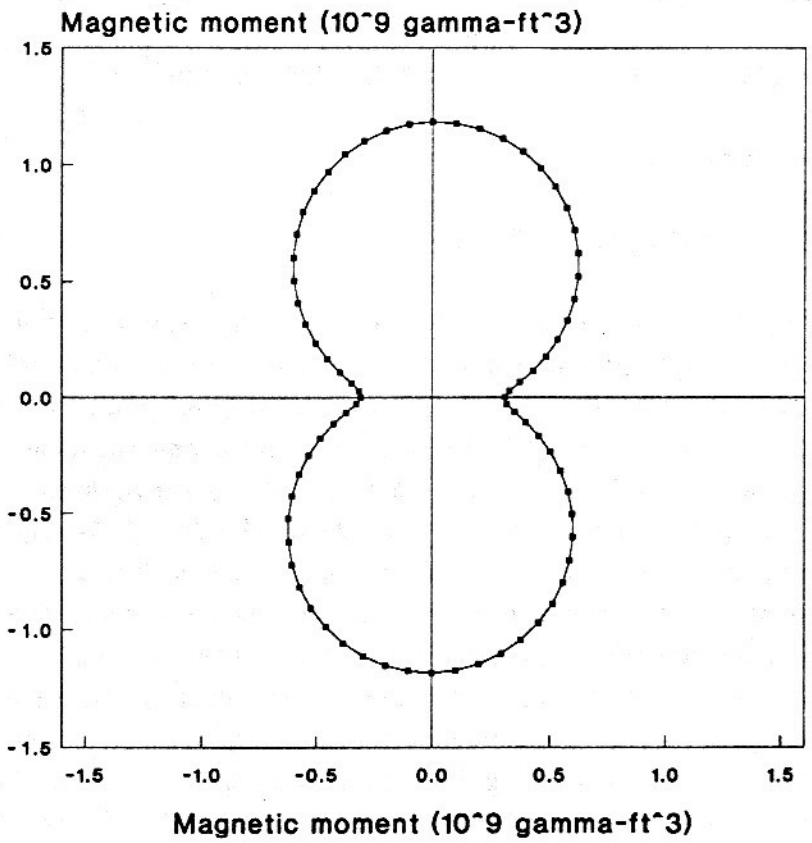


Figure 2. Magnitude of the horizontal component of the induced magnetic moment of a submarine as a function of heading in submarine-fixed polar coordinates.

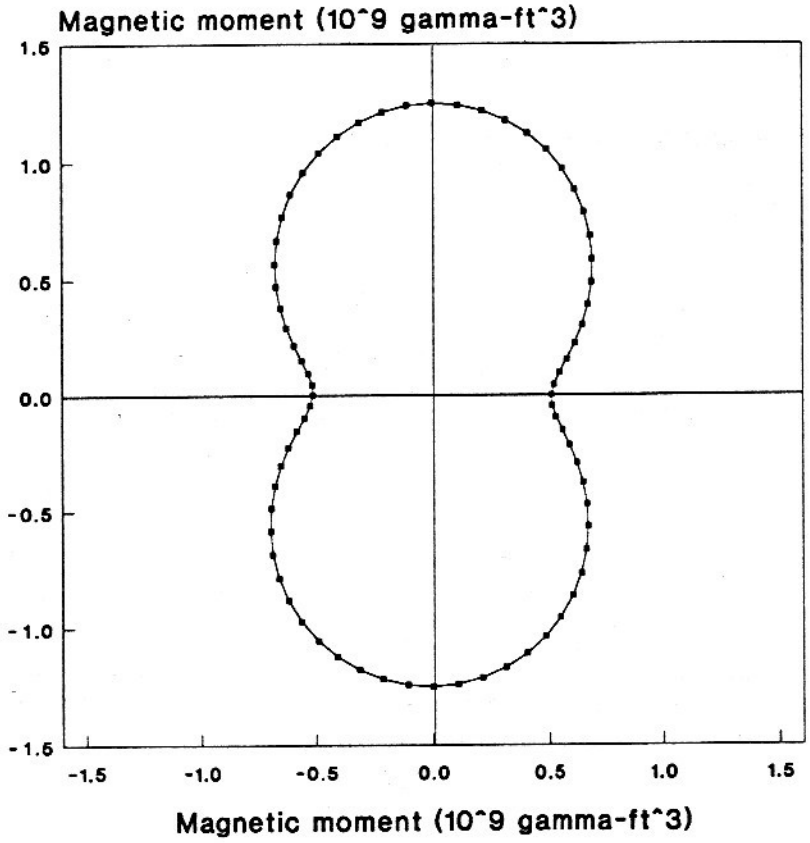


Figure 3. Magnitude of the resultant induced/equilibrium magnetic moment of a submarine as a function of heading in polar coordinates.

Figures 1, 2, and 3 show only the magnitudes of the moment vectors. Figure 4 shows the direction of the vector in the horizontal plane and figure 5 shows its direction in the vertical plane.

Figure 4 is a plot of the angular deviation of the induced horizontal moment vector from true north as a function of submarine heading obtained by adding values of submarine heading to values obtained from equation (9). Note that the deviation stays within the limits of +37.0° and -34.8° from true north or, more simply, as will be seen later, within ±35.9° of magnetic north.

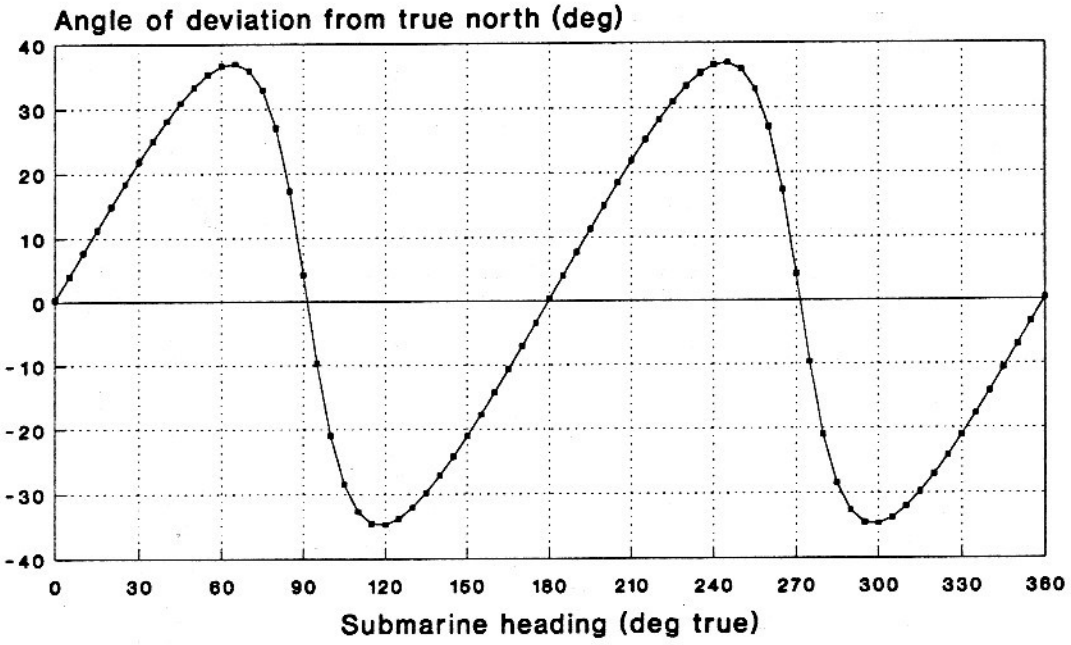


Figure 4. Deviation of the induced horizontal moment vector from north as a function of submarine heading.

Figure 5 is a plot of the elevation angle (i.e., the negative of the depression angle given by equation (11)) of the induced/equilibrium moment of the 3000-ton submarine as a function of heading. Note that for north-south orientations, the moment vector is depressed least and for east-west orientations, it is depressed the most. This variation occurs because this angle depends upon the ratio of the vertical to the longitudinal moment and the longitudinal moment is greatest for north-south headings. Thus the value of θ_I or the ratio M_{VE}/M_{HI} could provide some information on submarine heading although there is a four-fold ambiguity in inferring submarine heading from the moment depression angle. For example, if a depression angle of 30° were observed, it could imply a submarine heading of 57°, 125°, 237° or 305°.

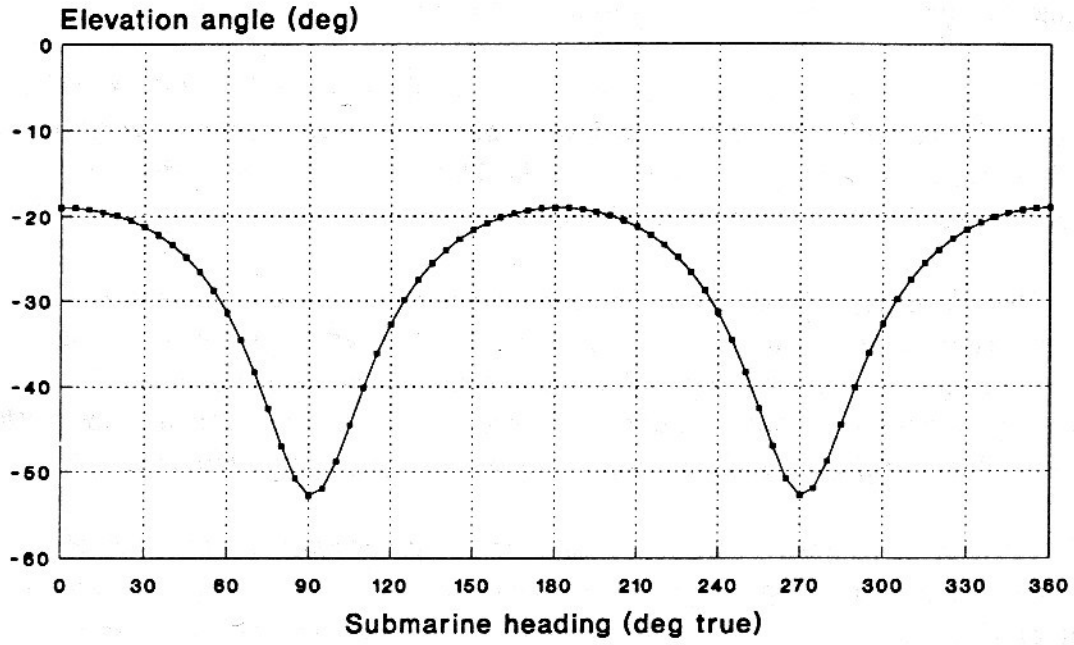


Figure 5. Elevation angle of induced/equilibrium moment as a function of submarine heading.

Permanent Magnetic Moment

The permanent magnetic moment is a function of the magnetic history of the submarine. Because a submarine has a cigar-like shape, its permanent moment tends to align itself primarily with the longitudinal axis. However, because the orientation of a submarine at sea tends to be random, prediction of the magnitude or even the direction (i.e., bow to stern vs. stern to bow) would be unreliable. If the submarine has been tied up in port for an extended period, or if it is regularly docked in a given orientation, a value for the permanent magnetic moment may be calculable. For a submarine on a nearly constant heading for a long period of time, one might expect the magnetic moment to build up asymptotically with time. If the vibration level of the submarine is high, or if it dives and thereby stresses the hull, the process will be accelerated. It appears to be impossible, except for peculiar special cases, to be able to predict the permanent longitudinal magnetic moment of a submarine.

The magnetic model of a submarine allows insertion of values for longitudinal and athwartship components of the permanent magnetic moment if such values are known or determinable. For example, if the magnetic anomaly from a submarine is observed when the submarine is on a given heading and again, shortly thereafter, when it is on the opposite

heading, and if the signatures are different, one could attribute the difference to the permanent magnetic moment and thereby calculate its value.

If a particular submarine remains in, say, the northern hemisphere, where the vertical component of the earth's field is directed down, a mathematically inseparable combination of permanent and induced magnetization will result. This combination gives rise to the previously discussed equilibrium vertical magnetic moment.

Despite its unpredictability, the permanent magnetic moment of a submarine is a reality which must be considered in any signature modelling effort. In this study, the permanent magnetic moment is handled parametrically; values are assigned and the consequences examined. This enables one to compare observed magnetic moments with modeled values to infer the magnitudes of the permanent and induced moments.

As with the induced moment, it is assumed that the horizontal component of the permanent magnetic moment comprises both longitudinal and athwartship components. The longitudinal permanent component is assumed to have a magnitude M_{LP} and a positive direction from stern to bow. Thus the combined induced and permanent longitudinal moment is given by $M_{LI} + M_{LP} = M_L$. Similarly, the athwartship permanent component is assumed to have a magnitude M_{AP} and a positive direction from starboard to portside and the combined induced and permanent athwartship is $M_{AI} + M_{AP} = M_A$.

Induced and Permanent Moments in Geographical Coordinates

Generally, the heading of a submerged submarine being prosecuted by MAD will not be known a priori. The only MAD observable (for a conventional scalar magnetometer) is the magnetic anomaly, from which one can determine, at best (on a single pass), the three orthogonal components of the resultant magnetic moment in geographical coordinates. However, it was seen in the previous illustrative examples that the magnetic moment vector is not, in general, aligned with the heading of the submarine. It is instructive to determine the relationship between submarine heading and the magnitude and direction of its magnetic moment.

First, it is useful to express equations (2), (3), and (4) in geographical coordinates rather than submarine-fixed coordinates. Assume a right-handed Cartesian coordinate system in which north, east, and vertically upward are the positive directions. The northerly component M_Y of the combined induced and permanent magnetic moments is then given by

$$M_Y = (M_{LI} + M_{LP}) \cos \alpha + (M_{AI} + M_{AP}) \cos(\alpha+90°)$$

$$= (M_{LI} + M_{LP}) \cos \alpha - (M_{AI} + M_{AP}) \sin \alpha$$

$$= M_L \cos \alpha - M_A \sin \alpha. \quad (12)$$

Similarly, the easterly component M_X of the combined induced and permanent magnetic moment is

$$M_X = (M_{LI} + M_{LP}) \sin \alpha + (M_{AI} + M_{AP}) \sin(\alpha+90°)$$

$$= (M_{LI} + M_{LP}) \sin \alpha + (M_{AI} + M_{AP}) \cos \alpha$$

$$= M_L \sin \alpha + M_A \cos \alpha. \quad (13)$$

The upward component M_Z of the equilibrium vertical moment is

$$M_Z = - M_{VE}. \quad (14)$$

The magnitude M_H of the horizontal moment is

$$M_H = (M_X^2 + M_Y^2)^{1/2}. \quad (15)$$

The magnitude M of the total ferromagnetic moment of the submarine is

$$M = (M_X^2 + M_Y^2 + M_Z^2)^{1/2}. \quad (16)$$

The angle of deviation φ of M_H from true north is

$$\varphi = \arctan (M_X/M_Y). \quad (17)$$

The elevation angle θ (i.e., the negative of the depression angle) of M relative to horizontal is

$$\theta = \arctan (M_Z/M_H). \quad (18)$$

Equations (12) through (16) are plotted as functions of submarine true heading α in figure 6. This graph shows the magnitudes of the northerly, easterly, and upward components of the magnetic moment of a 3000-ton submarine having a permanent longitudinal moment of 3×10^8 gamma-ft^3 and induced moments consistent with being located at 25°N, 58°E. In addition, figure 6 shows the magnitude of the horizontal component

and the magnitude of the resultant vector as a function of heading. Figure 6 should be compared to figure 1. A major difference between these two figures is that figure 6 gives values of components referred to earth-fixed directions whereas figure 1 gives values referred to submarine-fixed directions. Another difference is that, in figure 6, the longitudinal moment comprises both permanent and induced components whereas in figure 1 the longitudinal moment has no permanent component.

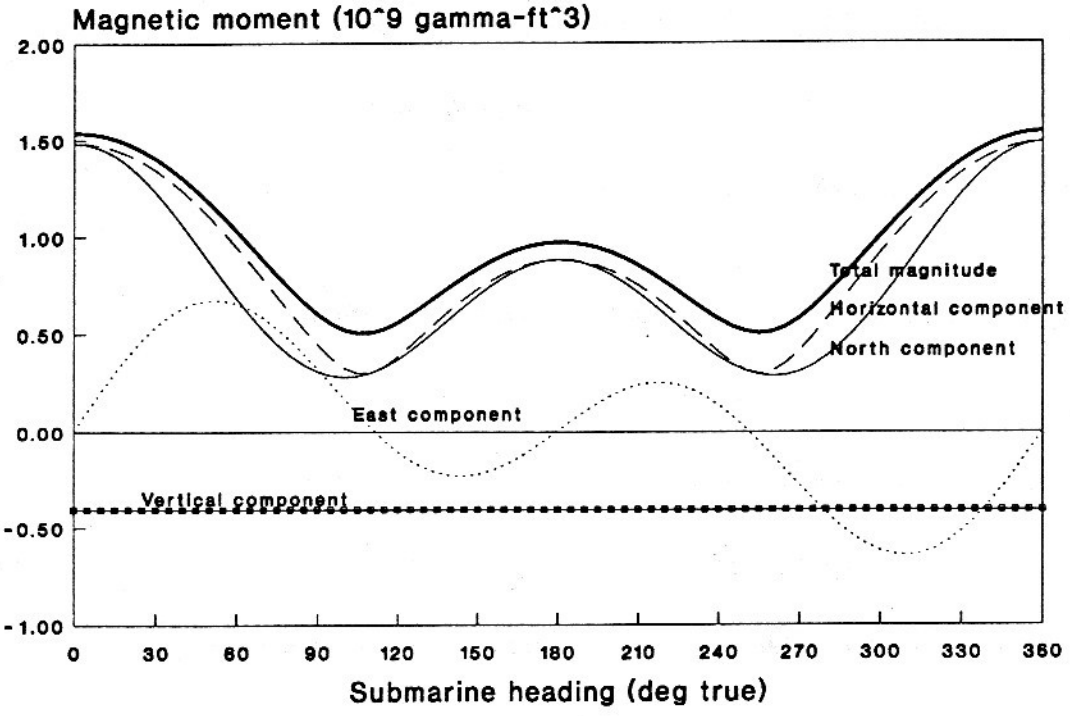


Figure 6. Components and resultant of induced and permanent magnetic moment of a 3000-ton submarine in geographical coordinates located at 25°N, 58°E as a function of heading.

Vector Loci of Horizontal Moments

If the northerly component of magnetic moment (equation (12)) is plotted as a function of the easterly component (equation (13)) using the heading α as a common parameter, for various values of permanent magnetic moment, a family of curves (limaçons) results. Each such curve represents the locus of the head of the horizontal magnetic moment vector (whose tail is fixed at the origin) as a function of submarine heading and therefore gives both the vector's magnitude and direction versus heading.

CASE I. Zero Horizontal Permanent Moment.

Figure 7 illustrates the simplest of these loci, for which the horizontal permanent moment is zero. As an example, the vector M_H drawn to the point on the curve corresponding to a magnetic heading of 20° is the resultant of M_X and M_Y and has a magnitude of 1.12×10^9 gamma-ft^3 and a deviation $\varphi = 14.6°$ east of magnetic north. That is, the magnetic moment vector is more northerly than the submarine's heading.

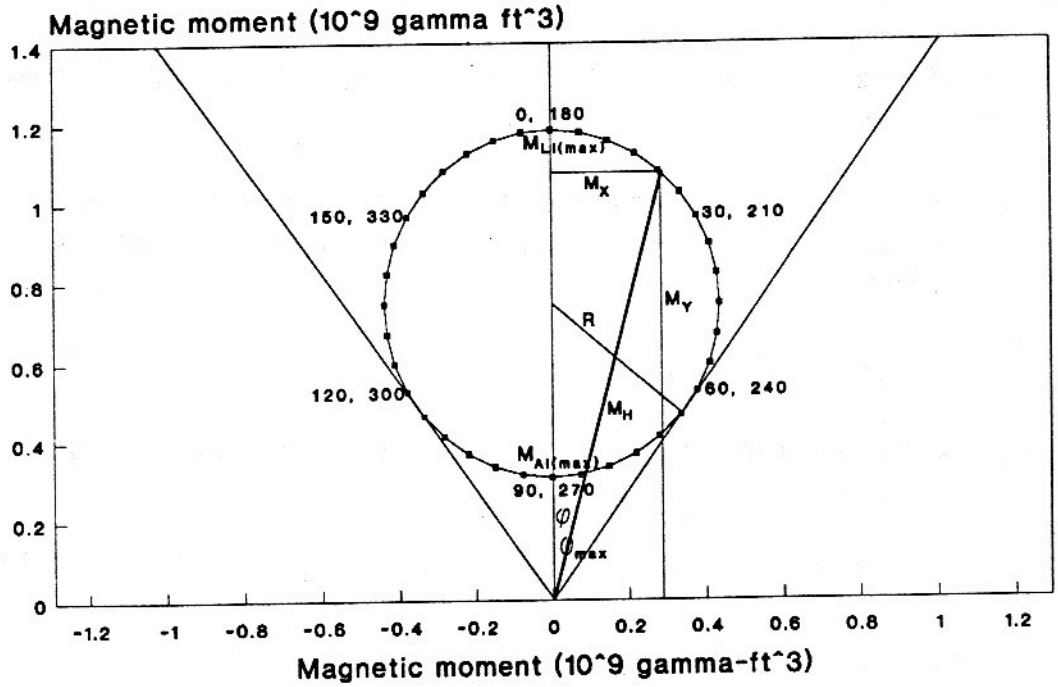


Figure 7. Plot of the northerly component of the induced magnetic moment as a function of the easterly component.

Figure 7 actually consists of two superimposed circles, one corresponding to headings from 0 to 180° and the other corresponding to headings ranging from 180 to 360°. The maximum value of the curve corresponds to the maximum value of the northerly component of the magnetic moment, which occurs when the longitudinal axis of the submarine is aligned with the earth's magnetic field (i.e., for headings of 0° and 180°, magnetic) and is equal to the maximum value of the longitudinal moment of the submarine. That is,

$$M_{YI(max)} = M_{LI(max)} = L\, H_H\, T. \tag{19}$$

Similarly, the minimum value of the curve equals the maximum value of athwartship moment of the submarine, which occurs when the submarine is aligned perpendicular to the earth's field (i.e., on a 90° or 270° magnetic heading). That is,

$$M_{YI(min)} = M_{AI(max)} = A\, H_H\, T. \tag{20}$$

The diameter D of the circular locus is therefore

$$D = M_{YI(max)} - M_{YI(min)} = (L - A)\, H_H\, T. \tag{21}$$

Equation (21) shows that if a spherically symmetrical submarine were to be built, i.e., one for which L = A, the diameter of the circular locus would be zero and the induced magnetic moment would have a magnitude and a direction that are independent of heading and always directed toward magnetic north.

One can derive a simple expression for the maximum deviation of a submarine's induced magnetic moment from magnetic north. From equation (21), it can be seen that the radius R of the circular locus is

$$R = D/2 = 1/2\, (L - A)\, H_H\, T. \tag{22}$$

From figure 7 and equations (20) and (22) it is seen that the distance d from the origin to the center of the circle is

$$d = A\, H_H\, T + 1/2\, (L - A)\, H_H\, T = 1/2\, (L + A)\, H_H\, T. \tag{23}$$

The angle of maximum deviation of M_{HI} from magnetic north is therefore

$$\varphi_{max} = \arcsin\, (R/d) = \arcsin\, [(L-A)/(L+A)]. \tag{24}$$

For the case illustrated in figure 7,

$$\varphi_{max} = \arcsin\, [(11.5 - 3.0)/(11.5 + 3.0)] = 35.9°. \tag{25}$$

Thus for a submarine whose coefficients for its longitudinal and athwartship components of magnetic moment are 11.5 and 3.0 ft^3/ton, respectively, the horizontal component of induced magnetic moment will not deviate from magnetic north by more than 35.9° regardless of the submarine's heading.

In principle, at least, one could work the problem backwards and infer the submarine's heading, with a four-fold ambiguity, from the measured direction of the

submarine's magnetic moment, assuming that (1) the direction of the horizontal moment vector can be inferred from measurements of the magnetic anomaly, (2) the coefficients L and A are known (or determinable) for the particular class of submarine, and (3) there is no permanent horizontal component of magnetic moment. If these conditions obtain, the data of figure 7 can be used to relate submarine heading to the direction of the horizontal component of magnetic moment as shown in figure 8. Consider, for example, the case in which the "observed" direction of the horizontal moment is 20° magnetic. Four different submarine headings (28°, 82°, 208° and 262°) could give rise to such an observed direction; however, if the magnitude of the vector is also considered, the uncertainty could be reduced to a two-fold 180° ambiguity.

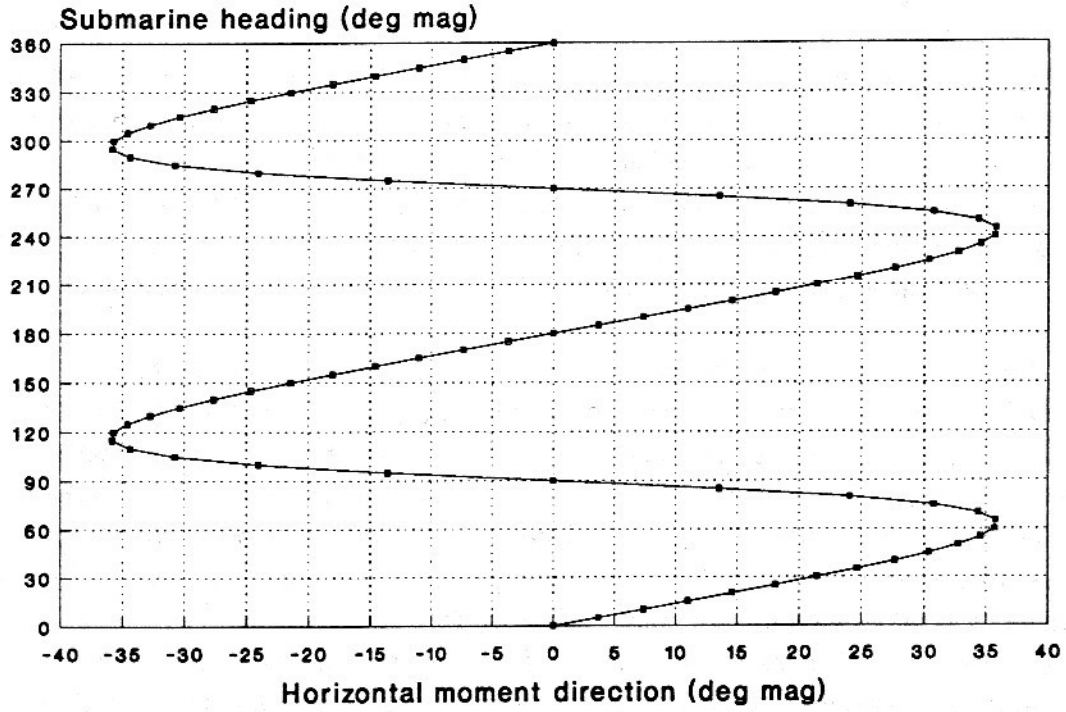


Figure 8. Inference of submarine heading from the direction of the induced horizontal moment vector.

CASE II. Horizontal Permanent Moment Considered as a Parameter.

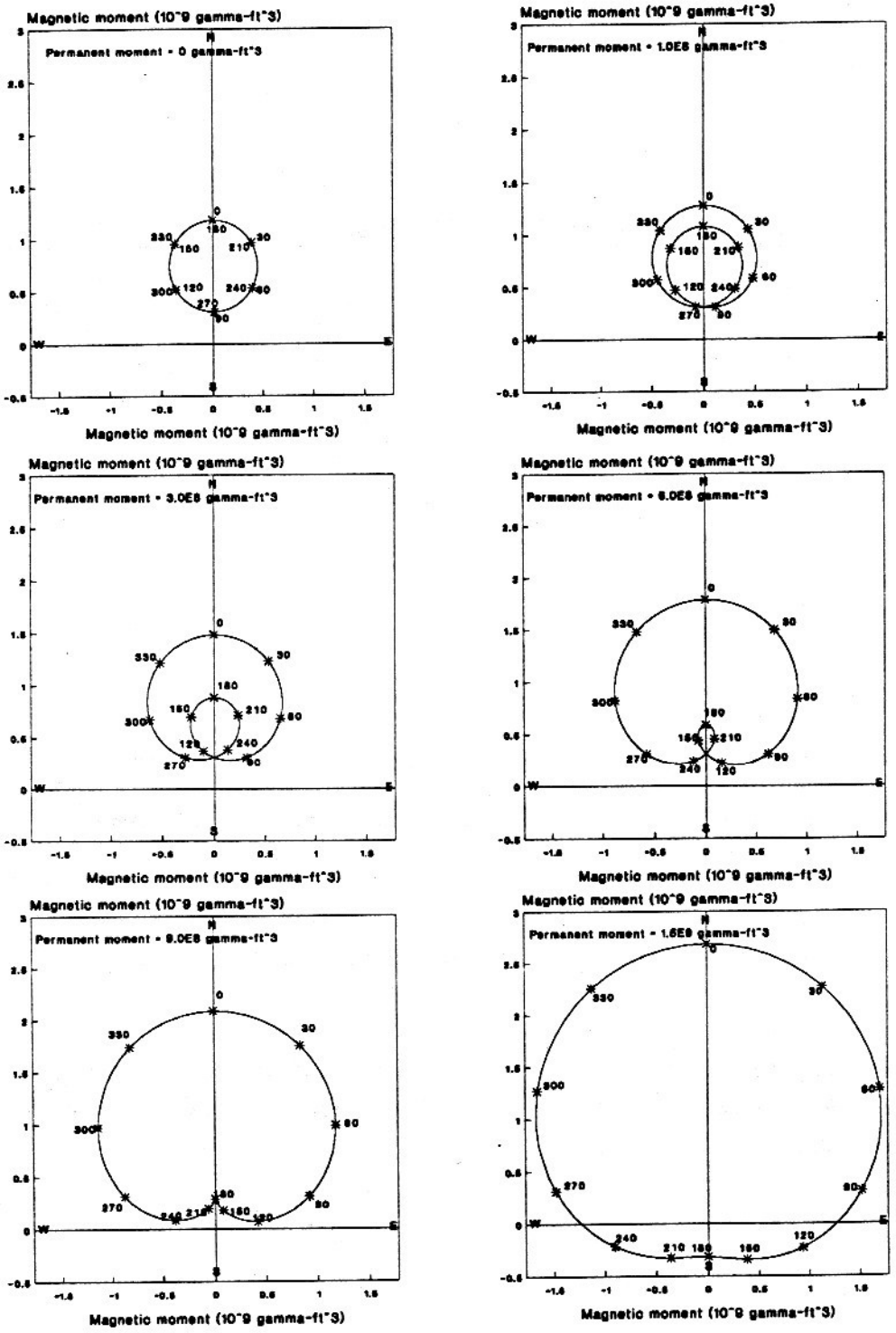
Equations (12) and (13) are now applied to the previously described hypothetical situation of a KILO class submarine operating in the Gulf of Oman at 25°N, 58°E. In this illustrative example, parametric values are assigned to the longitudinal permanent magnet

moment M_{LP}, northerly and easterly components of the horizontal moment are calculated as a function of true heading, and the northerly components plotted as a function of the easterly components to produce limaçons depicting the loci of the resultant vectors.

Figure 9 illustrates the evolution of the loci as the permanent longitudinal moment takes on successive values of 0, $1x10^8$, $3x10^8$, $6x10^8$, $9x10^8$, and $1.5x10^9$ gamma-ft^3 for the case of a maximum induced longitudinal moment ($L H_H T$) of $1.18x10^9$ gamma-ft^3 and a maximum induced athwartship moment ($A H_H T$) of $3.1x10^8$ gamma-ft^3. In this example, the permanent athwartship moment is assigned a value of zero; that is, the permanent horizontal moment is assumed to lie along the longitudinal axis of the submarine. The first graph in figure 9 is substantially the same as figure 7 except that figure 9 is plotted in true geographic coordinates whereas figure 7 is plotted in magnetic coordinates. The difference is the geomagnetic declination of 1.1°E at the selected location. The effect is to rotate the plots in figures 9 clockwise 1.1° relative to figure 7.

Increasing the permanent longitudinal moment produces two very obvious effects: (1) For most headings, the horizontal moment increases as illustrated by the increase in size of the locus; (2) The angle subtended at the origin by the limaçon increases with increasing permanent moment; when the permanent longitudinal moment exceeds the maximum induced longitudinal moment, the angle becomes 360° and the resultant horizontal moment could even take on a southerly direction although its magnitude might be quite small.

From the data used to produce figure 9, the maximum angles of deviation of the horizontal moment vector from magnetic north were computed and plotted in figure 10 as a function of the ratio of permanent longitudinal moment to maximum induced longitudinal moment. Physically, it is very unlikely that the permanent moment would ever exceed, or even equal, the corresponding maximum induced moment without some human contrivance. It is most likely that the permanent longitudinal moment will not exceed about 25% of the maximum induced longitudinal moment. Schneider (reference (c)) assumes that the permanent longitudinal moment will not exceed the maximum athwartship induced moment or, according to his model, 1.00/4.19 = 24% of the induced longitudinal moment. In the model being used here (reference (b)), this ratio equals 3.0/11.5 = 26%. If these criteria are applied, it appears that the maximum deviation angle will always be less than 50°.



Tick marks indicate submarine heading in degrees true.

Figure 9. Loci of magnitude and direction of horizontal component of induced and permanent magnetic moment of a 3000-ton submarine at location 25°N, 58°E as a function of submarine heading for permanent longitudinal moments of 0, $1x10^8$, $3x10^8$, $6x10^8$, $9x10^8$, and $1.5x10^9$ gamma-ft^3.

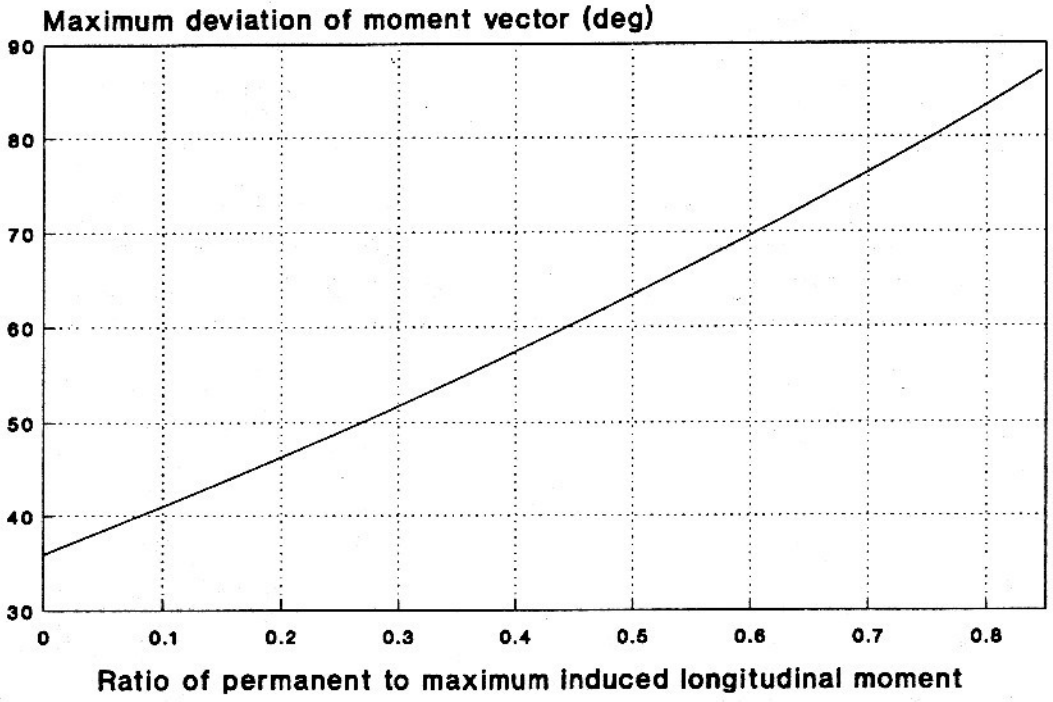


Figure 10. Maximum deviation of the horizontal moment vector from magnetic north vs. the ratio of permanent to maximum induced longitudinal moment.

In summary, the horizontal magnetic moment vector of an untreated submarine points in a general northerly direction from about 310° to 050° magnetic regardless of the submarine's heading.

V. MAGNETIC FIELD AND ANOMALY FROM A FERROMAGNETIC DIPOLE

A glossary of symbols with their definitions and units is given in Appendix A. Appendix B provides the reference framework for derivations given in subsequent appendices.

Point Dipole

The vector field produced by a point magnetic dipole is given in Section III (equation (1)) by the expression

$$\mathbf{B} = - \mathbf{M}/R^3 + (3\ \mathbf{M}\cdot\mathbf{R})\ \mathbf{R}/R^5. \tag{26}$$

It would be desirable to expand equation (26) into three equations giving the components of magnetic induction from the submarine in earth-fixed coordinates.

To establish a reference frame that is fixed to the earth, a coordinate system is set up with its origin at the sea surface and its x, y, and z axes directed east, north and vertically upward, respectively. Let X_s, Y_s, and Z_s be the coordinates of the submarine (i.e, the center of the dipole) and X, Y, and Z be the coordinates of the point where the magnetic field is to be determined (i.e., the location of the sensor). Thus, the easterly, northerly, and vertically upward components of the magnetic induction from a point dipole, as derived in Appendix C, are respectively

$$B_{Dx} = \{3\ [M_x\ (X-X_S) + M_y\ (Y-Y_S) + M_z\ (Z-Z_S)]\ (X-X_S) - M_x\ R^2\}\ /R^5 \tag{27}$$

$$B_{Dy} = \{3\ [M_x\ (X-X_S) + M_y\ (Y-Y_S) + M_z\ (Z-Z_S)]\ (Y-Y_S) - M_y\ R^2\}\ /R^5 \tag{28}$$

$$B_{Dz} = \{3\ [M_x\ (X-X_S) + M_y\ (Y-Y_S) + M_z\ (Z-Z_S)]\ (Z-Z_S) - M_z\ R^2\}\ /R^5. \tag{29}$$

where

$$R = [(X-X_s)^2+(Y-Y_s)^2+(Z-Z_s)^2]^{1/2}. \tag{30}$$

The magnitude B_D of the magnetic induction from a point dipole follows from equations (27) through (29) and the Pythagorean theorem as

$$B_D = (B_{Dx}^2 + B_{Dy}^2 + B_{Dz}^2)^{1/2} \tag{31}$$

Equations (27) through (30) provide the means for calculating three orthogonal components of the magnetic induction at any remote position caused by a point dipole.

However, the signal sensed by a total-field-measuring magnetometer (i.e., the scalar magnetic field) is not that given by equation (31) but rather the magnitude of the vector sum of the field produced by the dipole and the (much larger) magnetic field of the earth. The magnetic "anomaly" is the difference between magnitude of the earth's magnetic field with the dipole present and its magnitude without the dipole present. If the easterly, northerly, and upward components of the earth's magnetic field (obtainable, for example, from exercising the IGRF model) are represented, respectively, by B_{Ex}, B_{Ey}, and B_{Ez}, and the magnitude of their resultant is B_E, the anomaly Γ from a ferromagnetic dipole can be calculated from the expression:

$$\Gamma = [(B_{Dx}+B_{Ex})^2 + (B_{Dy}+B_{Ey})^2 + (B_{Dz}+B_{Ez})^2]^{1/2} - B_E. \qquad (32)$$

Alternatively, as shown in Appendix H, the anomaly Γ can be calculated to a very good approximation as the component of the dipole field along the earth's field vector as follows:

$$\Gamma \approx (B_{Dx}\, B_{Ex} + B_{Dy}\, B_{Ey} + B_{Dz}\, B_{Ez}) / B_E. \qquad (33)$$

The formalism of equations (27) through (33) allows calculations to be made for the submarine (represented as a point dipole) and the sensor aircraft assuming any position in space relative to fixed geographical and geomagnetic references. (However, a flat earth is assumed.) The submarine and sensor coordinates can be expressed as functions of time, thereby enabling a dynamic situation in which both the submarine and sensor are moving. The heading of the submarine is contained implicitly in the northerly and easterly components of magnetic moment M_N and M_E (equations (12) and (13)). Although the model can accommodate changes is submarine depth during a run, it is assumed that the submarine is level during an encounter and that there is no roll, pitch or yaw motion. Similarly, the model can handle changes in aircraft heading and/or altitude during a run; however, for the examples presented in this report, headings and altitudes were not varied during runs.

It is a common practice, in calculations of magnetic moments of submarines from measured anomalies and in calculations of MAD detection ranges from known submarine magnetic moments, to truncate equation (26) to the simple scalar equation

$$B \approx M / R^3. \qquad (34)$$

Comparing equations (26) and (34) shows that the latter gives the same magnitude as the former for the magnetic induction along the perpendicular bisector of the dipole (i.e., for which $\mathbf{M}\cdot\mathbf{R} = 0$), twice the magnitude along the dipole axis (i.e., for which $\mathbf{M}\cdot\mathbf{R} = MR$), and a continuum of intermediate values for other angles.

To illustrate the foregoing, figure 11 provides twelve plotted examples of the magnetic anomaly produced in the earth's field by a point magnetic dipole from equation (33) and, for comparison, plots of equation (34) for the arbitrary set of conditions described below. Graphs of equation (34) always exhibit a simple concave-downward curve with a single maximum; graphs of magnetic anomalies (e.g., equation (33)) may exhibit one, two, or three extrema.

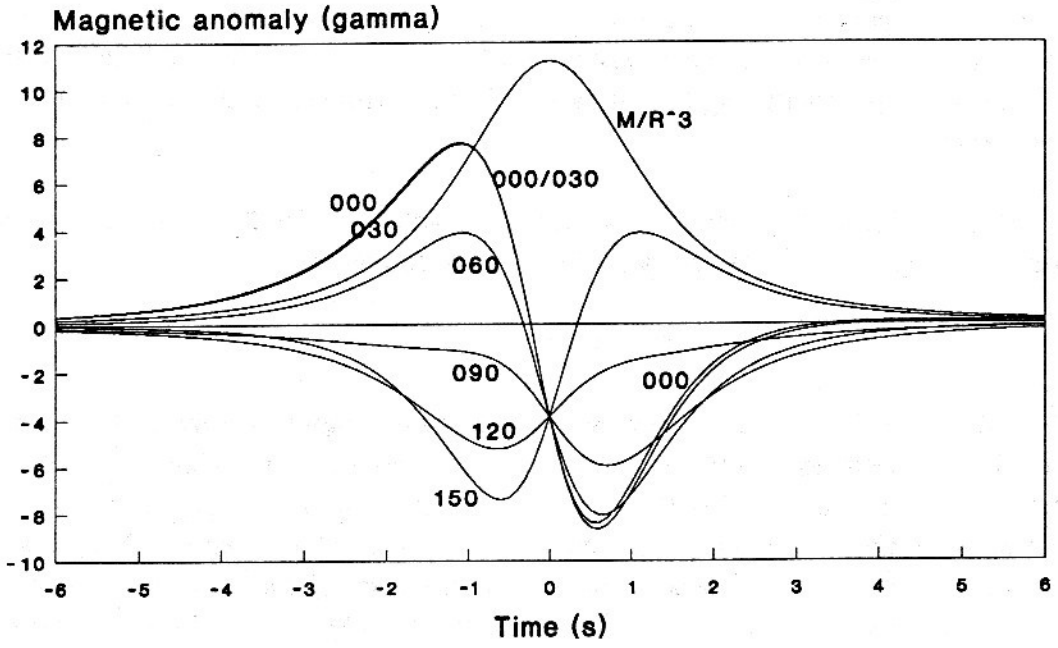
One can arrive at a quick estimate of the magnetic moment M of a submarine from measured data by use of equation (34), which may be rewritten as

$$M \approx B\,R^3, \tag{35}$$

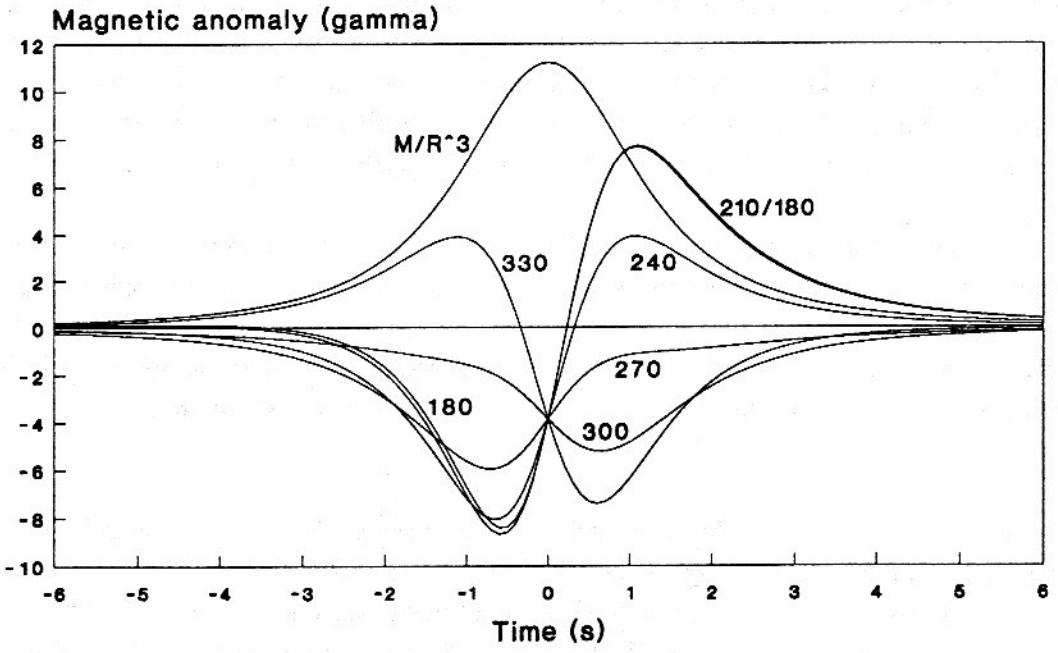
in which B is taken as the peak-to-peak magnitude of the magnetic anomaly (or the peak magnitude if only one extremum exists) and R is the minimum slant range to the target. To illustrate the use of equation (35), the magnetic anomalies plotted in figure 11 were calculated for twelve aircraft course directions directly over a hypothetical KILO-class submarine on a 30-degree true heading in the Gulf of Oman. For all cases the magnetic moment had a constant value $M = 1.405 \times 10^9$ gamma-ft^3. The aircraft altitude was assumed to be 300 ft and the submarine depth was taken as 200 ft. The submarine was assumed to behave as a point dipole. Equation (35) was then applied to the data used in preparing figure 11 and values of M were calculated using this simplified formula and plotted as a function of aircraft course direction in figure 12. A cosine squared curve was fitted to the twelve points. Figure 12 shows that the value of M obtained by use of equation (35) varies about the correct value of M, departing from it by a maximum of 53%. In this illustrative example, for aircraft course directions of about 60°, 150°, 240°, and 330°, equation (35) gives the correct answer.

If the data used to prepare figure 11 are examined, it is noted that the separation in time between each maximum and its corresponding minimum is 1.7 s. Anomaly values were calculated for intervals of 0.1 s and the simulated aircraft speed was set at 300 ft/s. Thus, the separation between extrema is 510 ft, which is very close (i.e., within the 30-ft resolution of the calculations) to the minimum slant range to the target on each of the passes for which two extrema were obtained.

To investigate further the relationship between separation of extrema and the slant range at CPA, magnetic anomalies were calculated for 15 aircraft passes on a true north course directly over the submarine at vertical separations ranging of 100 to 1500 ft. The separation between the extrema was then plotted in figure 13 as a function of the aircraft-to-target vertical separation and a straight line was fitted to the plotted points. Figure 13 shows that, to within the resolution of the calculations, the separation between the extrema equals the minimum aircraft-to-target separation on each pass. This implies that operationally one could determine the distance of the target from the flight path from an examination of the target signature for cases in which two extrema appear.



(a)



(b)

Figure 11. Magnetic anomalies calculated for a point dipole for twelve sensor aircraft course directions over the target.
(a) Aircraft course directions 000, 030, 060, 090, 120 and 150 degrees true.
(b) Aircraft course directions 180, 210, 240, 270, 300 and 330 degrees true.

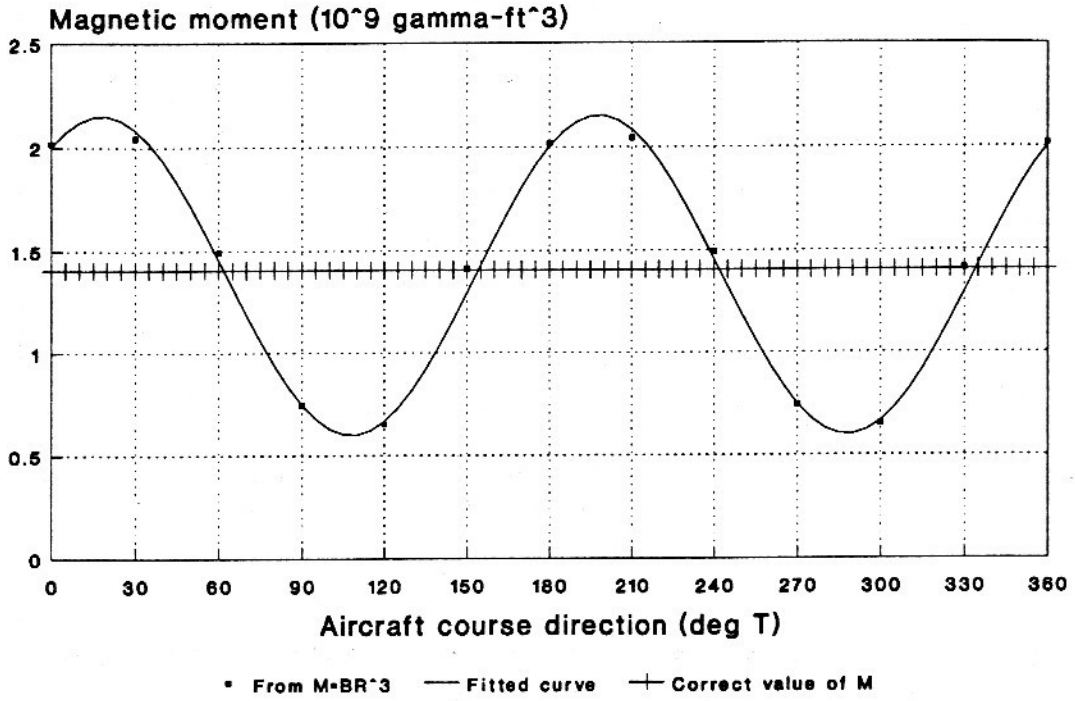


Figure 12. Comparison of values of magnetic moment obtained with the simple formula $M = B R^3$ to the correct values for a point dipole as a function of sensor course direction.

For cases in which only a single extremum occurs in the anomaly (e.g., in east-west crossings), the width of the anomaly is similarly a function of minimum distance to the target. If the first derivative of such a signature is taken with respect to position along the aircraft path, a convenient metric of signature width is obtained. The separation between extrema of the derivative curve corresponds to about 85% of the slant range at CPA.

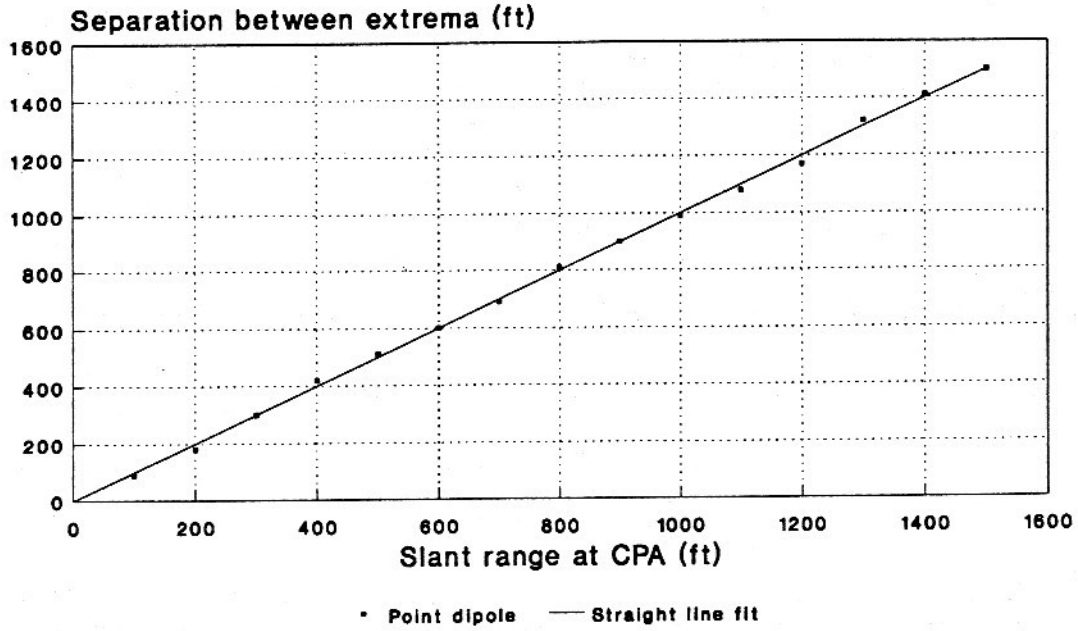


Figure 13. Separation between extrema of anomaly from a point ferromagnetic dipole as a function of minimum sensor-to-target slant range.

It is recognized that the foregoing calculations were performed for specific, although arbitrary, cases. A more general approach would be to derive a single equation for the anomaly from a point ferromagnetic dipole, take the first derivative of it with respect to sensor position along its path, and set the derivative to zero to obtain a function giving the locations at which extrema exist.

Failure of Point Dipole Assumption at Short Range

In the derivation of expressions for the magnetic field, one usually makes the simplifying assumption that the dimensions of the source are very small in comparison to the distance at which the field is observed. This is true regardless of whether the field is considered to originate from a current-carrying loop or from two poles of opposite polarity. This assumption is inherent in equation (26). For observation distances that are not at least several times greater than the dimensions of the magnetic source, the point dipole assumption breaks down. In general, if one is interested only in detecting the magnetic anomaly produced by a submarine, this is not important. However, if one is concerned with modeling and analyzing magnetic signatures, and if the data being analyzed were obtained at distances about equal to the length of a submarine, significant errors could occur. Indeed, these errors could result in larger than correct ranges to the target and larger than correct values of target

magnetic moment. In addition, such errors could easily mask, at short range, other more subtle effects, such as the field from the steady galvanic corrosion currents. One can obtain a better fit of measured data of the magnetic field in close proximity to a submarine by assuming that the field does not originate from a single point dipole but rather from any one of the following: (1) a distribution of point dipoles within the boundaries of the submarine, (2) a single point dipole at the center of the submarine, plus correction terms consisting of a suitable set of point multipoles, (3) a prolate spheroidal "dipole" with approximately the same outer dimensions as the submarine plus correction terms consisting of a suitable set of prolate spheroidal multipoles, and (4) a prolate spheroidal "dipole" plus correction terms consisting of a set of point dipoles.

The problem of modelling the magnetic field of a submarine is analogous to that of modelling the magnetic field of the earth, as discussed in Section III. As in the case of the earth, one can model to any desired degree of accuracy at the price of increasing complexity. For measurements of submarine magnetic signatures from large fixed-wing aircraft, it is unlikely that the separation between aircraft and submarine will ever be less than about 200 ft, or perhaps 35% of the length of a large submarine. Because this separation will always be large compared to the relatively small vertical and athwartship dimensions of a submarine, one could assume that these components of the magnetic moment can be treated as point dipoles. However, as the ability to analyze magnetic signatures improves, the same may not apply to the longitudinal component of the moment. To address such a situation, it may be necessary to invoke more complicated models.

Perhaps the next more complicated model might be to assume the existence of two magnetic poles separated by a finite distance equal to some large fraction of the length of the submarine. In Appendix D, an expression is derived for the components of the magnetic induction produced by a ferromagnetic dipole of arbitrary length, location, and orientation. The concluding equations from Appendix D are presented here:

$$B_{Dx} = (MX - MX_S - 1/2\, M_x d)/(D_1 d) - (MX - MX_S + 1/2\, M_x d)/(D_2 d) \quad (36)$$

$$B_{Dy} = (MY - MY_S - 1/2\, M_y d)/(D_1 d) - (MY - MY_S + 1/2\, M_y d)/(D_2 d) \quad (37)$$

$$B_{Dz} = (MZ - MZ_S - 1/2\, M_z d)/(D_1 d) - (MZ - MZ_S + 1/2\, M_z d)/(D_2 d) \quad (38)$$

in which

$$D_1 = [(X-X_S-1/2M_x d/M)^2 + (Y-Y_S-1/2M_y d/M)^2 + (Z-Z_S-1/2M_z d/M)^2]^{3/2} \quad (39)$$

$$D_2 = [(X-X_S+1/2M_x d/M)^2 + (Y-Y_S+1/2M_y d/M)^2 + (Z-Z_S+1/2M_z d/M)^2]^{3/2}. \quad (40)$$

Equations (36), (37), and (38) are the extended dipole counterparts of point dipole equations (27), (28), and (29), respectively. The only new parameter introduced here is the dipole length d. For values of d that are very small in comparison with the target-to-sensor slant range, both sets of equations yield equal output values. Equation (32) or (33) can be used with equations (36) through (40) to calculate the anomaly from an extended ferromagnetic dipole.

Figure 14 illustrates how, for an assumed set of conditions, the observed magnetic anomaly from a longitudinal moment of magnitude 1 x 10^8 gamma-ft^3 would depend upon the separation of the poles for an aircraft pass directly overhead along the length of the submarine at a vertical separation of 250 ft. Curves are given for a point dipole and for dipoles of length 100, 200, 300, 400 and 500 ft.

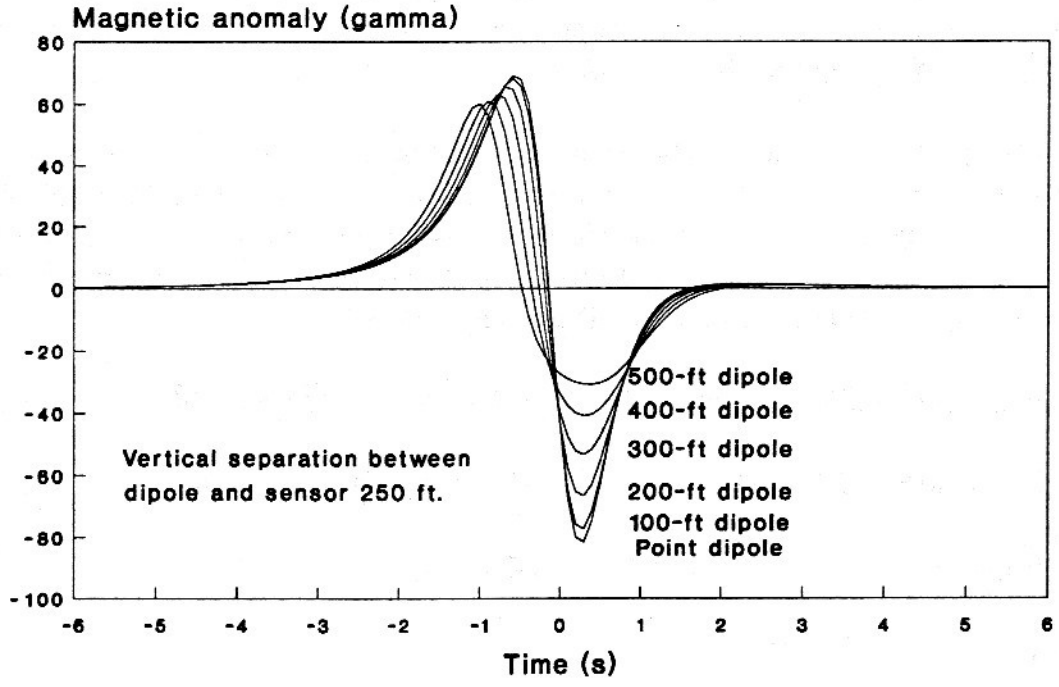


Figure 14. Dependence of calculated magnetic anomaly signature on assumed dipole length for constant magnetic moment.

For a pole separation of 100 ft, there is a reduction in peak value of about 5% relative to the point dipole. (Because magnetic moment equals the product of pole strength and pole separation, and because the magnetic moment is assumed constant in all cases, the pole strength decreases as pole separation increases.) As the separation of the poles increases, the peak values decrease further, and the distance between the respective maxima and minima become nearly equal to the pole separation. The falloff rate with distance decreases gradually from an inverse cube dependence to inverse square. (It is interesting to note that, for the particular geometry assumed in figure 14, the separation between the maximum and the minimum equals, to a very good approximation, the square root of the sum of the square of the dipole length and the square of the slant range at the point of closest approach.) For the case of a point dipole, the distance between the maximum and the minimum equals approximately the distance between the target and the sensor at the point of closest approach.

Another model that could be used if more rigor would be required to describe signatures adequately would be to assume that the submarine behaves as a uniformly magnetized solid prolate spheroid. In this case, the magnetic properties of the submarine can be described equivalently in terms of a dipole distribution whose linear density varies as a function of position along the longitudinal axis of the submarine as illustrated in figure 15. In this case, the magnetic moment integrated along the length of the submarine is 1×10^9 gamma-ft^3.

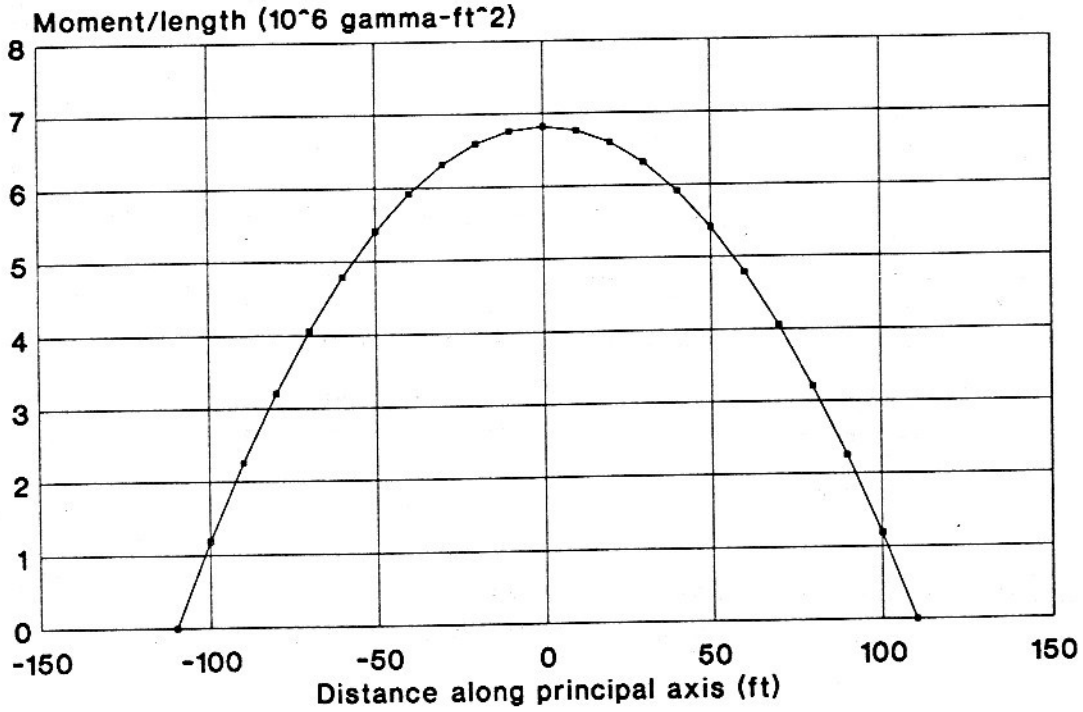


Figure 15. Linear density of magnetic moment for a prolate spheroidal dipole as a function of position along the dipole axis.

Data taken from reference (e) were used in preparing figure 16, which shows how calculated peak values of the magnetic anomaly differ from a reference values depending on observation distances and the properties of the assumed source. Three sources are considered in addition to an assumed correct source: a point dipole, a uniformly magnetized solid prolate spheroid, and a two-pole, uniformly magnetized solid cylinder. For distances greater than five target lengths to the side (or above) the target, all agree within about one percent. However, at distances of one target length, peak signals calculated from the point dipole model exceed the reference signal by 29% whereas the other models deviate by about only 6%, one overestimating and the other underestimating. Accordingly, it appears that a correct description would be one intermediate between the distributed moment of the spheroidal source and the two-pole cylinder source. In this study, both the point dipole model and an extended dipole model are used to describe the magnetic induction from a ferromagnetic dipole.

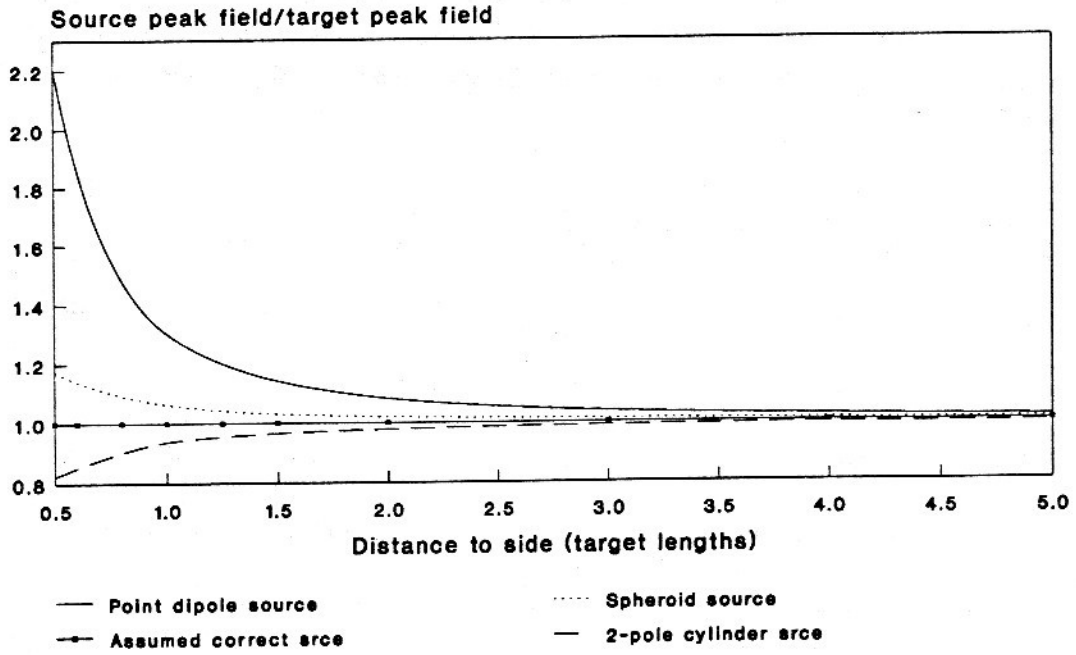


Figure 16. Ratios of magnetic field values referenced to a ferromagnetic source assumed to be a correct representation of a submarine as a function of distance for three types of sources.

VI. MAGNETIC FIELD AND ANOMALY FROM A STEADY HORIZONTAL ELECTRIC CURRENT ELEMENT

As indicated in Section I, a submarine immersed in sea water behaves like a short-circuited galvanic cell. The bronze propeller is the positive terminal, the sacrificial zincs are the negative terminal, the sea water is the electrolyte, and the propeller drive shaft and bearings and the submarine structure are the "external" circuit. The positive terminal is fairly well defined; however, the negative terminal is distributed along the length of the submarine, giving rise to a complicated current pattern. The conventional current flows from the propeller, through the drive shaft, bearings, and hull, and then through the water back to the propeller. The current density in the water is greatest in the region between the propeller and the hull, and decreases gradually with increasing distance from the stern. The amount of spreading of the current through the water varies inversely as the conductivity of the water.

The magnetic induction arising from an infinitesimal electric current element is given in vector form by the Biot-Savart law:

$$\mathbf{dB} = \mu_0 i/(4\pi)\ (\mathbf{dl} \times \mathbf{R}/R^3) \qquad (41)$$

in which **dB** is the contribution to the magnetic induction at some point P at a distance R from a conductor of length and direction given by the vector **dl**, which carries a current i. See figure 17. The radius vector **R** is directed from **dl** to point P. The permeability constant μ_0 has the value $4\pi \times 10^{-7}$ weber/(A·m). As the vector (cross) product $(\mathbf{dl} \times \mathbf{R}/R^3)$ indicates, the direction of **dB** is perpendicular to both **dl** and **R** and its magnitude is proportional to the sine of the angle between vectors **dl** and **R**. In contrast to the ferromagnetic dipole field, this field consists of a series of rings having the longitudinal axis of the submarine as their axis and directed upward on the port side and downward on the starboard.

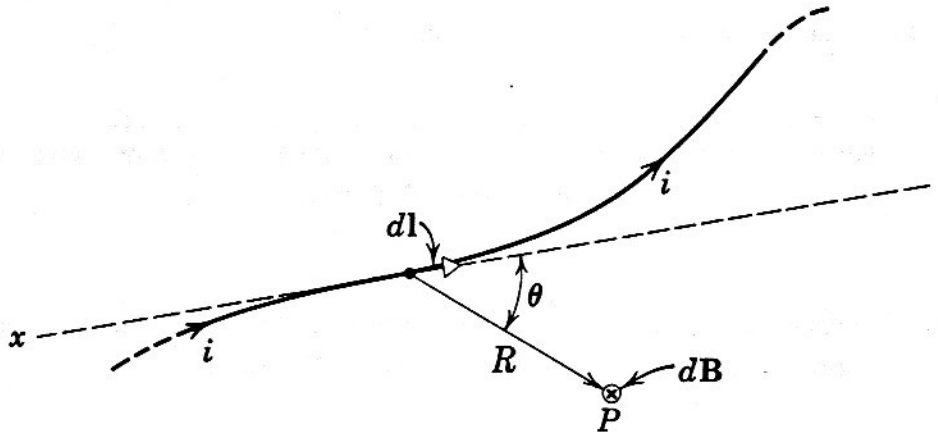


Figure 17. Biot-Savart law for the magnetic induction from an infinitesimal electric current element.

By sacrificing directional information, equation (41) can be recast in scalar form as

$$B = (100\ IL \sin\theta) / R^2 \qquad (42)$$

in which B is the magnitude of the magnetic field in gamma (nT) at a distance R from a current element p = IL (a straight conductor of length L (meter) carrying a current I (ampere); θ is the angle between the positive direction of IL and the point of observation P.

Figure 18 is a plot of the magnitudes of three orthogonal components of the magnetic induction produced by a steady horizontal electric current dipole of moment 100 A·m along the direction of a straight-line horizontal path perpendicular to the dipole axis at a minimum separation of 500 ft calculated by use of the Biot-Savart law. The dipole is assumed to be aligned parallel to the x-axis and the magnetometer is assumed to be moving parallel to the y-axis, with the positive direction being from starboard to port. The z-axis is directed vertically upward. (Note that figure 18 shows the magnetic induction from the current dipole only; it is not the anomaly produced in the earth's magnetic field by the dipole.)

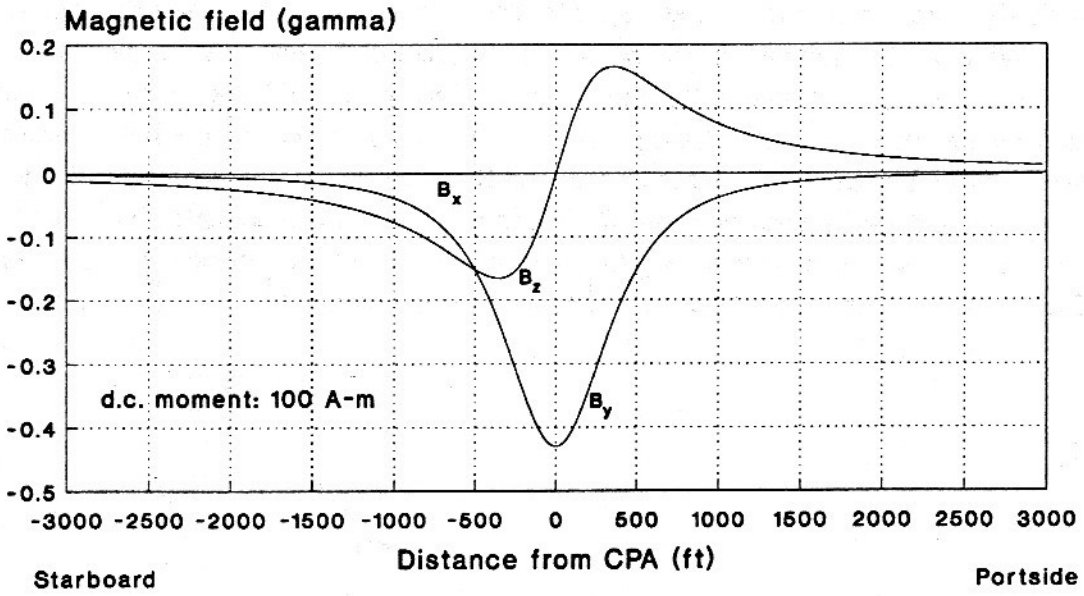


Figure 18. Orthogonal components of the magnetic induction from an infinitesimal horizontal electric current element calculated by use of the Biot-Savart law.

A few sample calculations permit a comparison of the magnitude of the electric current dipole field with that of the ferromagnetic dipole magnetic field. Suppose there is an electric current I = 10 A flowing through the drive shaft between the propeller and the hull. Because the current through the hull drops off with distance from the propeller, the effective length of the current moment may be only about 0.3 L. (Conversely, one could say that the average current along the entire length of the hull is 3 A.) Thus, from equation (42), the resulting magnetic induction at a distance of 500 ft (152.4 m) from a submarine of length L = 100 m along the perpendicular bisector of IL would be

$$B = 100\ IL/R^2 = 100 \times 10 \times 30 / 152.4^2 = 1.29 \text{ gamma.} \qquad (43)$$

For comparison, at the same point, the magnitude of the field from a ferromagnetic dipole of moment $M = 1 \times 10^9$ gamma-ft^3 (2.83×10^7 nT·m^3) would be (from equation (34))

$$B = M/R^3 = 1 \times 10^9 / 500^3 = 8.00 \text{ gamma.} \qquad (44)$$

Because the field from the ferromagnetic moment varies as R^{-3} whereas that from the electric current element varies more gradually as R^{-2}, a crossover occurs beyond which the electric current effect is larger. By setting equation (42) equal to equation (34) and solving for R (being careful to convert to consistent units) we obtain for the assumed set of values

$$R = M / (100\ IL \sin\theta) = 2.83 \times 10^7 / (100 \times 10 \times 30) = 943.9 \text{ m} = 3097 \text{ ft.} \qquad (45)$$

Unfortunately (for exploiting magnetic fields from steady galvanic currents), at this range the magnetic field is down to 0.034 gamma, which is unlikely to be detectable in flight.

The previous sample calculation is expanded in figure 19 to show the magnitude of the magnetic field, as a function of slant range, for three assumed values of ferromagnetic moment **M** and three assumed values of current moment **IL**. Figure 19 shows not only the rather pessimistic value calculated in the preceding paragraph but also others which may be feasible to measure; for example, for the case of a current moment of 3000 A·m and a ferromagnetic moment of 1×10^9 gamma-ft^3, the magnetic field from the current dipole exceeds that from the ferromagnetic dipole at all ranges greater than 310 ft and, at that range, has a detectable magnitude of 33.7 gamma.

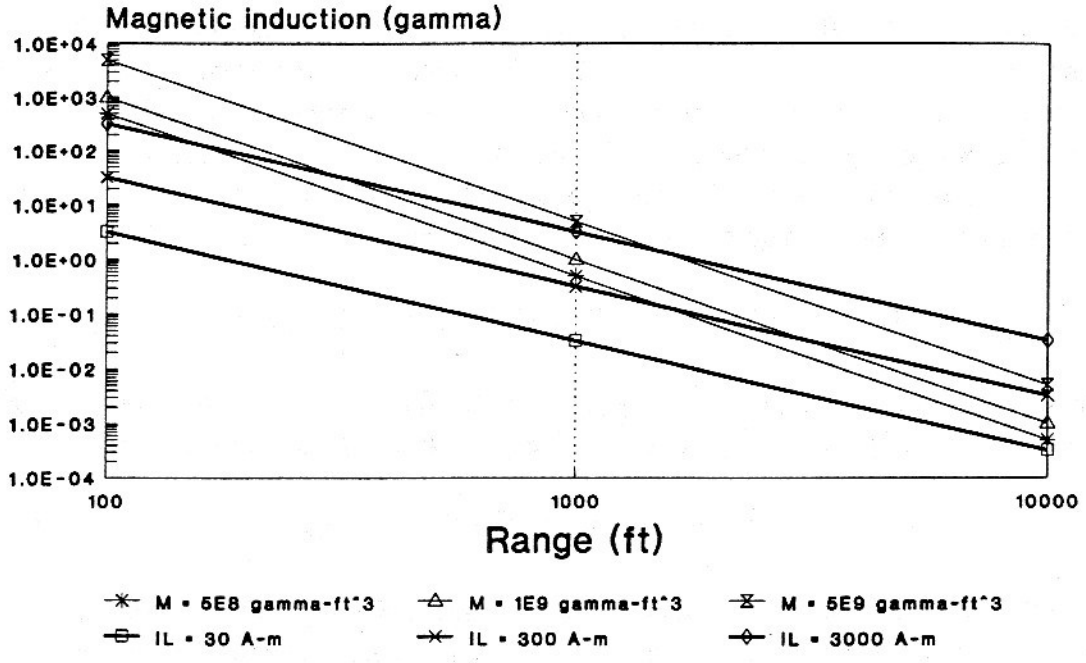


Figure 19. Comparison of magnetic induction from ferromagnetic moments and electric current moments as functions of range perpendicular to the dipole axes.

In Appendix E, equations are derived for three orthogonal components (east, north and vertically upward) of magnetic induction from an isolated electric current element by use of the law of Biot and Savart. These equations, which are presented here as equations (46), (47), and (48), are in the same compatible format as those describing the magnetic induction from point and extended ferromagnetic dipoles.

$$B_{CEx} = 1076.39\ p\ [(Z-Z_S)\cos\alpha)]/R^3 \tag{46}$$

$$B_{CEy} = -1076.39\ p\ [(Z-Z_S)\sin\alpha]/R^3 \tag{47}$$

$$B_{CEz} = 1076.39\ p\ [(Y-Y_S)\sin\alpha - (X-X_S)\cos\alpha]/R^3 \tag{48}$$

Equation (32) or (33) can be used with equations (46) through (48) to calculate the anomaly from an isolated electric current element.

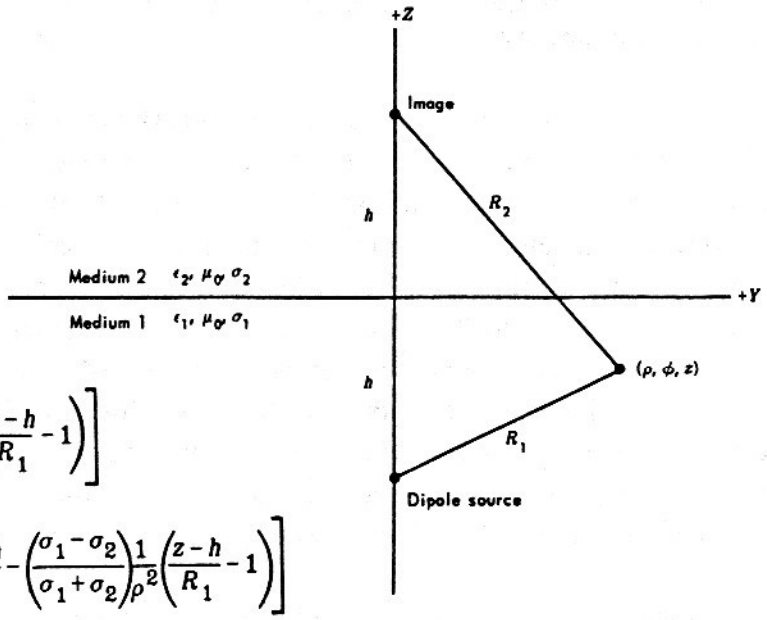
In the foregoing discussion, the magnetic field effects from the return current in seawater were ignored. Because the return current is equal and opposite to the current through the hull, certain components of the magnetic fields produced by each tend to cancel.

Indeed, if one applies Ampere's law along a closed path through which the net current is zero, the line integral of magnetic induction along that path equals zero. (The situation is analogous to a coaxial cable carrying equal and opposite currents in its two conductors; for a long coaxial cable, for which end effects can be disregarded, the magnetic field is confined to the space between the conductors and is not detectable outside the cable.)

Kraichman (reference (f)) provides equations that enable one to calculate the magnetic field in one semi-infinite medium (e.g., atmosphere) above another semi-infinite medium (e.g., sea) in which a horizontal current element is positioned on the z-axis at a distance -h below the interface, parallel to the x-axis and positively directed. See figure 20. Kraichman defines two distance parameters R_1 and R_2 in cylindrical coordinates as the

$$R_1 = \left[\rho^2 + (z-h)^2\right]^{1/2}$$

$$R_2 = \left[\rho^2 + (z+h)^2\right]^{1/2}$$



$$H_{\rho_2} = \frac{-p \sin\phi}{4\pi}\left[\frac{z-h}{R_1^3} + \left(\frac{\sigma_1-\sigma_2}{\sigma_1+\sigma_2}\right)\frac{1}{\rho^2}\left(\frac{z-h}{R_1} - 1\right)\right]$$

$$H_{\phi_2} = \frac{-p \cos\phi}{4\pi}\left[\frac{z-h}{R_1^3} - \left(\frac{\sigma_1-\sigma_2}{\sigma_1+\sigma_2}\right)\frac{z-h}{R_1^3} - \left(\frac{\sigma_1-\sigma_2}{\sigma_1+\sigma_2}\right)\frac{1}{\rho^2}\left(\frac{z-h}{R_1} - 1\right)\right]$$

$$H_{z_2} = \frac{p \sin\phi}{4\pi}\left(\frac{\rho}{R_1^3}\right)$$

Figure 20. Equations for the magnetic field above a semi-infinite conducting medium in which a static horizontal electric current dipole is immersed (from Kraichman, 1976).

distances to a field point P (ρ, φ, z) from, respectively, the current element in the lower medium and its image directly above it in the upper medium. Figure 20 illustrates the geometry and gives Kraichman's equations for three orthogonal components of the magnetic field in the upper medium (medium 2). The steady electric current moment p = IL and the electrical conductivities of medium 1 and medium 2 are σ_1 and σ_2, respectively. If the earth's atmosphere is taken as medium 2, its conductivity σ_2 may be taken as zero and the equations for the three components of magnetic field reduce to

$$H_\rho = -p/(4\pi) \sin\varphi \{(z-h)/R_1^3 + [(z-h)/R_1 - 1]/\rho^2\} \quad (49)$$

$$H_\varphi = p/(4\pi) \cos\varphi [(z-h)/R_1 - 1]/\rho^2 \quad (50)$$

$$H_Z = p/(4\pi) \sin\varphi [\rho/R_1^3] \quad (51)$$

It is interesting to note in equations (49), (50), and (51) that, for any given value of current moment p, the magnetic field is independent of seawater conductivity. (Of course, p is implicitly dependent upon conductivity.) It is also interesting to note in these equations that the altitude z of the field point (i.e., the sensor altitude) and the depth -h of the source point always appear in the combination of z-h. This means that the magnetic field in the air varies only with the vertical separation between the submarine and the sensor and not with depth and altitude separately.

After a conversion of magnetic field intensity H to magnetic induction B, equations (49) and (50) were used to plot in figure 21 the magnitudes of orthogonal components of the magnetic induction along a line parallel to the perpendicular bisector of the current moment. The conditions assumed in preparing figure 21 are identical to those assumed for figure 18. Both figures are plotted on the same scale to permit easy comparison. It is seen that the curves corresponding to B_x and B_z are the same in both cases. Indeed, it can be shown that equation (51) can be recast as the vertical component of equation (42). On the other hand, there is a significant difference between the curves for B_y in figures 18 and 21. The peak (negative) value for B_y obtained by use of the Biot-Savart law is twice as great as that obtained by applying Kraichman's equation (49). In addition, the plot of B_y in figure 18 does not reveal the two broad maxima appearing in the plot of B_y in figure 21.

Equation (49) can be expressed as the sum of two terms. The first of these corresponds to the relevant component of magnetic induction B_y obtained from the Biot-Savart law applied to an electric current element, that is, to the current flowing through the hull of the submarine. The second term corresponds to the magnetic field produced by the return current flowing through the seawater. Figure 22 shows the result of plotting these two terms separately, in addition to their algebraic sum, for the same set of conditions as figures (18) and (21). Note the broader maximum for the field from the return current, indicating that it is potentially detectable at greater distances abeam of the submarine than the field from the hull current. Use of the Biot-Savart law, i.e., assuming that the field arises solely from a simple isolated horizontal electric current element, could result in underestimating the magnitude of the magnetic field at the longer ranges while overestimating it at the shorter ranges.

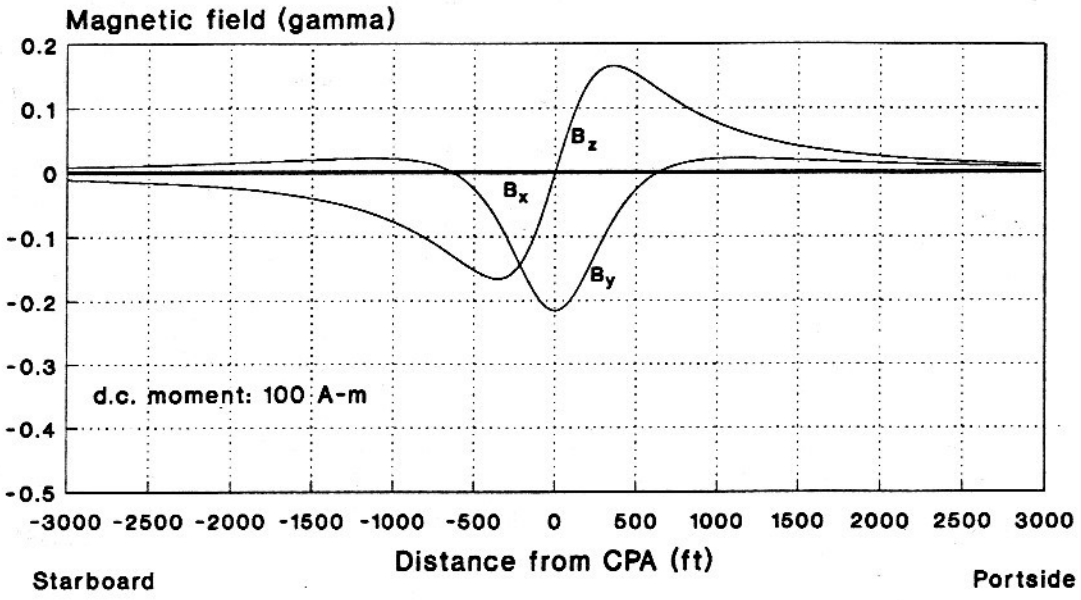


Figure 21. Orthogonal components of the magnetic field from a horizontal electric current element calculated by use of Kraichman's equations (3.24), (3.25), and (3.26).

In summary, the return current through the seawater reduces the peak magnitude of B(y) to 50% of the value produced by the current in the hull alone. However, because the seawater return current is spread out over a much larger conducting volume, the magnetic field it produces (of opposite polarity) may be detectable at longer ranges.

Figure 23 shows plots of B_y for three parallel flight paths over an electric current dipole in seawater at vertical separations of 250 ft, 500 ft, and 1000 ft. For any particular angle off axis, the values of these three functions vary in the proportion of 16:4:1, indicative of an inverse square law relation. This is most readily seen for the case in which the distance from CPA is zero.

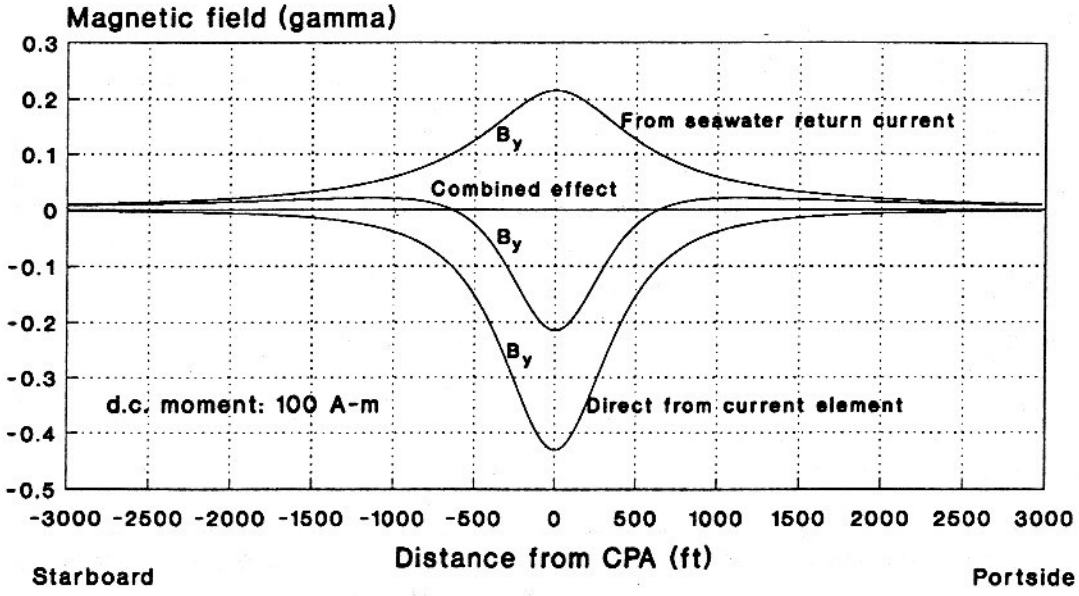


Figure 22. Magnetic field from a horizontal electric current dipole along a path perpendicular to the dipole axis showing the contributions from the hull current and the seawater return current.

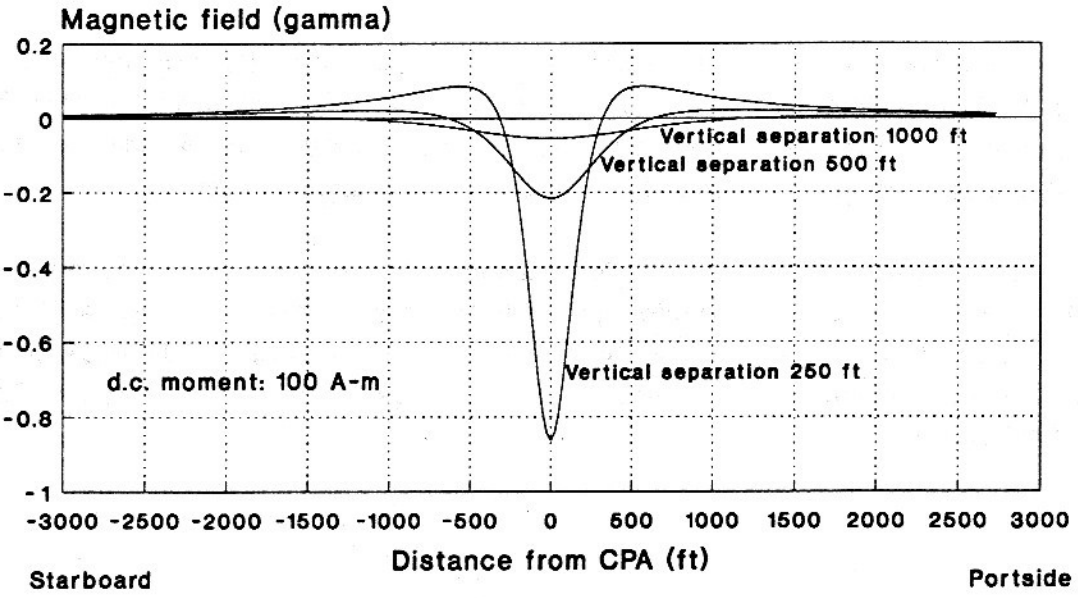


Figure 23. Magnetic field from a steady electric current dipole in seawater as a function of lateral range and vertical separation between source and sensor.

In Appendix F, Kraichman's equations are converted to an earth-fixed coordinate system and adapted to the same consistent framework used previously for calculating the magnetic induction from ferromagnetic dipoles.

Equations (52), (53), and (54), which are derived in Appendix F, give the east, north, and upward components of the magnetic induction (in gamma) in air in a coordinate system that is centered at an immersed horizontal steady electric current element for distances given in feet.

$$B_{CEx} = [(-1076.39\ p)/(Rr^2)]\{xy\ [z/R^2 + 2(z-R)/r^2] \sin \alpha + [(x^2-y^2)(z-R)/r^2 - zy^2/R^2] \cos \alpha\} \quad (52)$$

$$B_{CEy} = [(-1076.39\ p)/(Rr^2)]\{xy\ [z/R^2 + 2(z-R)/r^2] \cos \alpha - [(x^2-y^2)(z-R)/r^2 - zy^2/R^2] \sin \alpha\} \quad (53)$$

$$B_{CEz} = 1076.39\ py/R^3. \quad (54)$$

If, relative to an earth-fixed coordinate system (as used elsewhere in this report), the coordinates of the source are X_S, Y_S, and Z_S and the coordinates of the field point (i.e., the sensor location at any time t) are X, Y, and Z, the following substitutions should be made:

$$r = \rho = (x^2 + y^2)^{1/2} \quad (55)$$

$$R = (x^2 + y^2 + z^2)^{1/2} \quad (56)$$

$$x = X - X_s \quad (57)$$

$$y = Y - Y_s \quad (58)$$

$$z = Z - Z_s \quad (59)$$

VII. DESCRIPTION OF THE MODEL

The mathematical model presented in this report is a modular but integrated model which permits calculation of magnetic signatures of submarines in a consistent reference system and in consistent units. One can define a scenario in which a submarine of a particular class is assumed to be operating at or near certain geographical coordinates on a given date. To serve as an specific example in this report, it is postulated that the target will be a third-world, KILO-class submarine operating in the Gulf of Oman in the vicinity of 25°N, 58°E on 1 June 1996. One then uses any one of several models (such as the IGRF) to calculate the components of the earth's magnetic field and applies that information to calculating the east, north, and upward components of the submarine's magnetic moment in that operating area as a function of submarine heading. (If such submarine data are already known independently, they may be used directly.) Next, one establishes a right-handed Cartesian coordinate system with its positive x-axis directed toward true east, its positive y-axis directed toward true north, and its positive z-axis directed vertically upward. The x-y plane is located at the ocean surface, which is assumed to be flat.

A glossary of symbols used in the appendices and their definitions and units are given in Appendix A. The positions of the target submarine and the sensor aircraft are expressed as simple linear functions of time in terms of their position coordinates at time zero, their speeds, and heading/course direction and ascent rates as described in Appendix B. In most cases, both the submarine and the aircraft are assumed to move at constant velocity (speed and direction) in any given run; however, to investigate "gradient noise" from the movement of the aircraft through the earth's magnetic field, the motion of the aircraft can be modified to simulate changes in altitude and course that could occur under gusty flying conditions.

The orientation of the submarine is described in terms of its true heading whereas the orientation of the aircraft is given in terms of its true course direction. This is done because heading is the relevant factor in determining the induced magnetic moment of the submarine; on the other hand, because the observed magnetic signature is independent of the orientation of the sensor but dependent upon its path through the anomaly, course direction is a relevant descriptor of the aircraft motion. While it is true that the actual path traveled by the submarine during an aircraft encounter is relevant, the difference between submarine heading and course direction will have negligible significance during the brief encounter period (about 10 s) of a slow-moving submarine.

Two approaches are given for calculating the magnetic induction arising from the ferromagnetic dipole moment of the submarine. In Appendix C, equations are derived for computing the three components of magnetic induction under the assumption that the submarine can be considered as a point dipole. This is a valid assumption provided the

separation R between the sensor and the target exceeds several target lengths. In Appendix D, similar but somewhat more complicated equations are derived to cover situations in which the point dipole assumption is not valid. In Appendix D, the equations for the components of magnetic induction are based on the assumption of an extended dipole consisting of a magnetic N-pole and an S-pole separated by a distance d, which may equal roughly 90% of the length of the submarine. If $d << R$, the extended dipole and point dipole equations yield equal results.

Two approaches are given for calculating the magnetic induction arising from the steady galvanic corrosion currents resulting from immersion of the submarine in seawater. In Appendix E, the submarine is assumed to behave as an isolated infinitesimal horizontal electric current element and the law of Biot and Savart is used to derive a set of equations that give the components of magnetic induction that result. The Biot-Savart law approach has been used by others to provide a relatively simple means for calculating approximate magnitudes. In this approach, only the current flowing through the submarine itself is considered and not the equal and opposite return currents through the seawater. In Appendix F, a more rigorous approach is taken which includes the effects of the seawater currents. In Appendix F, equations provided by Kraichman in reference (f) are recast into a form that is consistent with the rest of this report. In Appendices E and F, the electric current moment is tacitly assumed to be at the same location as the ferromagnetic dipole moment although the former is likely be within the aft third of the submarine and the latter about amidship.

As stated in Section III, the magnetic field of the earth plays a dual rôle: that of governing the magnetic moment of the submarine, and that of serving as the "carrier" for the magnetic anomaly of the submarine. In Appendix G, a procedure is developed in which the components of the earth's magnetic field over a region of space can be expressed in terms of three linear equations. These equations are referred to the same coordinate system as the positions of the submarine and the aircraft and the magnetic anomalies. In the specific example given in Appendix G, the magnetic field of the earth is calculable over a 1° by 1° "square" of latitude and longitude and over an altitude range of 0 to 1 nmi with a maximum error of 5 gamma relative to the IGRF model. The use of these equations in conjunction with the equations developed in Appendices C, D, E, and F for the magnetic induction from a submarine enable one to calculate the resultant vector magnetic induction of the earth-submarine combination as a function of geographical location.

The final aspect of the magnetic signature model is the calculation of the resultant vector of the magnetic induction of the earth, the magnetic induction from the ferromagnetic moment of the submarine, and the magnetic induction from the electric current moment of the submarine as a function of sensor position. This is accomplished, as shown in Appendix H, by simply adding the x, y, and z components of each of the three contributing vectors. The magnitude of the resultant vector can then be obtained by use of the Pythagorean

theorem. If only the anomaly is desired, and not the total field of earth and submarine, one need simply subtract the magnitude of the earth's field from the magnitude of the resultant. The foregoing is an exact method.

Appendix H gives, in addition, an approximate method of calculating the anomaly based on the assumption that the magnetic induction from the submarine will be very small in comparison with that of the earth. The derivation in Appendix H shows that to a very good approximation, the anomaly is equal simply to the component of the submarine's magnetic induction vector in the direction of the earth's magnetic induction vector.

VIII. EXERCISING THE MODEL

The model was programmed in Lotus 1-2-3, Release 2.3 to investigate the properties of the magnetic anomaly of a submarine and to illustrate the capabilities of the model. Because a vast number of combinations of input parameters is possible, it was decided to establish the set of arbitrary baseline conditions given in Table 1 and then to make variations on it.

TABLE 1. BASELINE PARAMETERS ASSUMED FOR COMPUTATIONS

Target Parameters	
Type	KILO-class submarine
Displacement (submerged)	3000 tons of seawater
Length	239.5 ft
Induced longitudinal moment coefficient	11.5 ft^3/ton
Induced athwartship moment coefficient	3.0 ft^3/ton
Equilibrium vertical moment coefficient	5.1 ft^3/ton
Permanent longitudinal moment	3.0×10^8 gamma-ft^3
Permanent athwartship moment	0 gamma-ft^3
Extended dipole length (0.9 x length)	215.55 ft
Static (d.c.) electric current moment	1000 A·m
Heading	030° true
Speed	10 kn
Depth	variable
Ascent rate	0 ft/s
Sensor Aircraft Parameters	
Speed	300 ft/s (177.6 kn)
Altitude	variable
Course direction	variable
Ascent rate	0 ft/s
Environmental Parameters	
Reference point in OPAREA	25°N, 58°E, sea level
Date	1 June 1996
Earth's field at reference point	
North component	34271 gamma
East component	662 gamma
Upward component	-26582 gamma
Declination (east)	1.1066°
Inclination (up)	-37.8°

EXAMPLE 1

Combined magnetic field of the earth, extended ferromagnetic dipole moment and static electric current moment

In this example, the aircraft at an altitude of 300 ft made twelve passes directly over the 100-ft deep submarine. The aircraft's course directions were varied from 0° to 360° true in increments of 30°. Figure 24 illustrates the twelve cases. Note that on courses that have a component in the northerly (magnetic) direction, the background level increases with time whereas the converse is true for courses that have a southerly (magnetic) component. Note also that two extrema exist in the signatures in eight of the twelve cases. Because the aircraft speed is 300 ft/s, the spacing between the 1-s tick marks along the abscissae corresponds to 300 ft of aircraft travel relative to the earth-fixed reference system. However, because the submarine is moving at 10 kn on a 030° heading, the speed of the aircraft relative to the submarine is 283 ft/s on its 030° course and 317 ft/s on its reciprocal course. Therefore, the spacing (in time) between the extrema for the 030° course is greater than for the 210° course.

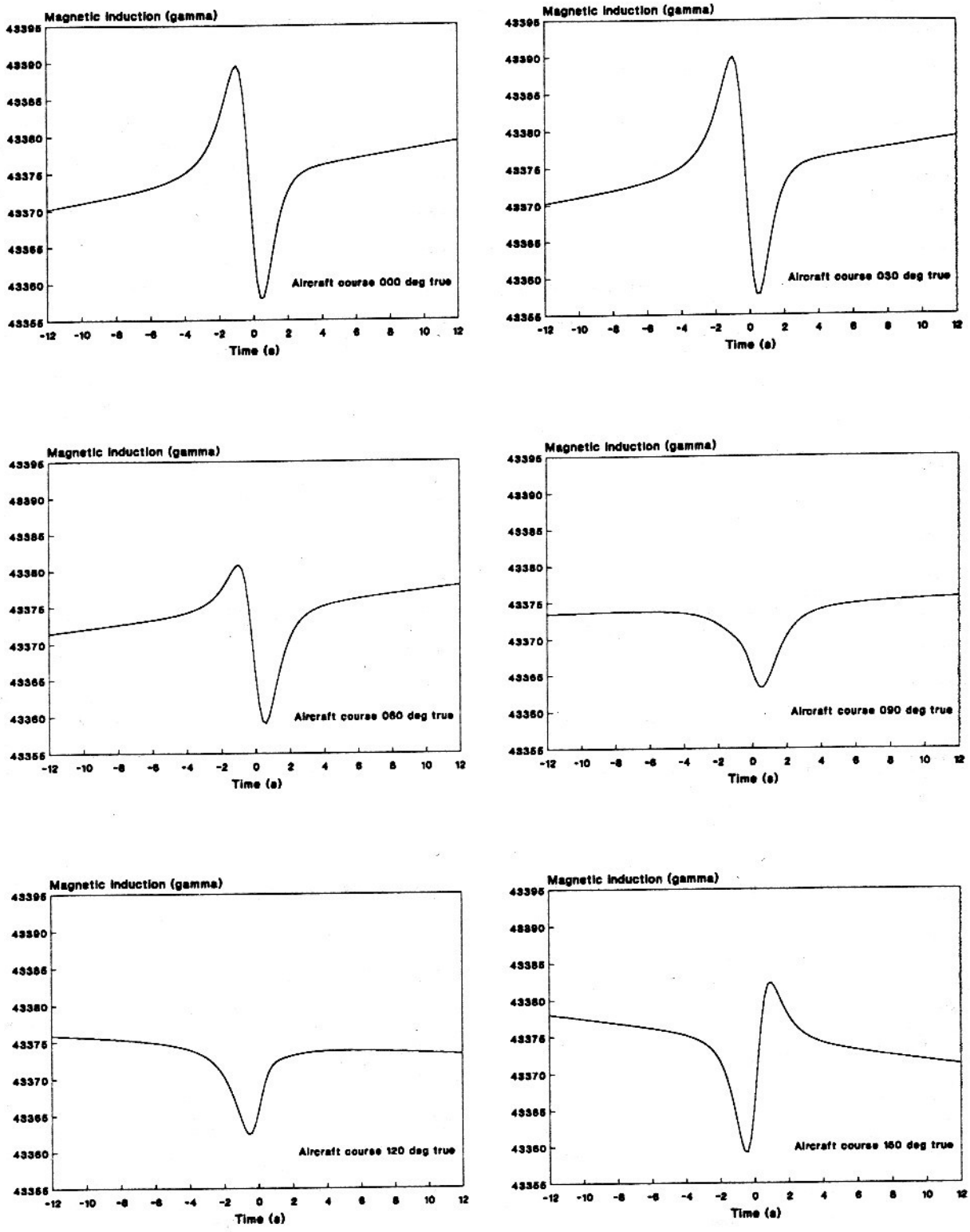


Figure 24A. Combined magnetic induction of the earth and the extended ferromagnetic and static electric current moments of a submarine.

Aircraft course directions 000, 030, 060, 090, 120 and 150 degrees true.

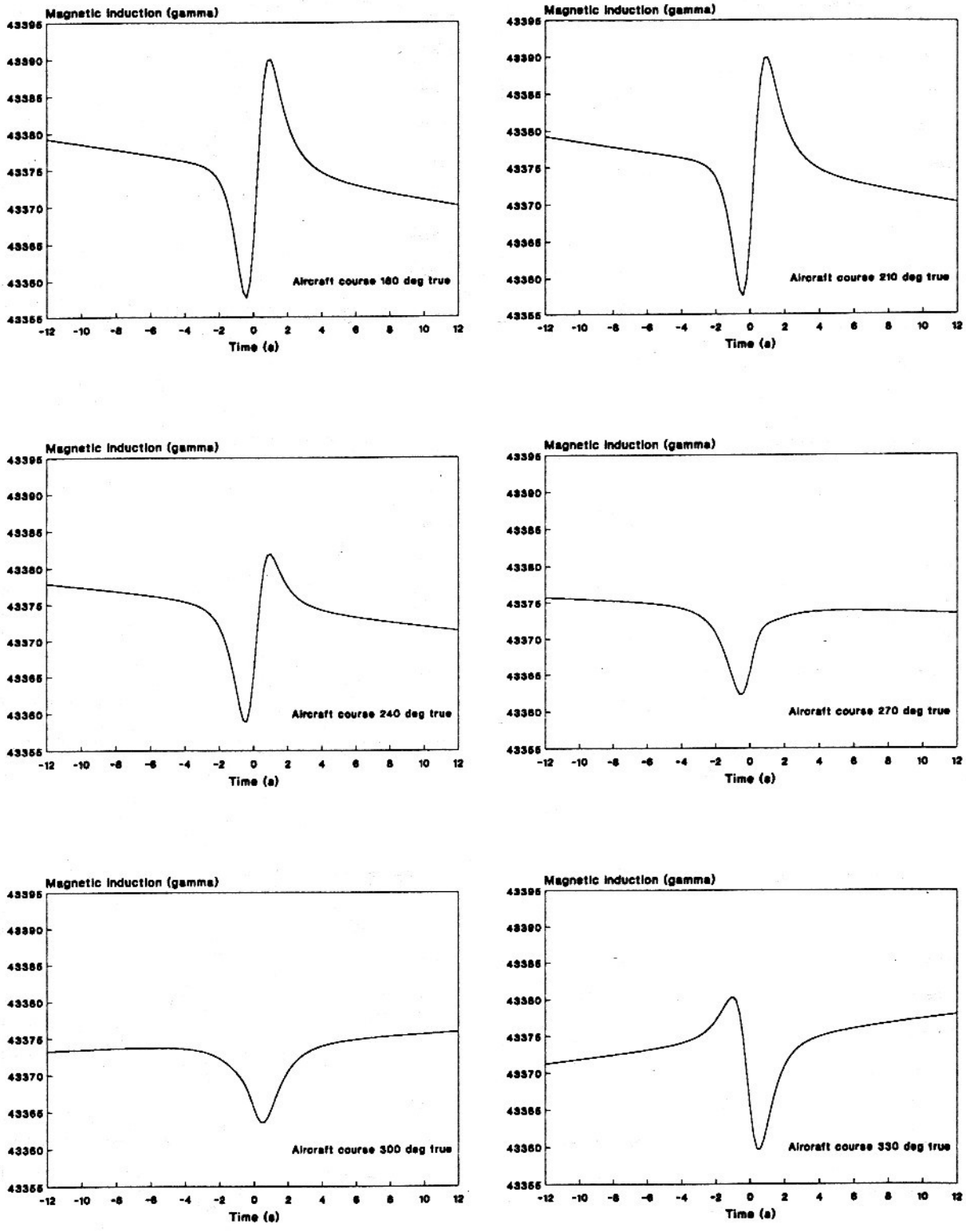


Figure 24B. Combined magnetic induction of the earth and the extended ferromagnetic and static electric current moments of a submarine.

Aircraft course directions 180, 210, 240, 270, 300 and 330 degrees true.

EXAMPLE 2

Comparison of ferromagnetic anomalies computed from extended dipole, point dipole, and "$B = M/R^3$" equations

Differences which arise in computed anomalies depending upon the method of calculation are illustrated in figure 25. The baseline conditions of Table 1 were assumed with the aircraft altitude taken as 250 ft and the submarine depth as zero. Eight course directions, at intervals of 45°, were selected for the sensor aircraft, which went directly over the submarine on each pass.

The use of $B = M/R^3$, because of its lack of angular dependence, yielded nearly equivalent results on all eight passes. (Some small differences did occur on the wings of the M/R^3 curves because of encounter geometry variations resulting from the different starting positions of the aircraft relative to the moving submarine on the different passes. The peak values are all identical, however. On the other hand, because the ferromagnetic moment M varies with submarine heading, the amplitude of the M/R^3 curves would vary with that parameter.) Note that the peak value of the M/R^3 curve is sometimes less than and sometimes greater than the peak-to-peak value of the anomaly; usually one is within a factor of two of the the other.

The anomalies calculated for the point dipole and the extended dipole track together for distances greater than about 450 ft (1.5 s) from the on-top position. At the shorter ranges the curves separate and the calculated peak-to-peak values are greater for the point dipole than for the extended dipole. On the other hand, the spacing (in time or distance) between extrema is greater for the extended dipole than for the point dipole. In addition, the locations of the extrema for the point dipole are shifted along the aircraft flight path relative to the extrema for the extended dipole.

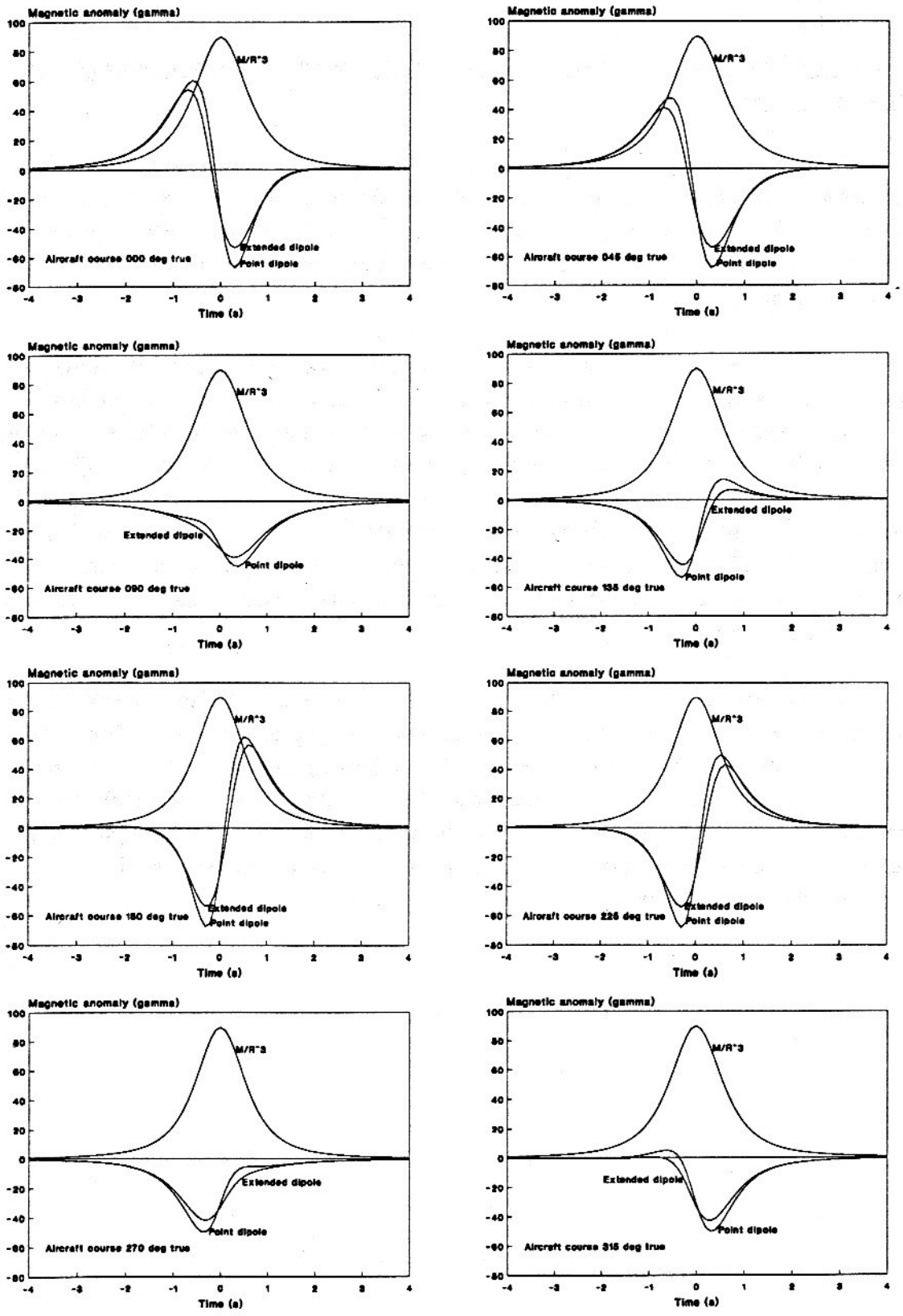


Figure 25. Comparison of magnetic anomaly signatures calculated by use of point and extended ferromagnetic dipole models.

EXAMPLE 3

Adjusting an anomaly calculated for a point dipole to approximate one calculated for an extended dipole

In this example, the difference between the point dipole anomaly and the extended dipole anomaly is examined under higher resolution for the more extreme situation of the aircraft at an altitude of only 100 ft while passing directly over the submarine at rest on the surface. The assumed heading/course for both the submarine and the aircraft is 0° magnetic (1.1066° true). For this situation, the east, north, and upward components of the submarine's magnetic moment are, respectively,

$$M_x = 2.863 \times 10^7 \text{ gamma-ft}^3$$

$$M_y = 1.482 \times 10^9 \text{ gamma-ft}^3$$

$$M_z = -4.067 \times 10^8 \text{ gamma-ft}^3.$$

Figure 26 illustrates the calculated anomalies for the two ferromagnetic models. Note that for the point dipole case, the extrema are separated by 100 ft (0.333 s at 300 ft/s), corresponding to the minimum sensor-to-target separation on the run, whereas, for the extended dipole case, the extrema are spaced at 180 ft. The maximum of the point dipole curve occurs 0.2 s (60 ft) after the maximum for the extended dipole. If one assumes

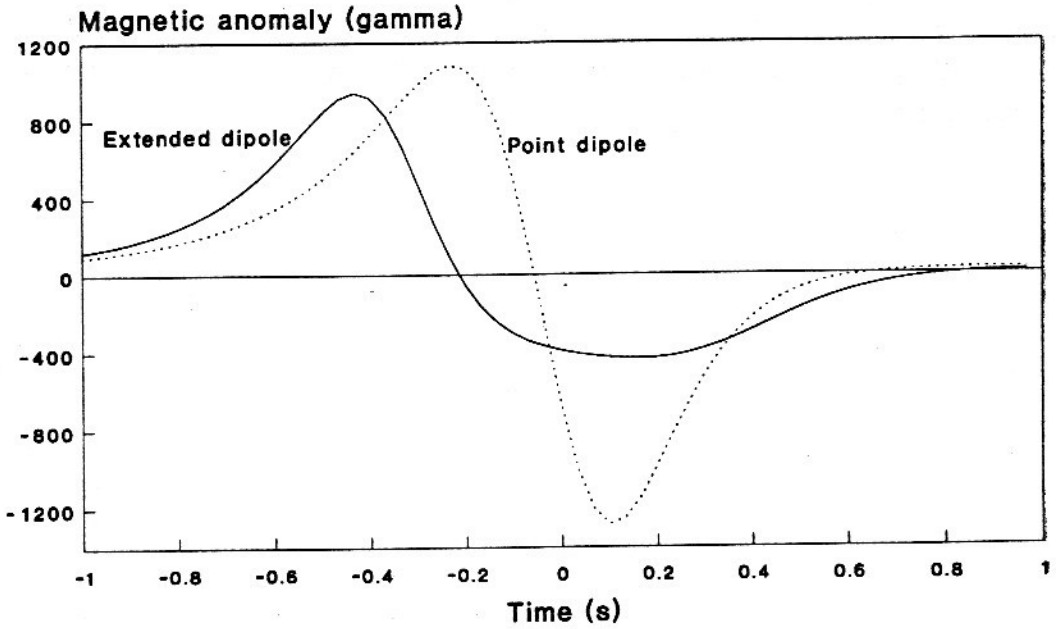


Figure 26. Comparison of anomalies calculated for extended and point ferromagnetic dipoles for very-low-altitude pass directly over target.

that the extended dipole represents the "correct" description of the submarine's ferromagnetic moment and wishes to align the extrema of the two curves, one can adjust the parameters used in calculating the point dipole anomaly. Thus, one can adjust the minimum slant range (for the point dipole case) to be 180 ft. This could be done by increasing the submarine's depth to 80 ft (or the aircraft altitude to 180 ft) or by shifting the target's location from its originally assumed location by $(180^2 - 100^2)^{1/2} = 150$ ft. However, increasing the presumed range to the target results in a weaker anomaly. Therefore, one must also increase the presumed magnetic moment of the target. By a "cut-and-try" approach, it was found that the extrema could be made to coincide if the target were presumed to be 145 ft to the west and 45 ft to the north of its "actual" position (a displacement of about 150 ft) and the components of the submarine's magnetic moment increased to the following values:

$$M_x = 4.438 \times 10^9 \text{ gamma-ft}^3$$

$$M_y = 2.965 \times 10^9 \text{ gamma-ft}^3$$

$$M_z = -1.220 \times 10^9 \text{ gamma-ft}^3.$$

That is, the extrema could be made to coincide only if the submarine's magnetic moment were presumed to be substantially larger than its originally assumed value. Figure 27 shows the adjusted point dipole anomaly relative to its unadjusted appearance and to the extended dipole anomaly. To achieve this degree of "match," the easterly component M_x of magnetic moment was increased by a factor of 155, while M_y and M_z were increased by factors of 2 and 3, respectively. For a submarine on a north magnetic heading, a value of M_x that is larger than M_y and M_z is totally unrealistic and illustrates the large errors that could result from applying the point dipole model at ranges that are not large in comparison with the length of the target.

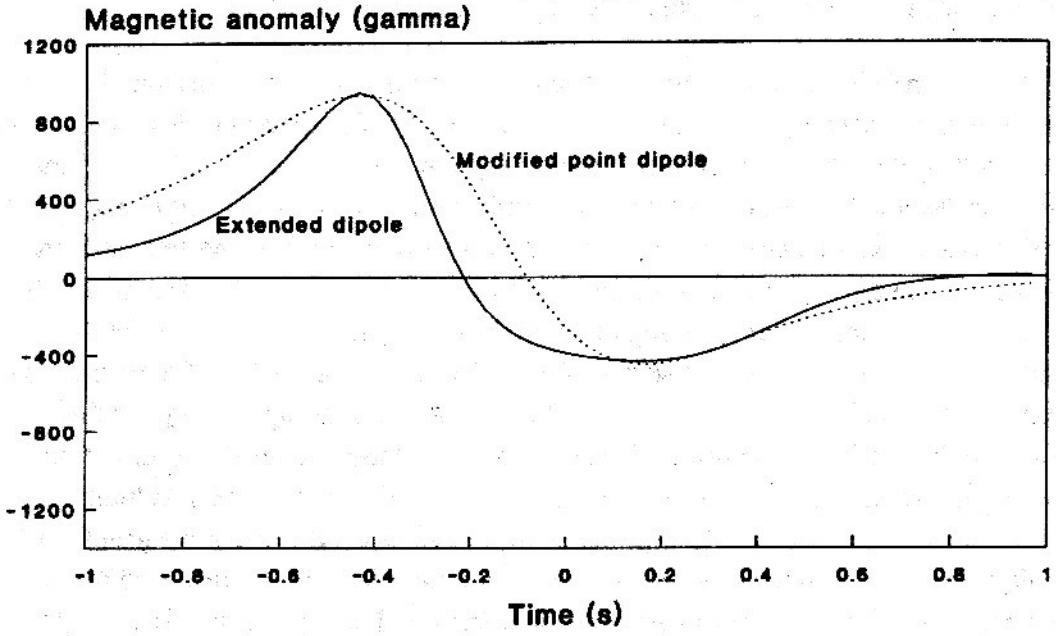


Figure 27. Anomaly from a ferromagnetic dipole modified in magnitude and location to approximate the anomaly from an extended dipole at its extrema.

EXAMPLE 4

Magnetic anomalies from static horizontal electric current elements

Two approaches to calculating magnetic anomalies from static horizontal electric current elemenents have been described. See Section VI and Appendices E and F. In this section, results obtainable with each approach are given. In the simpler approach, the submarine is assumed to behave as an isolated infinitesimal electric current element and the law of Biot and Savart is applied; in this case, return currents through the seawater are not considered. In the more complicated case, the electric current element is assumed to be immersed in a semi-infinite conducting medium (seawater) and the magnetic field is calculated at points in an overlying semi-infinite nonconducting medium (atmosphere). In this case, the return electric currents flow in the seawater, extending out beyond the immediate vicinity of the submarine. These currents are largely opposite in direction to those flowing through the submarine. Therefore, they tend to reduce the resultant magnetic field in the submarine's vicinity. However, at larger distances, the counter currents produce potentially detectable magnetic fields. The magnetic field from both direct and return currents were calculated by use of equations published by Kraichman in reference (f).

Figure 28 illustrates the magnetic anomalies calculated for the isolated current element and for the current element in seawater for eight aircraft course directions directly over a submarine having an improbably large electric current moment of 1000 A·m. The baseline conditions of Table 1 apply. The aircraft altitude was assumed to be 200 ft and the submarine depth 100 ft.

The eight pairs of curves presented in figure 28 show similarities and dissimilarities resulting from the two methods of computation. In each pair, the peak-to-peak magnitudes agree within a factor of about 2.8 and thus the simpler approach could be used for estimating electric current moments. For signature modelling, however, it appears necessary to use the more complicated approach.

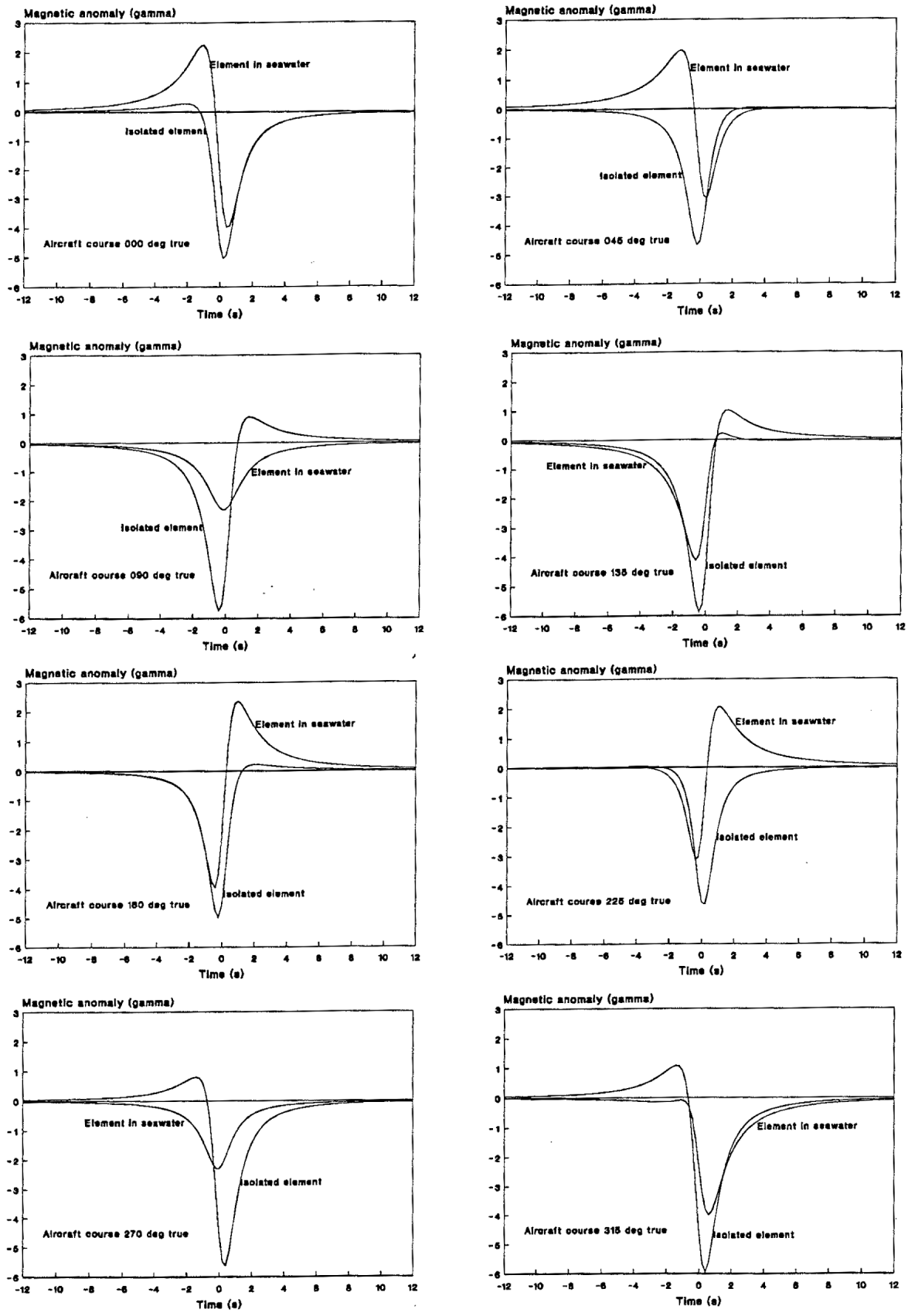


Figure 28. Comparison of magnetic anomalies calculated for an isolated electric current element and for an electric current element immersed in seawater.

EXAMPLE 5

Combination of magnetic anomalies from ferromagnetic dipole and static electric current element

In this example, the model is exercised separately for the magnetic anomaly produced by a ferromagnetic dipole and by a static electric current element. The magnetic induction components from these two sources are then added vectorially and the resulting anomaly computed in the usual manner. Once again, the baseline conditions of Table 1 were applied with a few exceptions: the submarine's speed was set at 0 kn and its heading at 000° true. The aircraft altitude was set at 300 ft and the submarine depth was 300 ft. For the resulting minimum slant range of 600 ft, it makes little difference whether the extended dipole model or the point dipole model is used for the ferromagnetic moment. (The extended dipole model was used.) The formalism derived in Appendix F was used to calculate the electric current effects. The rather large baseline value of p = 1000 A·m was used for the electric current moment to enable the reader to see more readily its contribution to the total. Because the anomaly from the electric current moment scales in direct proportion to p, the reader can visualize the effect of using smaller values. The results for aircraft passes along eight course directions directly over the submarine are shown in figure 29. Note that even with the large assumed value of p, the contribution from the electric current moment is dominated by that from the ferromagnetic dipole. For east-west crossings, the anomaly from the electric current is vanishingly small. This occurs, despite the fact that the magnetic induction is greatest directly over the submarine, because the magnetic induction vector from the submarine is perpendicular to the magnetic induction of the earth and therefore has no component in that direction. In other runs (not shown in this report) in which the aircraft did not pass directly over the target, the anomaly increased with miss distance out to several hundred feet (despite a dropoff in magnetic induction) because of the way in which the fields of the submarine and the earth combine.

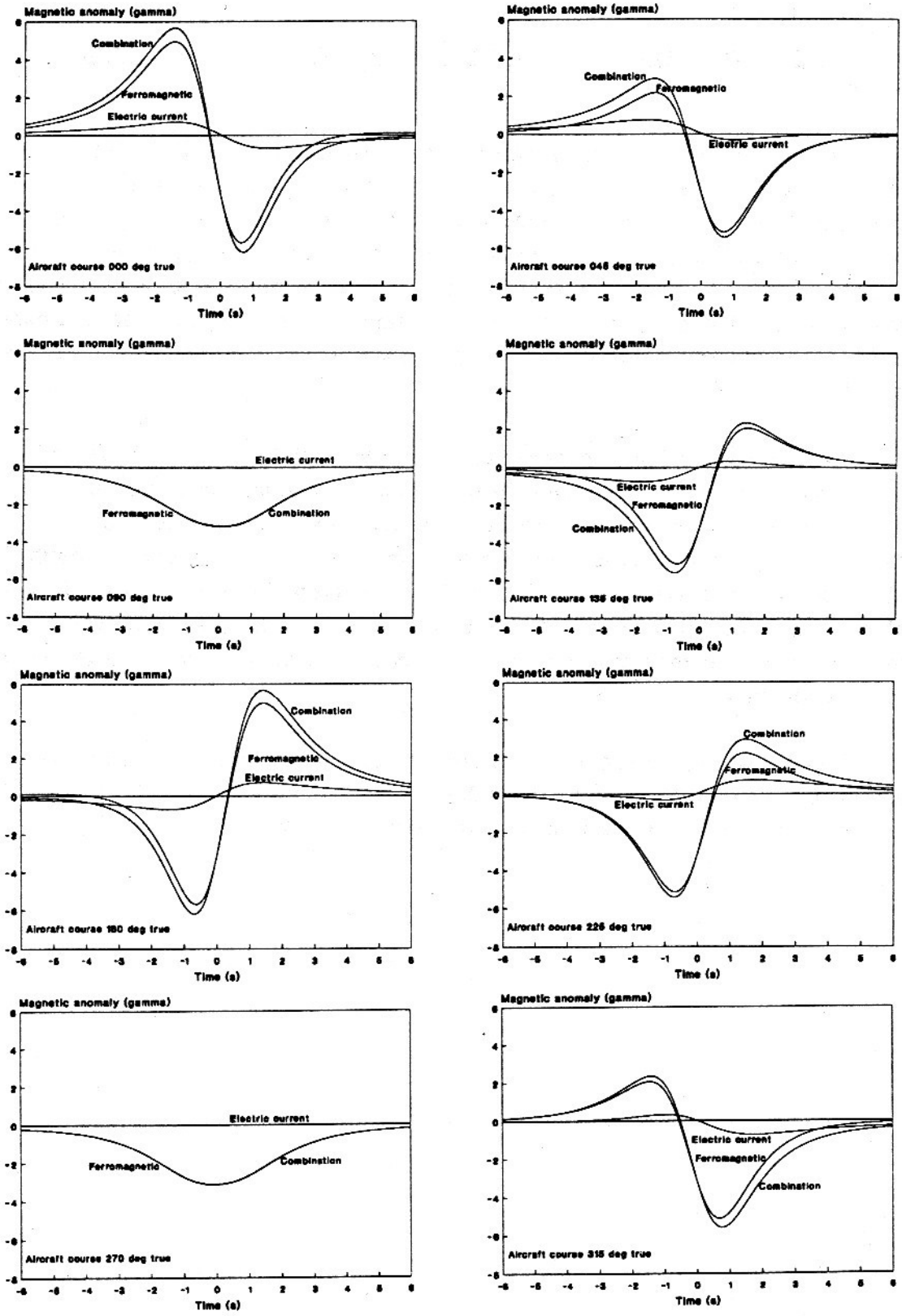


Figure 29. Magnetic anomalies from ferromagnetic dipole, static electric current element, and the combination of the two.

EXAMPLE 6

Dependence of magnetic anomaly on submarine heading for constant aircraft course direction

The combined extended ferromagnetic dipole and electric current element model was exercised to examine the effects of various submarine headings on the calculated anomaly. In this example, the aircraft, at an altitude of 300 ft, made eight passes heading true north directly over the surfaced submarine, whose speed was zero and whose heading was varied at increments of 45°. The results are shown in figure 30. There appears to be no dramatic change in the shape of the anomaly with change in submarine heading; this stands in stark contrast to the variation that occurs with changes in sensor aircraft course direction shown in figure 11.

Note that the anomalies are greatest for the north-south headings and least for the east-west headings, principally because the magnitude of the submarine's induced ferromagnetic moment varies in that manner. Also note, that when the extended ferromagnetic dipole model is used, the separation between extrema is greater for north-south headings than for east-west headings of the submarine when the sensor aircraft is on a northerly course. (Contrast this with the observation made regarding figure 11 which showed no variation in the distance between extrema as a function of aircraft course direction when the point dipole model was used.)

From this and the foregoing, it is apparent that the magnetic anomaly presented by a scalar magnetometer, such as the AN/ASQ-208, reveals better information about the heading of its host aircraft than about the heading of the target submarine.

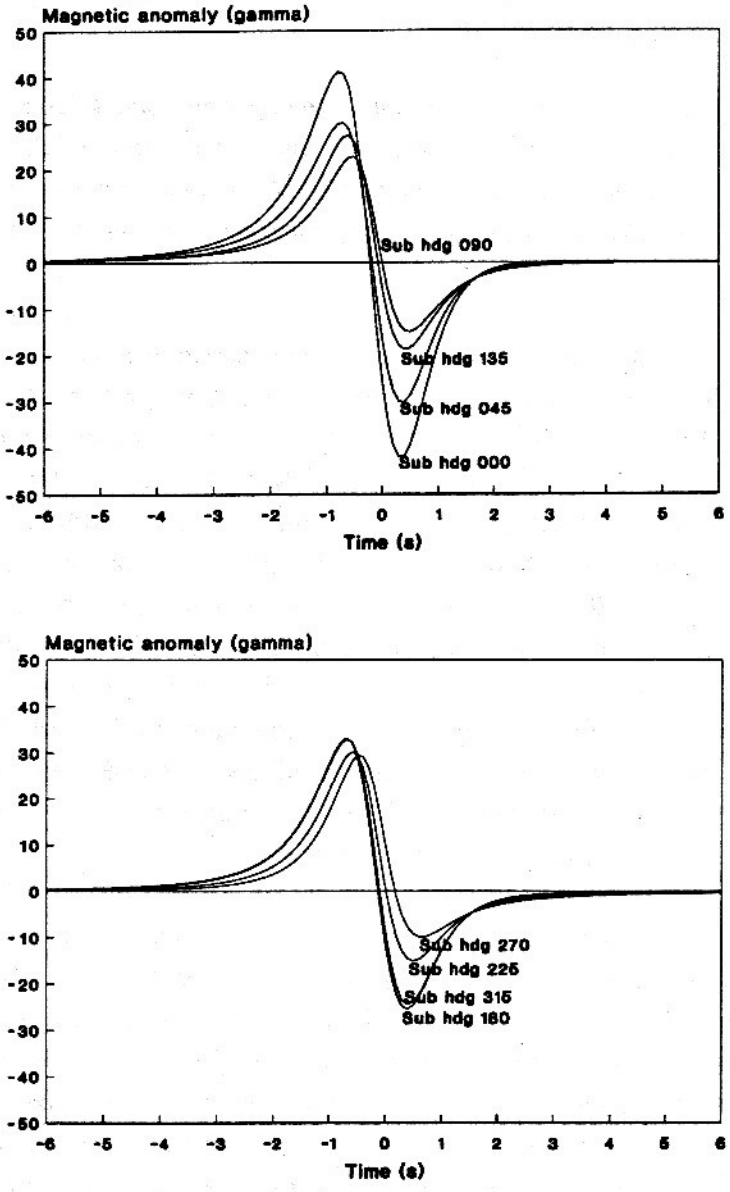


Figure 30. Effect of changes in target submarine heading on calculated magnetic anomaly for constant sensor aircraft heading.

EXAMPLE 7

Dependence of separation between extrema of magnetic anomaly on component of dipole moment in direction of sensor aircraft travel

Earlier in this report reference was made to the apparent dependence of the separation between extrema of magnetic anomalies upon the length of the extended dipole giving rise to the anomaly and upon the sensor-to-target range at CPA. In qualitative terms, the longer the dipole and the greater its distance from the sensor, the greater the separation between extrema.

To investigate further the dependence of extrema separation on submarine heading, the combined extended dipole and electric current element model was exercised at a resolution corresponding to 60 samples per second or 1 sample for each 5 ft of aircraft travel for submarine headings of 000°, 030°, 060°, and 090°, with the aircraft always on a true north course at 100-ft altitude. The submarine was at rest on the surface. Magnetic anomalies calculated for these four runs are shown in figure 31. The separations between extrema in figure 31 are, respectively, 180, 165, 145, and 105 ft. It should be noted that, in the extended dipole model, the northerly component of dipole length varies with submarine heading, being greatest when the submarine is oriented north-south and least when it is oriented east-west. The northerly components of dipole length (i.e., the projections of dipole length in the direction of aircraft travel) for the four submarine headings were 208, 189, 143, and 110 ft, respectively. Accordingly, the separation of the extrema varies monotonically with the projected length of the dipole in the direction of aircraft travel.

As noted earlier, the separation between extrema is a function of sensor-to-target minimum slant range when the point ferromagnetic dipole model is used. The foregoing indicates an additional dependence on the length of the component of the ferromagnetic dipole in the direction of aircraft travel when the extended dipole model is used. It is assumed that at short ranges the extended dipole model is more representative of the target than the point dipole model. Although the preceding observations are based only on a quick-look examination of a few computer runs, it appears that extrema separation may be a useful property for inferring submarine heading.

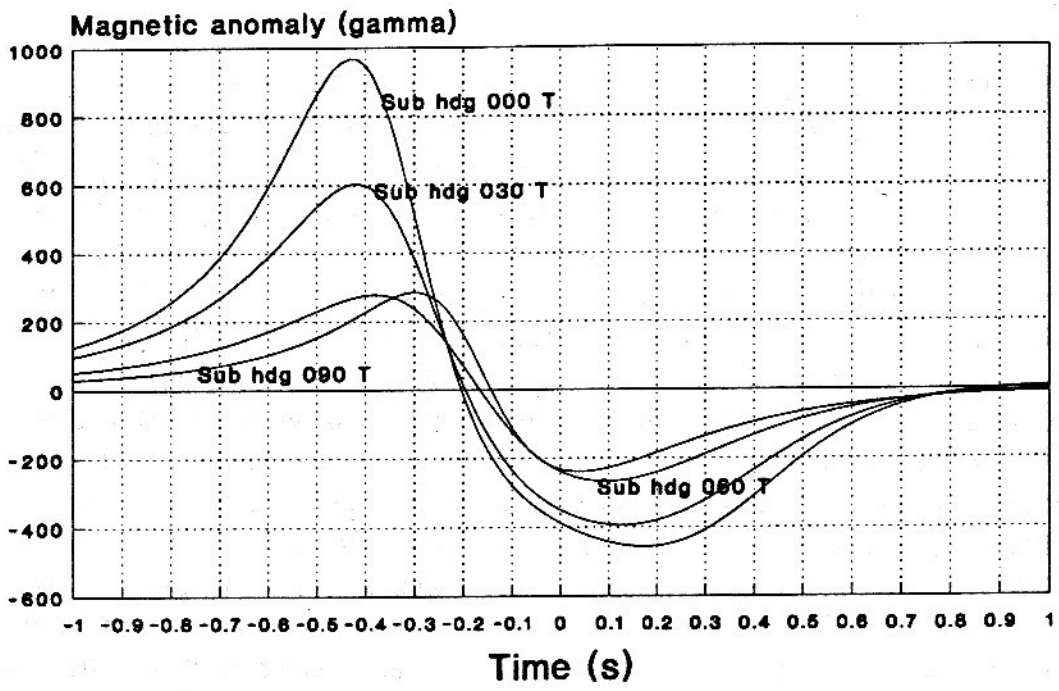


Figure 31. Separation of anomaly extrema calculated from combined extended ferromagnetic dipole and electric current element model for four submarine headings.

EXAMPLE 8

Dependence of vector components of magnetic induction on submarine heading

EXAMPLE 6 showed that a scalar magnetometer reveals information about submarine heading that is rather subtle compared to the information it reveals about aircraft course direction. The model was exercised to investigate whether some other approach, namely, using a vector magnetometer, would improve the situation. Indeed, the AN/ASQ-208 contains a three-axis vector magnetometer that is used for compensating for aircraft motion. This fluxgate vector magnetometer, which has an inherent sensitivity about two orders of magnitude less than the helium resonance scalar magnetometer, measures components of the magnetic field along the longitudinal, transverse, and vertical axes of the aircraft. These components, along with other aircraft data, could be used to determine the magnetic components in an earth-fixed coordinate system, namely, the east, north and upward components. These components were calculated for the same conditions as EXAMPLE 6 and are shown in figure 32. A comparison of figure 32 with figure 30 reveals a much richer signature in the presentation of the vector components. The east component, for example, flips polarity with certain heading changes. Although the sensitivity of the vector magnetometer is sufficient for recording submarine signatures only at relatively short ranges and the extraction of signatures from noisy data may be difficult, the possibility of gaining additional tactical data about the target may justify further investigation.

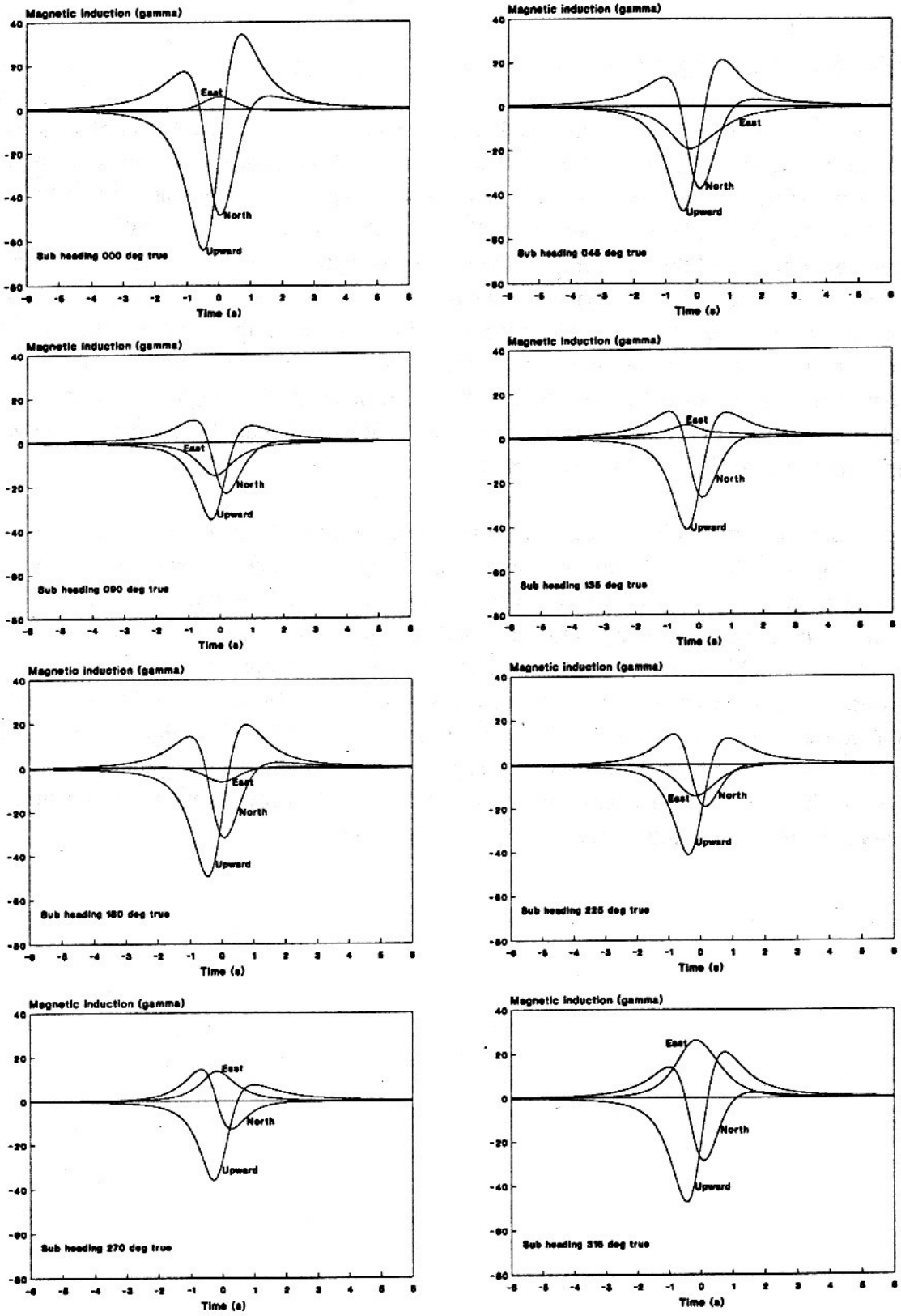


Figure 32. Vector components of combined magnetic induction from a ferromagnetic dipole and a static electric current element.

EXAMPLE 9

Calculation of magnetic anomalies by exact and approximate methods

Two methods, an exact method and an approximate method, for calculating magnetic anomalies are described in Appendix H. In this example, discrepancies that may arise by use of the approximate method are examined. It was said in Appendix H that the approximate method is valid provided the magnetic induction from the submarine was "small" in comparison with that of the earth at the point of observation. In such a situation, it is only the component of submarine's magnetic induction vector in the direction of the earth's vector that has a significant effect. Because the magnetic induction from the submarine may be of the order of 10 gamma and that of the earth of the order of 40,000 gamma, it would appear that one is "small" compared to the other. However, if one is performing analyses of signatures obtained at very short ranges, anomalies may reach hundreds of gamma and the effects on the signatures could be significant.

The model was exercised under the baseline conditions of Table 1 for the submarine on a heading of 1.1066° true (000° magnetic) at zero depth and speed. The aircraft made two passes on courses of 000° and 090° magnetic directly over the submarine at rest on the surface. To produce an anomaly in the thousand gamma regime, an altitude of 100 ft was selected. The combined extended ferromagnetic dipole and electric current element model was used. Calculations were performed for intervals of 0.01667 s (i.e., a resolution of 5 ft) over a total time of only 2 s per run. The results are shown in figure 33, which shows barely detectable differences between curves in each pair. The maximum difference was only 17.5 gamma on the curves whose peak-to-peak value was more than 1400 gamma. Thus, there appears to be no compelling reason to use one method over the other.

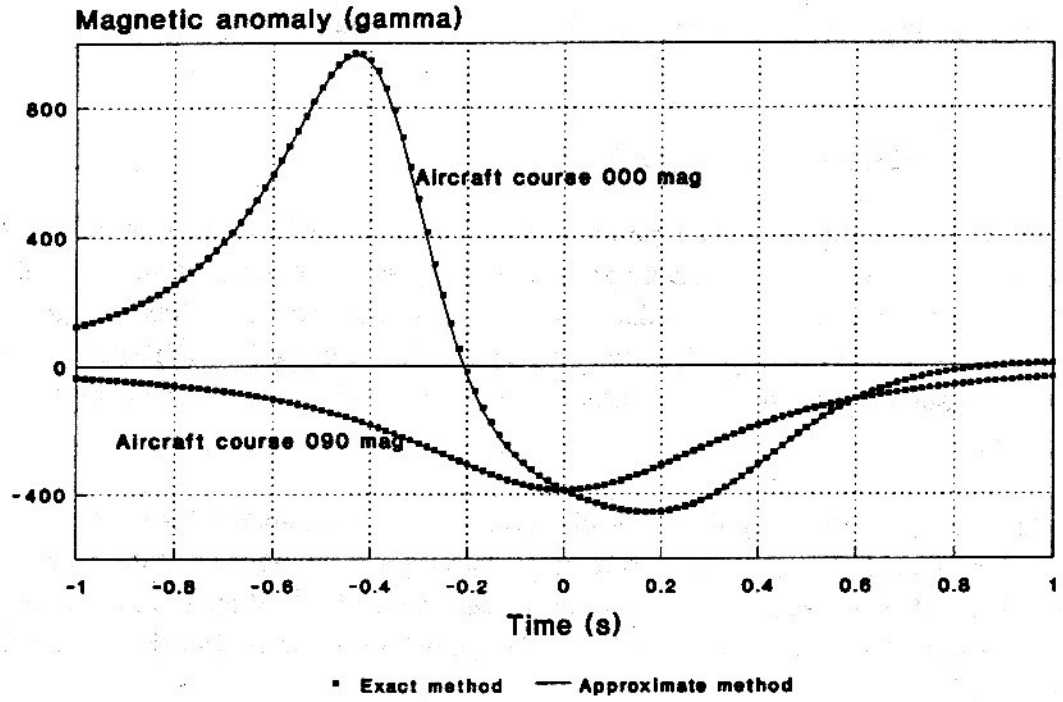


Figure 33. Magnetic anomalies calculated by exact and approximate methods.

IX. DISCUSSION

The following are a number of observations made during the course of this study that are at least obliquely related to the primary objective of the study.

Analysis of Magnetic Anomaly Signatures

The primary purpose of this report was to develop and present equations that can be used for calculating submarine magnetic anomaly signatures that can be related to actual submarine signatures as a means of deducing useful tactical information. However, potential uses of the model can extend significantly beyond this primary objective. For example, the model enables one to perform, quickly and inexpensively, many "what if" experiments under ideal conditions.

An example of the foregoing is the observation that the separation between the extrema of an anomaly signature appears to be a relatively simple function of the range to the target at CPA and of the projected length of the target's dipole in the direction of aircraft travel. A similar relation seems to exist for the first derivative of anomalies that have only a single extremum.

Extended Dipole Model

The analyses described in this report show the need for using an extended dipole model to describe magnetic anomalies observed at short sensor-to-target ranges. In deriving expressions for the particular extended dipole model used in this study, it was assumed that the dipole could be defined in terms of an N-pole and an S-pole separated by a finite distance (equal, for example, to about 90% of the length of a submarine). However, it was found that in some realistic situations the poles were located outside of the submarine. This was most apparent in cases in which the submarine was on an east-west orientation and the largest component of the magnetic moment was the vertical component. It may be argued that the poles are only a mathematical artifice; nevertheless it is somewhat disconcerting if the aircraft is able to fly between the submarine and one of its poles, or even worse, through the pole itself.

Intuitively, one would think that the poles should lie within the dimensions of the submarine; this would imply that the magnitudes of the longitudinal, athwartship and vertical components of magnetic moment would be in proportion to the submarine's dimensions. Because the beam dimension of a submarine may be only about 1/10 as great as its length,

one might expect the maximum athwartship component of magnetic moment to be only 1/10 as great as the maximum longitudinal component. However, this is apparently not the case because, in the model for the magnetic moment that was used (reference (b)), the ratio was 1/3.83. One could constrain the poles to remain within the confines of the submarine by reducing the dipole length and increasing the pole strength in inverse proportion to maintain a constant moment. This, however, could severely limit the length that the dipole could assume, resulting in little difference relative to a point dipole.

Another concern about the present extended dipole model is that although it can be used to calculate magnetic anomalies easily if the components of magnetic moment are given, it has not yet been determined how to invert the equations to calculate magnetic moment components given measured real-world anomaly data.

Platform Noise

The model described in this report enables one to compensate for one type of platform noise, namely, gradient noise, because it contains a sub-model of the earth's magnetic field, albeit over a rather limited region of space. Thus the model can reveal differences in the observed magnetic field of the earth that result from changes in aircraft position as a function of time that may accompany maneuvers or buffeting; if the motions of the aircraft are sensed, this noise can be calculated and subtracted from the received signals during processing. At present, the model is not capable of handling noise that results from rotational motion of the aircraft. However, noise from changes in orientation is also calculable and could be subtracted from the received signals during processing as an alternative to current methods of compensation.

Platform noise is really an unwanted signature from the aircraft; its orientation-dependent properties could be calculated in the same manner as the magnetic field of a submarine. That is, the aircraft possesses induced and permanent components of magnetic moment in its longitudinal, athwartship, and vertical directions which are a function of its heading and the local magnetic field of the earth. Coefficients could be determined for each of these axes, similar to those of the submarine, and with their use, the orientation-dependent field of the aircraft calculated at the sensor location. The resulting varying field could be subtracted from the magnetometer output as a means of compensation. Thus, by inserting measured aircraft position and orientation data into magnetic models of the aircraft and of the earth, a large portion of the task of compensation could be handled.

Geological Noise Model

The model described in this report currently accepts earth's magnetic field data of very low spatial frequency (e.g., about 0.0005 cycle/nmi from the IGRF model), which can be used to calculate and mitigate gradient noise. However, for certain operating areas, (e.g., the Gulf of Oman) magnetic field data of higher spatial frequencies exist which could also be incorporated into this model or into a compensation algorithm used on ASW aircraft. Although the spatial frequencies that will be available in the near future are not likely to permit elimination of geological noise, a substantial reduction could be obtained which would reduce the amount of filtering required even at present. (Frequencies up to perhaps 5 cycles/nmi would probably be needed to do a complete job.)

Geomagnetic Noise Model

Geomagnetic noise models exist which enable one to calculate statistical values of noise amplitudes as a function of frequency, geographical location, time of day, and day of the year. An example of such a model is *Geoshell*, which was developed by Pacific-Sierra Research Corporation. Such a model could be incorporated into this magnetic signature model to generate noise which would be added to and displayed with the magnetic signature data. Adding noise from the various sources (platform, geological, and geomagnetic) would increase the realism of simulated signals and would permit estimation of noise-limited detection ranges for use in engagement models.

Alternating Magnetic Field from Modulation of Corrosion Currents

This aspect of the modelling effort remains to be done.

X. CONCLUSIONS / RECOMMENDATIONS

- A model that can be inverted or a method of inverting the present extended dipole equations is needed for calculating the magnetic anomaly at distances that are not large compared to the dimensions of the target.

- The use of the simple equation $M = B R^3$ gives a fairly good value for for the magnitude of the magnetic moment of a submarine at a given location and on a given heading. If the heading of the submarine is known, the magnetic moment can be calculated for other headings and geographical locations.

- Because the magnetic moment of a submarine is such a strong function of its geographical location and heading, it would appear to be more meaningful to specify its magnetic source strength in terms of the coefficients V, L, and A instead of specifying its magnetic moment as a single number with a large variance. During data-gathering flights, the class of submarine should be identified and estimates of the submarine's heading made on each pass.

- A mathematical analysis should be performed of the equations that describe submarine anomalies to show the relation between the separation of extrema of the anomaly and the distance from the sensor to the target at CPA for distances that are not necessarily large in comparison with the length of the target. A similar analysis for anomalies exhibiting only a single extremum should be performed in terms of the separation between the maximum and the minimum of the first derivative of the anomaly with respect to distance along the sensor aircraft's path.

- The use of the vector magnetometer that is a part of the AN/ASQ-208 should be investigated as a means for obtaining more detailed short-range signature information than is provided by the scalar magnetometer.

- The horizontal component of an untreated submarine's magnetic moment will almost always lie in a direction between 310° and 050° magnetic regardless of the submarine's heading. Therefore, inferences of target heading based on such information are likely to be imprecise and ambiguous.

- If the point dipole model (rather than an extended dipole model) is used for comparing synthetic signatures with real-world signatures obtained at short ranges, significant errors result when components of magnetic moment and minimum target range are computed.

- The extended dipole model should be used to generate synthetic signatures to serve as inputs to the processor for assessing the validity of algorithms used in determining the magnitudes, directions and positions of real-world magnetic moments.

- The "approximate" method for calculating magnetic anomalies (i.e., the method in which the anomaly is assumed to be only the component of the submarine's field in the direction of the earth's field) is sufficiently accurate for any realizable situation.

XI. REFERENCES

(a) U.S. Department of Commerce, National Oceanic and Atmospheric Administration, National Geophysical Data Center pamphlet *Values of Earth's Magnetic Field from Mathematical Models*, SE-0501, January 1988.

(b) E. I. Peizer, *Magnetic Moments and Fields of Submarines (U)*, Naval Ordnance Laboratory (C) *Magnetic Anomaly Detector (MAD) Symposium*, NOLTR 72-49, D. F. Bleil, Editor, 1 March 1972.

(c) R. Schneider, Jr., *MAD Concepts Report*, Naval Air Development Center (C) Report NADC-73220-20, 15 November 1973.

(d) *Jane's Fighting Ships 1989-90*, Ninety-second edition, Edited by Captain Richard Sharpe, RN.

(e) N. M. Ginsberg and K. E. Bishop, *System Concepts and Error Analysis of the Trident Submarine Magnetic Range (U)*, Naval Ordnance Laboratory (C) Technical Report NOLTR 74-221, 16 December 1974.

(f) M. B. Kraichman, *Handbook of Electromagnetic Propagation in Conducting Media*, Second Printing, U. S. Government Printing Office Stock No. 008-040-00074-5, 1976.

APPENDIX A

SYMBOLS, DEFINITIONS AND UNITS USED IN APPENDICES

t	time (s)
t_0	initial time (s)
v_A	aircraft speed (kn)
φ_A	aircraft course direction (deg true)
C_A	aircraft ascent (climb) rate (ft/s)
X	aircraft east coordinate at t = t (ft)
Y	aircraft north coordinate at t = t (ft)
Z	aircraft altitude at t = t (ft)
X_0	aircraft east coordinate at t = 0 (ft)
Y_0	aircraft north coordinate at t = 0 (ft)
Z_0	aircraft altitude at t = 0 (ft)
$\mathbf{M}$	vector ferromagnetic moment of a submarine (gamma-ft^3)
M	magnitude of the ferromagnetic moment of a submarine (gamma-ft^3)
M_X	east component of submarine magnetic moment (gamma-ft^3)
M_Y	north component of submarine magnetic moment (gamma-ft^3)
M_Z	upward component of submarine magnetic moment (gamma-ft^3)
v_S	submarine speed (kn)
α	submarine heading (deg true) ($\approx$ course direction)

C_S submarine ascent rate (ft/s)

X_S submarine east coordinate at t = t (ft)

Y_S submarine north coordinate at t = t (ft)

Z_S submarine altitude (negative of depth) at t = t (ft)

X_{S0} submarine east coordinate at t = 0 (ft)

Y_{S0} submarine north coordinate at t = 0 (ft)

Z_{S0} submarine altitude (negative of depth) at t = 0 (ft)

$\mathbf{B_D}$ vector magnetic induction at sensor location from a ferromagnetic dipole at submarine location (gamma)

B_D magnitude of the magnetic induction at sensor location from a ferromagnetic dipole at submarine location (gamma)

B_{Dx} east component of magnetic induction at sensor location from a ferromagnetic dipole at submarine location (gamma)

B_{Dy} north component of magnetic induction at sensor location from a ferromagnetic dipole at submarine location (gamma)

B_{Dz} upward component of magnetic induction at sensor location from a ferromagnetic dipole at submarine location (gamma)

$\mathbf{B_E}$ earth's magnetic induction vector at sensor location (gamma)

B_E magnitude of earth's magnetic induction at sensor location (gamma)

B_{Ex} east component of earth's magnetic induction at sensor location point (gamma)

B_{Ey} north component of earth's magnetic induction at sensor location (gamma)

B_{Ez} upward component of earth's magnetic induction at sensor location (gamma)

$\mathbf{R}$ vector extending from the ferromagnetic dipole to the sensor (ft)

R	slant range from source point to field point (ft)
d	length of extended submarine ferromagnetic dipole (ft)
σ	pole strength of extended submarine ferromagnetic dipole (gamma-ft^2) (σ is also used in Kraichman's equations to denote electrical conductivity.)
d_x	east component of extended dipole length (ft)
d_y	north component of extended dipole length (ft)
d_z	upward component of extended dipole length (ft)
X_{NP}	east coordinate of submarine's N-pole (ft)
Y_{NP}	north coordinate of submarine's N-pole (ft)
Z_{NP}	upward coordinate of submarine's N-pole (ft)
X_{SP}	east coordinate of submarine's S-pole (ft)
Y_{SP}	north coordinate of submarine's S-pole (ft)
Z_{SP}	upward coordinate of submarine's S-pole (ft)
R_N	slant range from N-pole to sensor (ft)
R_S	slant range from S-pole to sensor (ft)
B_N	magnitude of magnetic induction at sensor from N-pole (gamma)
B_S	magnitude of magnetic induction at sensor from S-pole (gamma)
B_{Nx}	east component of magnetic induction at sensor location from N-pole (gamma)
B_{Ny}	north component of magnetic induction at sensor location from N-pole (gamma)
B_{Nz}	upward component of magnetic induction at sensor location from N-pole (gamma)
B_{Sx}	east component of magnetic induction at sensor location from S-pole (gamma)

B_{Sy} north component of magnetic induction at sensor location from S-pole (gamma)

B_{Sz} upward component of magnetic induction at sensor location from S-pole (gamma)

Γ magnetic anomaly at sensor location (gamma)

APPENDIX B

REFERENCE FRAMEWORK FOR COMPUTATIONS

A right-handed Cartesian coordinate system is set up as shown in figure B-1. The x, y, and z dimensions are associated with true east, true north, and vertically upward, respectively.

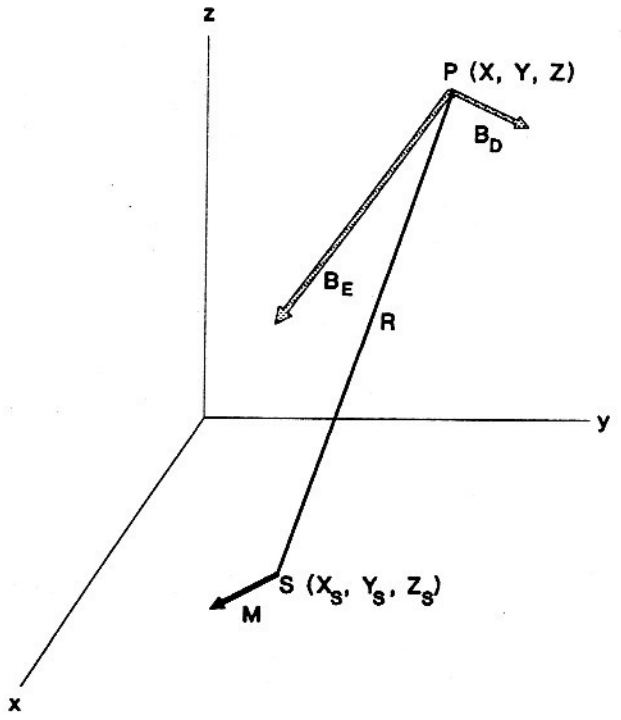


Figure B-1. Coordinate system.

The earth is assumed to be flat in the area of interest and the xy plane is situated at the sea surface. The origin of the coordinate system can be located at any arbitrary latitude and longitude. The source point S, a magnetic dipole associated with a submarine, has coordinates X_S, Y_S, and Z_S (ft) at time t (s); it moves at a constant velocity v_S (kn) on a heading of α degrees true and ascends at a constant rate C_S (ft/s). (The heading α is also assumed to be the submarine's course direction; during any aircraft pass over the submarine

this assumption should not introduce any serious error because of the relatively low speed of the submarine and the short duration of an aircraft pass.) At time t = 0, the submarine ferromagnetic dipole coordinates are X_{S0}, Y_{S0}, and Z_{S0}.

The ferromagnetic moment of the submarine is a vector **M** (gamma-ft^3), which is the vector sum of permanent and induced longitudinal, vertical, and athwartship moments, resolved, in turn, into components M_x, M_y, and M_z. The magnetic moment may arise from either a dipole of infinitesimal length (i.e., a "point" dipole) or of any arbitrary finite length (i.e., an "extended" dipole).

The submarine's ferromagnetic moment produces a magnetic field which, at field point P, is represented by the magnetic induction vector $\mathbf{B_D}$ (gamma). $\mathbf{B_D}$ is resolved into components of magnitude B_{Dx}, B_{Dy}, and B_{Dz}. Point P is the location of a scalar magnetometer in an aircraft which has coordinates X, Y, and Z (ft) at time t. At time t = 0, the sensor coordinates are X_0, Y_0, and Z_0. The aircraft moves at a constant velocity v_A (kn) with a course direction of φ_A degrees true and climbs at a constant rate C_A (ft/s). The earth's magnetic induction vector at P is $\mathbf{B_E}$ (gamma), which is resolved into components of magnitude B_{Ex}, B_{Ey}, and B_{Ez}.

The coordinates of the sensor as a function of time are

$$X = X_0 + (6080/3600)\, v_A\, t \sin \varphi_A \tag{B-1}$$

$$Y = Y_0 + (6080/3600)\, v_A\, t \cos \varphi_A \tag{B-2}$$

$$Z = Z_0 + C_A\, t. \tag{B-3}$$

The coordinates of the ferromagnetic dipole of the submarine as a function of time are

$$X_S = X_{S0} + (6080/3600)\, v_S\, t \sin \alpha \tag{B-4}$$

$$Y_S = Y_{S0} + (6080/3600)\, v_A\, t \cos \alpha \tag{B-5}$$

$$Z_S = Z_{S0} + C_S\, t. \tag{B-6}$$

The vector **R** (ft) extends from the ferromagnetic dipole to the sensor at field point P. Its magnitude, the slant range R, is given by

$$R = [(X-X_S)^2+(Y-Y_S)^2+(Z-Z_S)^2]^{1/2}. \tag{B-7}$$

APPENDIX C

MAGNETIC INDUCTION FROM AN INFINITESIMAL ("POINT") FERROMAGNETIC DIPOLE OF ARBITRARY LOCATION AND ORIENTATION

The magnetic induction from a point magnetic dipole is given in vector notation by the expression

$$\mathbf{B_D} = - \mathbf{M}/R^3 + 3(\mathbf{M} \cdot \mathbf{R})\, \mathbf{R}/R^5. \tag{C-1}$$

Resolve the vectors $\mathbf{B_D}$, $\mathbf{M}$, and $\mathbf{R}$ into components parallel to the east (x), north (y), and vertically upward (z) axes.

Let

$$\mathbf{B_D} = \mathbf{i}\, B_{Dx} + \mathbf{j}\, B_{Dy} + \mathbf{k}\, B_{Dz} \tag{C-2}$$

$$\mathbf{M} = \mathbf{i}\, M_x + \mathbf{j}\, M_y + \mathbf{k}\, M_z \tag{C-3}$$

$$\mathbf{R} = \mathbf{i}\, R_x + \mathbf{j}\, R_y + \mathbf{k}\, R_z = \mathbf{i}\,(X-X_S) + \mathbf{j}\,(Y-Y_S) + \mathbf{k}\,(Z-Z_S). \tag{C-4}$$

The magnitudes of these three vectors, respectively, are

$$B_D = (B_{Dx}^2 + B_{Dy}^2 + B_{Dz}^2)^{1/2} \tag{C-5}$$

$$M = (M_x^2 + M_y^2 + M_z^2)^{1/2} \tag{C-6}$$

$$R = [(X-X_S)^2 + (Y-Y_S)^2 + (Z-Z_S)^2]^{1/2}. \tag{C-7}$$

Substituting equations (C-2), (C-3), and (C-4) into equation (C-1) yields

$$\mathbf{i}\, B_{Dx} + \mathbf{j}\, B_{Dy} + \mathbf{k}\, B_{Dz} = - (\mathbf{i}\, M_x + \mathbf{j}\, M_y + \mathbf{k}\, M_z)\, /R^3$$

$$+ 3\,(M_x R_x + M_y R_y + M_z R_z)\,(\mathbf{i}\, R_x + \mathbf{j}\, R_y + \mathbf{k}\, R_z)\, /R^5. \tag{C-8}$$

Resolve equation (C-8) into components along the three axes:

$$\mathbf{i}\, B_{Dx} = - \mathbf{i}\, M_x/R^3 + 3\,(M_x R_x + M_y R_Y + M_z R_z)\, \mathbf{i}\, R_x/R^5 \tag{C-9}$$

$$\mathbf{j}\, B_{Dy} = - \mathbf{j}\, M_y/R^3 + 3\,(M_x R_x + M_y R_Y + M_z R_z)\, \mathbf{j}\, R_y/R^5 \tag{C-10}$$

$$\mathbf{k}\, B_{Dz} = -\,\mathbf{k}\, M_z/R^3 + 3\,(M_x\, R_x + M_y\, R_Y + M_z\, R_z)\,\mathbf{k}\, R_z/R^5. \qquad \text{(C-11)}$$

Therefore, the magnitudes of the east, north, and upward components of the magnetic induction of a point ferromagnetic dipole are

$$B_{Dx} = \{3\,[M_x\,(X-X_S) + M_y\,(Y-Y_S) + M_z\,(Z-Z_S)]\,(X-X_S) - M_x\,R^2\}\,/R^5 \qquad \text{(C-12)}$$

$$B_{Dy} = \{3\,[M_x\,(X-X_S) + M_y\,(Y-Y_S) + M_z\,(Z-Z_S)]\,(Y-Y_S) - M_y\,R^2\}\,/R^5 \qquad \text{(C-13)}$$

$$B_{Dz} = \{3\,[M_x\,(X-X_S) + M_y\,(Y-Y_S) + M_z\,(Z-Z_S)]\,(Z-Z_S) - M_z\,R^2\}\,/R^5. \qquad \text{(C-14)}$$

APPENDIX D

MAGNETIC INDUCTION FROM AN EXTENDED FERROMAGNETIC DIPOLE OF ARBITRARY LENGTH, LOCATION AND ORIENTATION

Consider an extended magnetic dipole consisting of a point N-pole and a point S-pole, each of pole strength σ, separated by a distance d, the length of the extended dipole. The center of the dipole is located at source point S and has coordinates X_S, Y_S, Z_S as shown in figure D-1. The coordinates of the N-pole and the S-pole are, respectively, X_{NP}, Y_{NP},

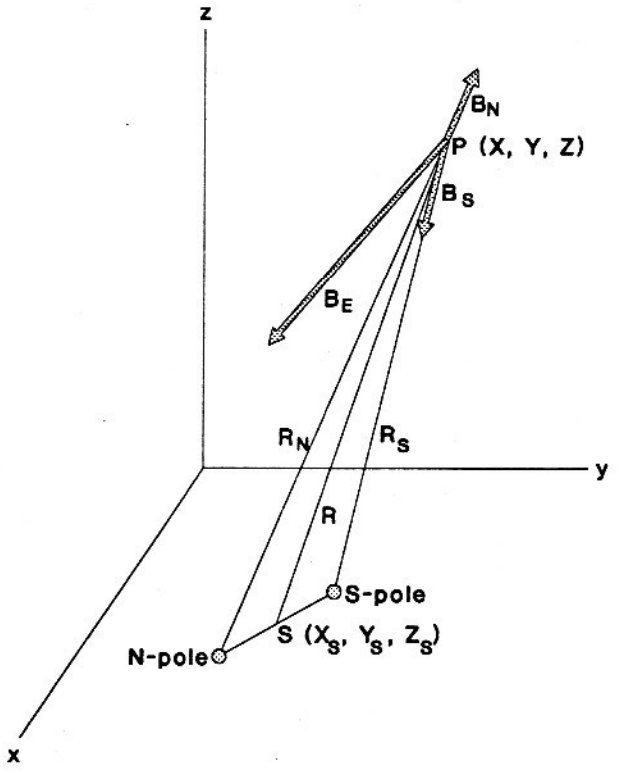


Figure D-1. Geometry for extended dipole derivation.

Z_{NP} and X_{SP}, Y_{SP}, Z_{SP}. Let P be a field point, having coordinates X, Y, Z, defining the location of the magnetic sensor at any time t. Let R be the slant range from S to P. Similarly, let R_N be the distance from the N-pole to P and let R_S be the distance from the S-pole to P.

Thus

$$R = [(X-X_S)^2 + (Y-Y_S)^2 + (Z-Z_S)^2]^{1/2} \quad \text{(D-1)}$$

$$R_N = [(X-X_{NP})^2 + (Y-Y_{NP})^2 + (Z-Z_{NP})^2]^{1/2} \quad \text{(D-2)}$$

$$R_S = [(X-X_{SP})^2 + (Y-Y_{SP})^2 + (Z-Z_{SP})^2]^{1/2}. \quad \text{(D-3)}$$

Let M be the magnitude of the vector magnetic moment of the dipole, and M_x, M_y, and M_z be its components in the east, north, and upward directions, respectively. Let d_x, d_y, and d_z represent the dipole's components of length in those directions, respectively. Then

$$d_x = d\, M_x/M \quad \text{(D-4)}$$

$$d_y = d\, M_y/M \quad \text{(D-5)}$$

$$d_z = d\, M_z/M. \quad \text{(D-6)}$$

The coordinates of the N-pole are

$$X_{NP} = X_S + 1/2\, d_x \quad \text{(D-7)}$$

$$Y_{NP} = Y_S + 1/2\, d_y \quad \text{(D-8)}$$

$$Z_{NP} = Z_S + 1/2\, d_z. \quad \text{(D-9)}$$

The coordinates of the S-pole are

$$X_{SP} = X_S - 1/2\, d_x \quad \text{(D-10)}$$

$$Y_{SP} = Y_S - 1/2\, d_y \quad \text{(D-11)}$$

$$Z_{SP} = Z_S - 1/2\, d_z. \quad \text{(D-12)}$$

The pole strength σ is given by

$$\sigma = M/d. \quad \text{(D-13)}$$

In accordance with Coulomb's law, the N-pole produces a magnetic induction vector at P whose magnitude B_N is

$$B_N = \sigma/R_N^2 \tag{D-14}$$

and whose direction is outward from the N-pole along the line joining it with P.

Similarly, the S-pole produces a magnetic induction vector at P whose magnitude B_S is

$$B_S = -\sigma/R_S^2 \tag{D-15}$$

and whose direction is inward toward the S-pole along the line from P.

B_N can be resolved into components along the x, y, and z axes (i.e., easterly, northerly and upward components, respectively) as

$$B_{Nx} = B_N(X-X_{NP})/R_N \tag{D-16}$$

$$B_{Ny} = B_N(Y-Y_{NP})/R_N \tag{D-17}$$

$$B_{Nz} = B_N(Z-Z_{NP})/R_N. \tag{D-18}$$

Similarly, B_S can be resolved into components as

$$B_{Sx} = B_S(X-X_{SP})/R_S \tag{D-19}$$

$$B_{Sy} = B_S(Y-Y_{SP})/R_S \tag{D-20}$$

$$B_{Sz} = B_S(Z-Z_{SP})/R_S. \tag{D-21}$$

The x, y, and z components of the magnetic induction vector $\mathbf{B_D}$ at P from the extended dipole at S can be obtained by combining equations (D-16) through (D-21) in pairs to obtain

$$B_{Dx} = B_{Nx} + B_{Sx} \tag{D-22}$$

$$B_{Dy} = B_{Ny} + B_{Sy} \tag{D-23}$$

$$B_{Dz} = B_{Nz} + B_{Sz}. \tag{D-24}$$

By substituting equations that appear earlier in this appendix into equations (D-22), (D-23), and (D-24) (e.g., starting with equations (D-16) through (D-21) and working

backwards), one can eliminate the intermediate parameters and arrive at a set of five summary equations for the three components of magnetic induction from an extended dipole:

$$B_{Dx} = (MX - MX_S - 1/2\ M_x d)/(D_1 d) - (MX - MX_S + 1/2\ M_x d)/(D_2 d) \quad \text{(D-25)}$$

$$B_{Dy} = (MY - MY_S - 1/2\ M_y d)/(D_1 d) - (MY - MY_S + 1/2\ M_y d)/(D_2 d) \quad \text{(D-26)}$$

$$B_{Dz} = (MZ - MZ_S - 1/2\ M_z d)/(D_1 d) - (MZ - MZ_S + 1/2\ M_z d)/(D_2 d) \quad \text{(D-27)}$$

in which

$$D_1 = [(X-X_S-1/2M_x d/M)^2 + (Y-Y_S-1/2M_y d/M)^2 + (Z-Z_S-1/2M_z d/M)^2]^{3/2} \quad \text{(D-28)}$$

$$D_2 = [(X-X_S+1/2M_x d/M)^2 + (Y-Y_S+1/2M_y d/M)^2 + (Z-Z_S+1/2M_z d/M)^2]^{3/2}. \quad \text{(D-29)}$$

The only input parameters appearing in equations D-25 through D-29 are the coordinates of the source and field points, the magnitude of the dipole's magnetic moment and its three components, and the length of the dipole.

APPENDIX E

MAGNETIC INDUCTION FROM AN ELECTRIC CURRENT ELEMENT DETERMINED FROM THE BIOT-SAVART LAW

The law of Biot and Savart may be written in vector form as

$$\mathbf{dB} = \mu_0 \, i \, \mathbf{dL} \times \mathbf{R} / (4 \pi R^3). \qquad \text{(E-1)}$$

In equation (E-1), **dB** is the magnetic induction (in tesla) produced at a field point P at a distance R (in meters) from an electric current element of length **dL** (in meters) carrying a current i (in amperes) located at a source point S. See figure E-1.

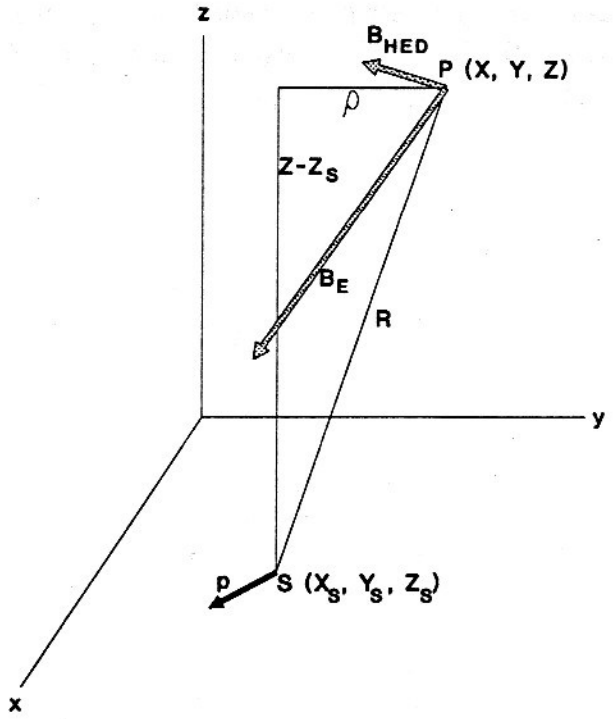


Figure E-1. Geometry for calculating magnetic induction from an electric current element.

The quantity

$$\mu_0 = 4 \pi \times 10^{-7} \text{ weber/A·m}. \qquad \text{(E-2)}$$

Insertion of equation (E-2) into equation (E-1) yields

$$\mathbf{dB} = 10^{-7}\, i\, \mathbf{dL} \times \mathbf{R} / R^3 \quad (\text{weber/m}^2). \tag{E-3}$$

But 1 weber/m^2 = 1 tesla = 10^9 nT = 10^9 gamma. For **dB** expressed in gamma and R expressed in ft, equation (E-3) becomes

$$\mathbf{dB} = 1076.39\, i\, \mathbf{dL} \times \mathbf{R} / R^3 \quad (\text{gamma}). \tag{E-4}$$

If it is assumed that R is much greater than the length of the current element, and if i **dL** is replaced by the current moment **p** (in A·m), the magnetic induction $\mathbf{B}_{CE}$ (substituted for **dB**) from the current element can be written as

$$\mathbf{B}_{CE} = 1076.39\, \mathbf{p} \times \mathbf{R}/R^3 \quad (\text{gamma}) \tag{E-5}$$

where R is in ft.

Let the coordinates of the source point S be X_S, Y_S, Z_S and the coordinates of the field point P be X, Y, Z. Resolve the vectors **p** and **R** into easterly, northerly, and upward components as follows:

$$\mathbf{p} = \mathbf{i}p_x + \mathbf{j}p_y + \mathbf{k}p_z \tag{E-6}$$

$$\mathbf{R} = \mathbf{i}(X-X_S) + \mathbf{j}(Y-Y_S) + \mathbf{k}(Z-Z_S). \tag{E-7}$$

The slant range R from S to P is

$$R\ [(X-X_s)^2 + (Y-Y_s)^2 + (Z-Z_s)^2]^{1/2}. \tag{E-8}$$

The vector product **p x R** can be expanded as

$$\begin{aligned}\mathbf{p} \times \mathbf{R} = {} & (\mathbf{i} \times \mathbf{j})\, p_x\, (Y-Y_S) + (\mathbf{i} \times \mathbf{k})\, p_x\, (Z-Z_S) \\ & + (\mathbf{j} \times \mathbf{i})\, p_y\, (X-X_S) + (\mathbf{j} \times \mathbf{k})\, p_y\, (Z-Z_S) \\ & + (\mathbf{k} \times \mathbf{i})\, p_z\, (X-X_S) + (\mathbf{k} \times \mathbf{j})\, p_z\, (Y-Y_S).\end{aligned} \tag{E-9}$$

Since **i x j** = **k**, **i x k** = -**j**, etc.,

$$\mathbf{p} \times \mathbf{R} = \mathbf{k}\, p_x (Y-Y_S) - \mathbf{j}\, p_x (Z-Z_S) - \mathbf{k}\, p_y (X-X_S) + \mathbf{i}\, p_y (Z-Z_S)$$

$$+ \mathbf{j}\, p_z (X-X_S) - \mathbf{i}\, p_z (Y-Y_S). \qquad \text{(E-10)}$$

Combining components along each axis yields

$$\mathbf{p} \times \mathbf{R} = \mathbf{i}\, [p_y (Z-Z_S) - p_z (Y-Y_S)] + \mathbf{j}\, [p_z (X-X_S) - p_x (Z-Z_S)]$$

$$+ \mathbf{k}\, [p_x (Y-Y_S) - p_y (X-X_S)]. \qquad \text{(E-11)}$$

Substituting equation (E-11) into an expansion of equation (E-5) yields the following three equations for the magnitudes of the components of the magnetic induction along each of the axes:

$$B_{CEx} = 1076.39\, [p_y (Z-Z_S) - p_z (Y-Y_S)]/R^3 \qquad \text{(E-12)}$$

$$B_{CEy} = 1076.39\, [p_z (X-X_S) - p_x (Z-Z_S)]/R^3 \qquad \text{(E-13)}$$

$$B_{CEz} = 1076.39\, [p_x (Y-Y_S) - p_y (X-X_S)]/R^3. \qquad \text{(E-14)}$$

Assume that the electric current element **p** is directed forward along the longitudinal axis of the submarine and it is horizontal. If the submarine's heading (in degrees true) is α,

$$p_x = p \sin \alpha \qquad \text{(E-15)}$$

$$p_y = p \cos \alpha \qquad \text{(E-16)}$$

$$p_z = 0. \qquad \text{(E-17)}$$

Then

$$B_{CEx} = 1076.39\, p\, [(Z-Z_S) \cos \alpha)]/R^3 \qquad \text{(E-18)}$$

$$B_{CEy} = -1076.39\, p\, [(Z-Z_S) \sin \alpha]/R^3 \qquad \text{(E-19)}$$

$$B_{CEz} = 1076.39\, p\, [(Y-Y_S) \sin \alpha - (X-X_S) \cos \alpha]/R^3. \qquad \text{(E-20)}$$

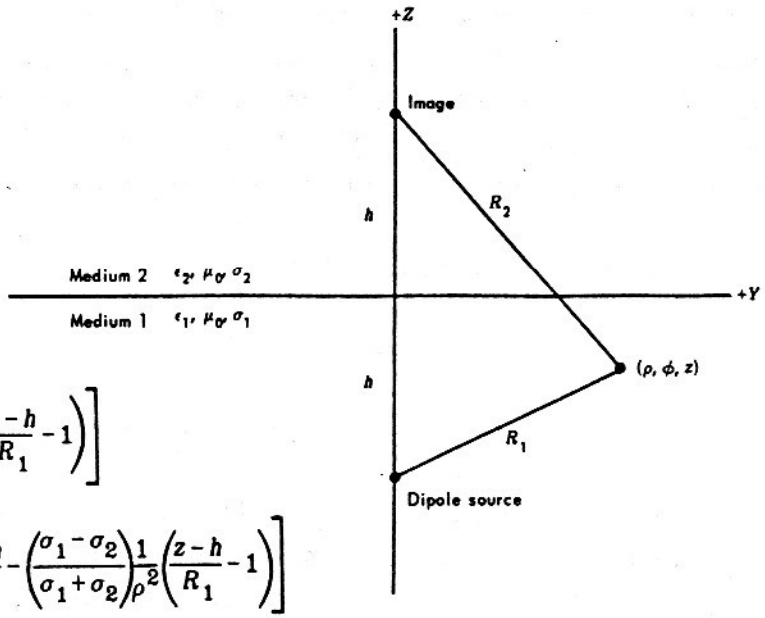
APPENDIX F

MAGNETIC INDUCTION IN AIR ABOVE A STATIC HORIZONTAL ELECTRIC DIPOLE IN SEAWATER

Kraichman (reference (f)) provides equations that enable one to calculate the magnetic field intensity **H** (in amperes/meter) in one semi-infinite medium (e.g., atmosphere) above another semi-infinite medium (e.g., sea) in which a horizontal current element is positioned on the z-axis at a distance -h below the interface, parallel to the x-axis and positively directed. See figure F-1.

$$R_1 = \left[\rho^2 + (z-h)^2\right]^{1/2}$$

$$R_2 = \left[\rho^2 + (z+h)^2\right]^{1/2}$$



$$H_{\rho_2} = \frac{-p \sin\phi}{4\pi}\left[\frac{z-h}{R_1^3} + \left(\frac{\sigma_1-\sigma_2}{\sigma_1+\sigma_2}\right)\frac{1}{\rho^2}\left(\frac{z-h}{R_1}-1\right)\right]$$

$$H_{\phi_2} = \frac{-p \cos\phi}{4\pi}\left[\frac{z-h}{R_1^3} - \left(\frac{\sigma_1-\sigma_2}{\sigma_1+\sigma_2}\right)\frac{z-h}{R_1^3} - \left(\frac{\sigma_1-\sigma_2}{\sigma_1+\sigma_2}\right)\frac{1}{\rho^2}\left(\frac{z-h}{R_1}-1\right)\right]$$

$$H_{z_2} = \frac{p \sin\phi}{4\pi}\left(\frac{\rho}{R_1^3}\right)$$

Figure F-1. Geometry and equations for the magnetic field intensity above a semi-infinite conducting medium in which a static horizontal electric current dipole is immersed (from Kraichman, 1976).

Kraichman defines two distance parameters R_1 and R_2 in cylindrical coordinates as the distances to a field point P (ρ, φ, z) from, respectively, the current element in the lower medium and its image directly above it in the upper medium. Figure F-1 illustrates the

geometry and gives Kraichman's equations for three orthogonal components of the magnetic field intensity in the upper medium (medium 2). The steady electric current moment p = IL and the electrical conductivities of medium 1 and medium 2 are σ_1 and σ_2, respectively. If the earth's atmosphere is taken as medium 2, its conductivity σ_2 may be taken as zero and the equations for the three components of magnetic field reduce to

$$H_\rho = -p/(4\pi) \sin\varphi \{(z-h)/R_1^3 + [(z-h)/R_1 - 1]/\rho^2\} \quad \text{(F-1)}$$

$$H_\varphi = p/(4\pi) \cos\varphi [(z-h)/R_1 - 1]/\rho^2 \quad \text{(F-2)}$$

$$H_Z = p/(4\pi) \sin\varphi [\rho/R_1^3]. \quad \text{(F-3)}$$

It should be noted in equations (F-1), (F-2), and (F-3) that the distance parameter R_2 does not appear and that z and h appear only in the combination z-h, which is the vertical separation between the source point and the field point. For convenience, replace z-h by z, R_1 by R, and ρ by r; that is, for the present, perform the mathematics in submarine-fixed coordinates. (Later, z will be replaced by $Z-Z_S$ to be consistent with the nomenclature used elsewhere in this report and a conversion to geographical coordinates will be made.)

From the foregoing, it follows that

$$r = (x^2 + y^2)^{1/2} \text{ and} \quad \text{(F-4)}$$

$$R = (x^2 + y^2 + z^2)^{1/2}. \quad \text{(F-5)}$$

Note that, if the field point should be directly over the source point (which would occur if the sensor passes directly over the target), r = 0, and singularities occur in equations (F-1) and (F-2). Difficulties can be avoided by inserting some very small number into x or y to prevent both from going to zero simultaneously.

It is desired ultimately to obtain three equations describing the easterly, northerly, and vertically upward components of the magnetic induction arising from the electric currents flowing through the submarine hull and the surrounding water that will be directly additive to similar components arising from the ferromagnetic moment. To switch to a Cartesian coordinate system, the following conversions are used:

$$x = r \cos\varphi \quad \text{(F-6)}$$

$$y = r \sin\varphi. \quad \text{(F-7)}$$

Thus, equations (F-1), (F-2), and (F-3) become, respectively,

$$H_r = -py/(4\pi Rr)\,[z/R^2 + (z-R)/r^2] \tag{F-8}$$

$$H_\varphi = px(z-R)/(4\pi Rr^3) \tag{F-9}$$

$$H_z = py/(4\pi R^3). \tag{F-10}$$

The components of H_r in the x and y directions are

$$H_{rx} = H_r \cos\varphi = H_r x/r \tag{F-11}$$

$$H_{ry} = H_r \sin\varphi = H_r y/r. \tag{F-12}$$

The components of H_φ in the x and y directions are

$$H_{\varphi x} = -H_\varphi \sin\varphi = -H_\varphi y/r \tag{F-13}$$

$$H_{\varphi y} = H_\varphi \cos\varphi = H_\varphi x/r. \tag{F-14}$$

Taking the sums of the x and y components yields

$$H_x = H_{rx} + H_{\varphi x} = (H_r x - H_\varphi y)/r \tag{F-15}$$

$$H_y = H_{ry} + H_{\varphi y} = (H_r y + H_\varphi x)/r. \tag{F-16}$$

Inserting equations (F-8) and (F-9) into equation (F-15) gives

$$H_x = [-pxy/(4\pi Rr^2)]\,[z/R^2 + 2(z-R)/r^2]. \tag{F-17}$$

Inserting equations (F-8) and (F-9) into equation (F-16) gives

$$H_y = [p/(4\pi Rr^2)]\,[(x^2-y^2)(z-R)/r^2 - zy^2/R^2]. \tag{F-18}$$

Equation (F-10) is repeated here unchanged:

$$H_z = py/(4\pi R^3). \tag{F-19}$$

Equations (F-17), (F-18), and (F-19) describe in MKS units the magnetic field intensity in air from a horizontal current element immersed in seawater expressed in

Cartesian coordinates fixed in the source. It is desired to convert these equations to yield magnetic induction in earth-fixed coordinates in which distances are expressed in feet.

In the absence of magnetic materials at the field point P, one can convert from magnetic field intensity H (in A/m) to magnetic induction B (in gamma) as follows:

$$1 \text{ A/m} = 4\pi \times 10^{-7} \text{ T} = 400\pi \text{ nT} = 400\pi \text{ gamma}. \tag{F-20}$$

Because 1 ft = 0.3048 m, one can express the linear dimensions (x, y, z, R, and r) in equations (F-17), (F-18), and (F-19) in ft by dividing the right sides of those equations by $(0.3048 \text{ m/ft})^2$.

Accordingly, if α is the submarine's true heading, the easterly, northerly, and upward components (B_{CEx}, B_{CEy}, and B_{CEz}, respectively) of magnetic induction at P from the horizontal electric current element at S, expressed in gamma are

$$B_{CEx} = 400\pi \, (H_x \sin \alpha - H_y \cos \alpha)/0.3048^2 \tag{F-21}$$

$$B_{CEy} = 400\pi \, (H_x \cos \alpha + H_y \sin \alpha)/0.3048^2 \tag{F-22}$$

$$B_{CEz} = 400\pi \, H_z/0.3048^2. \tag{F-23}$$

Thus,

$$B_{CEx} = [(-1076.39 \, p)/(Rr^2)]\{xy \, [z/R^2 + 2(z-R)/r^2] \sin \alpha + [(x^2-y^2)(z-R)/r^2 - zy^2/R^2] \cos \alpha\} \tag{F-24}$$

$$B_{CEy} = [(-1076.39 \, p)/(Rr^2)]\{xy \, [z/R^2 + 2(z-R)/r^2] \cos \alpha - [(x^2-y^2)(z-R)/r^2 - zy^2/R^2] \sin \alpha\} \tag{F-25}$$

$$B_{CEz} = 1076.39 \, py/R^3. \tag{F-26}$$

Equations (F-24), (F-25), and (F-26) give the east, north, and upward components of the magnetic induction (in gamma) in air in a coordinate system that is centered at an immersed horizontal steady electric current element for distances given in feet. If, relative to an earth-fixed coordinate system (as used elsewhere in this report), the coordinates of the

source are X_S, Y_S, and Z_S and the coordinates of the field point are X, Y, and Z, the following substitutions should be made:

$$r = (x^2 + y^2)^{1/2} \tag{F-27}$$

$$R = (x^2 + y^2 + z^2)^{1/2} \tag{F-28}$$

$$x = X - X_s \tag{F-29}$$

$$y = Y - Y_s \tag{F-30}$$

$$z = Z - Z_s. \tag{F-31}$$

APPENDIX G

CALCULATION OF EARTH'S MAGNETIC FIELD COMPONENTS IN THE VICINITY OF A GEOGRAPHICAL REFERENCE POINT

Equations describing the east, north, and upward components of the earth's magnetic field over a small region of space can be developed by a simple linear interpolation of data obtainable from more complicated global spherical harmonic models such as the International Geomagnetic Reference Field (IGRF). The method described below yields values that agree well with IGRF values over a 1-degree (latitude) by 1-degree (longitude) "square" for altitudes up to one nautical mile.

The method is described in terms of a numerical example at a reference point of 25°N, 58°E, and zero altitude (with respect to the ellipsoid that approximates the earth's shape). The region covered is over the Gulf of Oman and is bounded by 24.5° and 25.5°N, 57.5° and 58.5°E, and altitude 0 to 1 nmi. Figure G-1 illustrates the locations of the six points (five at zero altitude and one at 1 nmi altitude) for which the IGRF model was used to calculate easterly, northerly, and upward components of the earth's field, i.e., B_{Ex}, B_{Ey}, and B_{Ez}, respectively.

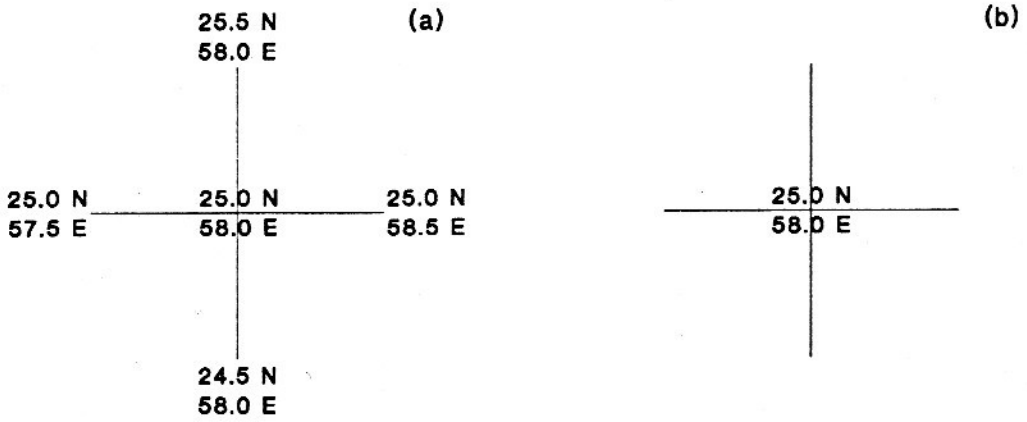


Figure G-1. Locations of points at which earth's magnetic field values were determined from IGRF model.
(a) Zero altitude
(b) One-nmi altitude

The values of the east, north, and upward components (gamma) of the earth's field at each of the locations identified in figure G-1 are given in the arrays that follow.

Zero altitude

East components (B_{Ex})			North components (B_{Ey})			Upward components (B_{Ez})		
	706			34046			-27245	
690	662	635	34234	34271	34309	-26545	-26582	-26618
	619			34491			-25911	

One-nmi altitude

East component (B_{Ex})	North component (B_{Ey})	Upward component (B_{Ez})
661	34239	-26554

The preceding data were used as the basis for the following equations. The coordinates of the sensor aircraft are X, Y, and Z and are given as distances (in feet) from the reference point (25°N, 58°E). Values were copied directly from the arrays above to allow the reader to follow the process used in formulating the equations.

$$B_{Ex} = 662 + (635-690)X/(60x6080 \cos 25°) + (706-619)Y/(60x6080) + (661-662)Z/6080 \quad \text{(G-1)}$$

$$B_{Ey} = 34271 + (34309-34234)X/(60x6080 \cos 25°) + (34046-34491)Y/(60x6080) + (34239-34271)Z/6080 \quad \text{(G-2)}$$

$$B_{Ez} = -26582 + (-26618-(-26545))X/(60x6080 \cos 25°) + (-27245-(-25911))Y/(60x6080) + (-26554-(-26582))Z/6080. \quad \text{(G-3)}$$

The foregoing equations can be rewritten in simpler form as

$$B_{Ex} = 662 - 0.00016635\ X + 0.00023849\ Y - 0.00016447\ Z \quad \text{(G-4)}$$

$$B_{Ey} = 34271 + 0.00022685\ X - 0.00121985\ Y - 0.00526316\ Z \quad \text{(G-5)}$$

$$B_{Ez} = -26582 - 0.00022080\ X - 0.00365680\ Y + 0.00460526\ Z. \quad \text{(G-6)}$$

As a check on the validity of these equations, values of B_{Ex}, B_{Ey}, and B_{Ez} were calculated for the eight corners of the 3263-nmi^3 volume bounded by latitudes 24.5° and 25.5°N, longitudes 57.5° and 58.5°E, and altitudes 0 and 1 nmi. (These points were chosen to be at the maximum distances within the volume from those used in developing equations (G-4), (G-5), and (G-6).) For comparison, values (24 in all) were also calculated by use of the IGRF model for the three components of the earth's magnetic field at the same eight locations. The maximum difference between the two sets of values was 5 gamma and the average difference was less than 2.7 gamma.

APPENDIX H

COMPUTATION OF MAGNETIC ANOMALY FROM COMPONENTS OF MAGNETIC INDUCTION CAUSED BY A SUBMARINE IN THE EARTH'S MAGNETIC FIELD

Method I (Exact)

The total steady magnetic induction $\mathbf{B_T}$ at field point P is the vector sum of the earth's magnetic induction $\mathbf{B_E}$, the magnetic induction $\mathbf{B_D}$ from the ferromagnetic dipole moment of the submarine, and the magnetic induction $\mathbf{B_{CE}}$ from the submarine's steady (static) electric current moment. That is,

$$\mathbf{B_T} = \mathbf{B_E} + \mathbf{B_D} + \mathbf{B_{CE}}. \tag{H-1}$$

Resolving each of these vectors into components in the easterly (x), northerly (y), and vertically upward (z) directions yields

$$\mathbf{B_E} = \mathbf{i}\, B_{Ex} + \mathbf{j}\, B_{Ey} + \mathbf{k}\, B_{Ez} \tag{H-2}$$

$$\mathbf{B_D} = \mathbf{i}\, B_{Dx} + \mathbf{j}\, B_{Dy} + \mathbf{k}\, B_{Dz} \tag{H-3}$$

$$\mathbf{B_{CE}} = \mathbf{i}\, B_{CEx} + \mathbf{j}\, B_{CEy} + \mathbf{k}\, B_{CEz}. \tag{H-4}$$

The magnitude B_E of vector $\mathbf{B_E}$ is

$$B_E = (B_{Ex}^2 + B_{Ey}^2 + B_{Ez}^2)^{1/2}. \tag{H-5}$$

Substituting equations (H-2), (H-3), and (H-4) into equation (H-1) and rearranging terms yields

$$\mathbf{B_T} = \mathbf{i}(B_{Ex}+B_{Dx}+B_{CEx}) + \mathbf{j}(B_{Ey}+B_{Dy}+B_{CEy}) + \mathbf{k}(B_{Ez}+B_{Dz}+B_{CEz}). \tag{H-6}$$

The magnitude of the magnetic induction at point P is

$$B_T = [(B_{Ex}+B_{Dx}+B_{CEx})^2 + (B_{Ey}+B_{Dy}+B_{CEy})^2 + (B_{Ez}+B_{Dz}+B_{CEz})^2]^{1/2}. \tag{H-7}$$

Equation (H-7) can be used to simulate the output of absolute or nearly absolute magnetometers such as the AN/ASQ-208. It may be advantageous to use B_T (instead of the more commonly used "magnetic anomaly") for processing magnetic signatures in that it is

not necessary to filter the magnetometer data first to eliminate earth's field gradient noise, a process that introduces signature distortion. In addition, if a high-pass filter is used to eliminate the gradient, noise caused by departures from straight and level flight of the sensor aircraft (e.g., erratic translational motion from buffeting) may be inseparably mixed in with the signal information. On the other hand, if equation (H-7) is used with earth's magnetic field data as a function of latitude, longitude, and altitude (obtainable from models such as IGRF), one can subtract out not only the gradient but also maneuver noise resulting from nonlinear motion of the sensor.

The magnetic anomaly Γ is the difference between the magnitude of the total magnetic induction at point P with the submarine present and the magnitude of the earth's magnetic induction in the absence of the submarine:

$$\Gamma = B_T - B_E. \tag{H-8}$$

Method II (Approximate)

It can be shown, as follows, that the magnetic anomaly from a submarine is, to an excellent approximation, simply the component of the magnetic induction from the submarine in the direction of the earth's field at point P.

First, equation (H-7) is simplified by combining the components of the magnetic induction from the ferromagnetic dipole and the electric current element (i.e., the submarine-generated components) as follows:

$$B_{subx} = B_{Dx} + B_{CEx} \tag{H-10}$$

$$B_{suby} = B_{Dy} + B_{CEy} \tag{H-11}$$

$$B_{subz} = B_{Dz} + B_{CEz}. \tag{H-12}$$

Then equation (H-7) becomes

$$B_T = [(B_{Ex}+B_{subx})^2 + (B_{Ey}+B_{suby})^2 + (B_{Ez}+B_{subz})^2]^{1/2}. \tag{H-13}$$

Squaring both sides of equation (H-13) and expanding the right side yields

$$B_T^2 = B_{Ex}^2 + 2\,B_{Ex}\,B_{subx} + B_{subx}^2 + B_{Ey}^2 + 2\,B_{Ey}\,B_{suby} + B_{suby}^2 + B_{Ez}^2 + 2\,B_{Ez}\,B_{subz} + B_{subz}^2. \tag{H-14}$$

If each component of the magnetic induction at point P from the submarine is much smaller than the corresponding component of the earth's magnetic induction, i.e.,

$$B_{subx} << B_{Ex}, \qquad B_{suby} << B_{Ey}, \qquad B_{subz} << B_{Ez},$$

equation (H-14) reduces to

$$B_T^2 \approx B_{Ex}^2 + 2\,B_{Ex}B_{subx} + B_{Ey}^2 + 2\,B_{Ey}B_{suby} + B_{Ez}^2 + 2\,B_{Ez}B_{subz}. \tag{H-15}$$

But, from equation (H-5)

$$B_{Ex}^2 + B_{Ey}^2 + B_{Ez}^2 = B_E^2. \tag{H-16}$$

Substituting equation (H-16) into (H-15) and rearranging terms yields

$$B_T^2 - B_{Ex}^2 \approx 2\,(B_{Ex}B_{subx} + B_{Ey}B_{suby} + B_{Ez}B_{subz}). \tag{H-17}$$

But

$$B_T^2 - B_{Ex}^2 = (B_T + B_{Ex})(B_T - B_{Ex}). \tag{H-18}$$

Therefore, from equations (H-17), (H-18), and (H-8), the anomaly Γ is

$$\Gamma = B_T - B_E \approx 2\,(B_{Ex}B_{subx} + B_{Ey}B_{suby} + B_{Ez}B_{subz})/(B_T + B_E). \tag{H-19}$$

If the magnetic induction from the submarine is very small compared to that of the earth,

$$B_T + B_E \approx 2\,B_E. \tag{H-20}$$

Substituting equation (H-20) into (H-19) and simplifying yields

$$\Gamma \approx (B_{Ex}B_{subx} + B_{Ey}B_{suby} + B_{Ez}B_{subz})/B_E. \tag{H-21}$$

Note that the earth's magnetic induction appears in equation (H-21) only as the ratios of each of its components to its total magnitude, i.e., B_{Ex}/B_E, B_{Ey}/B_E, and B_{Ez}/B_E. Thus, equation (H-21) enables one to compute the anomaly directly from the three components of the submarine's magnetic induction weighted in proportion to the respective components of the earth's magnetic induction.

As a matter of academic interest, it may be noted that the argument of equation (H-21) equals the scalar (dot) product of the earth's magnetic induction and the submarine's magnetic induction vectors

$$B_{Ex}B_{subx} + B_{Ey}B_{suby} + B_{Ez}B_{subz} = \mathbf{B_E} \cdot \mathbf{B_{sub}}. \qquad \text{(H-22)}$$

Thus equation (H-21) can be written in vector notation as

$$\Gamma \approx \mathbf{B_{sub}} \cdot \mathbf{B_E}/B_E, \qquad \text{(H-23)}$$

which states that the magnetic anomaly of a submarine equals the component of its magnetic induction in the direction of the earth's magnetic induction vector.